Universita' degli Studi "Roma Tre"

DIPARTIMENTO DI MATEMATICA E FISICA

DOTTORATO DI RICERCA IN FISICA
XXVIII CICLO

LEADING ISOSPIN BREAKING EFFECTS AND ELECTROMAGNETIC CORRECTIONS OF HADRONIC QUANTITIES IN LATTICE QCD

Candidate:
Dott.ssa Eleonora Picca

Supervisor:
Prof. Vittorio Lubicz

2015

Contents

Introduction

Isospin Symmetry is an approximate symmetry of strong interactions and, although the effect of this breaking is less than percent, it has very important consequences.

In an isospin symmetric world, the up (u) and down (d) quarks are identical particles. It is known than in Nature isospin symmetry is explicitly broken by the non–zero mass and electric charge differences of the u and d quarks. The mass difference $\Delta m_{ud} = m_d - m_u$ represents one percent or less of any typical QCD energy scale. Similarly, the typical relative size of the electromagnetic (EM) breaking of isospin symmetry is given by the fine structure constant $\alpha_{em} \simeq 0.007$. For those reasons we can reasonably state that, for observables with a non-vanishing isospin symmetric part, isospin symmetry is a good approximation of reality with an $\mathcal{O}(1\%)$ relative error. However, these small isospin breaking corrections are crucial to describe the structure of atomic matter in the Universe [1]. One of the most important consequences of the difference between u and d quarks is that the proton and neutron have different masses and charges. The mass splitting is accurately measured and it is given by [2]

$$\Delta M_{pn} = M_p - M_n = -1.2933322(4)\ \text{MeV}. \tag{1}$$

The sign of the mass splitting ΔM_{pn} makes the proton, and thus the hydrogen atom, a stable particle. The physical quantity ΔM_{pn} plays an important role also in the β–decay $n \to p + e + \nu_e$, because it determines the size of the phase space volume. The existence of this decay at early times of the Universe, i.e. for $t \sim 0$ and temperature $T \sim 1$ MeV, allows to infer that the ratio of the number of neutrons n_n and protons n_p is approximatively equal to:

$$\frac{n_n}{n_p} \simeq \exp\left(\frac{\Delta M_{pn}}{T}\right), \tag{2}$$

that is an important initial condition of Big Bang Nucleosynthesis.

Even if the nucleon isospin mass splitting is a well known quantity, predicting it from first principles is still an open problem because of the complex non–perturbative interactions of quarks inside the nucleon. The proton carries an additional electromagnetic charge comparing to the neutron, so just from QED one would expect $\Delta M_{pn} > 0$. However, the fact that the experimental value of ΔM_{pn} has the opposite sign indicates that the strong isospin breaking effects are competing against the EM effects (i.e.

$m_d > m_u$) with a larger magnitude. This implies that an important part of the structure of nuclear matter as we know it relies on a subtle cancellation between the small EM and strong breaking effects of isospin symmetry in the nucleon system. Therefore, it is fundamental to have a theoretical understanding of the nucleon isospin mass splitting.

Is also interesting to understand how to deduce the individual m_u and m_d quark masses and their difference. One way to do this is to consider that the kaon is a pseudo-Goldstone boson of chiral symmetry breaking and so the mass splitting $\Delta M_K^2 = M_{K^+}^2 - M_{K^0}^2$ is particularly sensitive to the strong isospin breaking. In order to calculate this effect, we have to find a way to evaluate the QED isospin breaking contributions. One well known result in this direction is the Dashen theorem [3] that states that in the $SU(3)$ chiral limit the electromagnetic kaon mass splitting is equal to the pion one. Since ΔM_π is known a pure QED effect with good accuracy (the strong IB corrections being quadratic in $m_u - m_d$), we conclude that $(\Delta M_K)_{EM} \simeq (\Delta M_\pi)_{EM} \simeq (\Delta M_\pi)_{EM}$.

Apart from the hadronic spectrum, the u and d quark difference reflects also on other physical observables such as decay constants and form factors. For instance, the corrections to the kaon decay constant f_K entering the $K_{\ell 2}$ decay [4] are crucial for the calculation of the CKM [5] matrix element V_{us}. In this work we are going to derive results of $m_u - m_d$, the mass splitting $M_{\pi^+} - M_{\pi^0}$ and QCD isospin breaking corrections to the $K_{\ell 2}$ decay rate.

The *up* and *down* mass difference is a small parameter with respect to the confinement scale Λ_{QCD} and electromagnetic isospin breaking effects are also small on hadronic observables because at low energy $\alpha_{em} \ll \alpha_s$. In particular we have

$$\frac{\hat{m}_d - \hat{m}_u}{\Lambda_{QCD}} \quad \sim \quad \hat{\alpha}_{em} = \frac{e^2}{4\pi} \quad \sim \quad 1\%. \tag{3}$$

For these reasons, most of the theoretical predictions on phenomenologically relevant hadronic observables have been derived by assuming the exact validity of isospin symmetry. Nowadays, at the level of precision presently achieved (see FLAG review [6]) for some flavour physics observables, isospin breaking effects cannot be neglected any longer.

At hadronic scale, i.e. $\mu \ll \Lambda_{QCD}$, we have a highly non–perturbative behavior of the strong interactions [7]. Therefore in this regime we can't use perturbation theory and we need to introduce non perturbative methods. In this work we use *Lattice QCD* (LQCD) [8, 9], a non–perturbative approach based only on first principles that consists in simulating QCD on a discrete and finite Euclidean space–time evaluating the path integrals via Montecarlo methods. One advantage of LQCD is that by the introduction of a finite 4–dimensional volume $V = L^3 \times T$ and a lattice spacing a, the theory is both IR and UV regularized. Furthermore, the LQCD degrees of freedom are finite. So we can use path integral formalism, which provides by itself a non perturbative approach. By discretizing the gauge and fermion fields, we can elaborate a lattice gauge field theory with some freedom, as long as in the continuum limit we recover the target

QCD theory. By choosing properly the lattice action we can minimize discretization effects, leaving $\mathcal{O}(a^2)$ as the dominant contribution.

In euclidean space–time the path integral has the form of a partition function and it can be calculated using numerical simulations. Given the large number of lattice points, Monte Carlo methods are employed with the importance sampling, by weighting the contributions to the integral using the Boltzmann factor. In this way only the relevant field configurations are taken into account, that are close to minimize the action. The finite volume, the lattice spacing and in many cases simulated light quark masses larger than the physical ones introduce systematic errors which have to be well controlled and accounted for.

Thanks to the increased computational power as well as to the algorithm and action improvements of the last decade, LQCD simulations have made significant progresses reaching a remarkable level of precision. In particular, this is due to the so-called un- quenched calculations, where the contribution of loops of dynamical sea quarks is properly taken into account.

Starting from the relevant two–points correlation functions calculated on the lattice, we computed the isospin breaking corrections to the pion mass, namely the splitting $M_{\pi^+} - M_{\pi^0}$, and to the kaon decay constant. Furthermore, we calculated the quark mass difference $m_d - m_u$.

A method to calculate leading isospin breaking effects on the lattice by including those associated with QED interactions has been recently developed [10, 11]. These effects are tiny because very small couplings, namely $m_d - m_u$ and α_{em}, multiply sizable matrix elements of hadronic operators. The approach is based on a perturbative expansion of the lattice path–integral in powers of $m_d - m_u$ and α_{em}, considering the two expansion parameters of the same size and neglecting higher orders. In this sense we talk of *leading isospin breaking* (LIB) effects.

A great advantage of our method is that, by working at fixed order in a perturbative expansion, we are able to factorize the small coefficients and to get relatively large numerical signals. For the same reason, we do not need to perform simulations at unphysical values of the electric charge, thus avoiding extrapolations of the lattice data with respect to α_{em}.

The expansion of the lattice path–integral in powers of α_{em} leads to correlators containing the integral over the whole space–time of two insertions of the quark electromagnetic currents, multiplied by the lattice photon propagator. These correlators have both infrared (zero modes), and ultraviolet divergences, that must be removed by providing an infrared safe finite volume definition of the lattice photon propagator and by imposing suitable renormalization conditions.

At first order of the expansion, the pion mass difference is generated only by QED corrections. For this reason it is a particularly clean theoretical prediction. Our result has been obtained by neglecting a quark disconnected contribution to M_{π^0} which is, however, of order $\mathcal{O}(m_{ud}\alpha_{em})$, with m_{ud} the average u and d quark mass. This contribution is expected to be numerically of the same order of the neglected second–order contributions to the expansion.

The kaon mass splitting is determined by both strong and electromagnetic isospin breaking effects. We implemented a renormalization prescription in order to separate these effects. Using this prescription, we calculated the kaon mass splitting $M_{K^+} - M_{K^0}$, together with the Dashen's theorem breaking parameter ϵ_γ and the u and d quark mass difference. These results are obtained using the so–called electro–quenched approximation, i.e. by considering dynamical sea quarks as neutral with respect to electromagnetism.

For the present study we used lattice gauge field configurations generated by *European Twisted Mass* (ETM) Collaboration at $N_f = 2+1+1$ sea quark flavors.

This work is organized as follows:

- In chapter 1 we will discuss the basic ingredients of lattice QCD, in particular how to discretize the fermion and the gauge fields and how to perform the renormalization on the lattice. There are different ways to discretize the continuum QCD action. For the fermions we employed the so–called *Wilson twisted mass* action [12] that, as we will see, has the property of reducing the discretization effects on physical quantities calculated on the lattice to $\mathcal{O}(a^2)$. Finally, we will briefly describe how to perform LQCD numerical simulations.

- In chapter 2 we will explain the method used in the calculation of the isospin breaking effects, that is basically a combined expansion in $m_d - m_u$ and α_{em} of the two–points correlation functions [10, 11]. We will discuss these expansions in the case of pions and kaons and use them as the starting point of our calculation. In particular we will explain how QED is introduced in our simulation using the non–compact formulation, i.e. by using as dynamical variable on the lattice the electromagnetic field A_μ.

  When including QED on the lattice, we have to deal with the fact that it is a long–ranged interaction, so we will have to take into account finite volume effects (FVE) [13] that are not exponentially suppressed, as in the case of QCD, but decrease as inverse powers of the lattice size.

- Chapter 3 contains the main original work performed in this thesis. Using the strategy described in chapter 2 we will obtain results for the pions mass splitting, the u and d mass difference and the kaon decay constant.

  The pion mass difference $M_{\pi^+} - M_{\pi^0}$ at the first order in the expansion in α_{em} and Δm_{ud} receives only the QED contribution. Furthermore, α_{em} doesn't need to be renormalized at this order. For these reasons, the pion mass splitting is a theoretically very clean observable. Our result is obtained by neglecting a quark disconnected contribution to M_{π^0} that, as already mentioned, is numerically of the same magnitude of higher order terms in the expansion not included in the analysis. We obtained

$$\boxed{M_{\pi^+} - M_{\pi^0} = 4.28(39)\ \text{MeV}}\ , \tag{4}$$

a result which is compatible with the previous determination with $N_f = 2$ [10], and with the experimental one [2]

$$(M_{\pi^+} - M_{\pi^0})_{EXP} = 4.5936(5)\ \text{MeV}\ , \tag{5}$$

We calculated the quark mass difference Δm_{ud} from the kaon mass splitting. We separated QED and QCD isospin breaking effects defining the quark masses in the $\overline{MS}$ scheme at $\mu = 2$ GeV, obtaining

$$\begin{aligned}
[M_{K^+} - M_{K^0}]^{QED}(2\ \text{GeV}) &= 2.04(21)\ \text{MeV} \\
[M_{K^+} - M_{K^0}]^{QCD}(2\ \text{GeV}) &= -5.98(20)\ \text{MeV},
\end{aligned}$$

from which we found

$$\boxed{[m_d - m_u](\overline{MS}, 2\ \text{GeV}) = 2.56(13)\ \text{MeV}}\ . \tag{6}$$

Also in this case our result is compatible with the previous $N_f = 2$ [10] calculation.

Finally we evaluated the corrections to the kaon decay constant, due to the up–down mass difference, that is related to the ratio of the K_{ℓ_2} and Π_{ℓ_2} decay rate correction, because pion doesn't get corrections at this order. We then found, using $SU(2)$ chiral perturbation theory for the chiral extrapolation,

$$\boxed{\left[\frac{f_{K^+}/f_{\pi^+}}{f_K/f_\pi} - 1\right]^{QCD} (\overline{MS}, 2\ \text{GeV}) = -0.00397(36)}\ . \tag{7}$$

Our result is higher than the estimate obtained by using chiral perturbation theory [14],

$$\left[\frac{f_{K^+}/f_{\pi^+}}{f_K/f_\pi} - 1\right]^{QCD}_{\chi PT} (\overline{MS}, 2\ \text{GeV}) = -0.0022(6). \tag{8}$$

by about $2 \times \sigma$.

Finally, I will end this thesis with some conclusions where I summarize the main results and indicate some future perspectives.

Chapter 1

Introduction to lattice QCD

QuantumChromoDynamics (QCD) [15] is a non–abelian gauge theory based on $SU(3)$ color group where the gauge bosons, the gluons, have color charges and therefore they self–interact. The gauge coupling constant α_s depends upon the energy scale of the phenomenon we are looking at. In particular, at high energy scales $\mu \gg \Lambda_{QCD} \simeq 0.3$ GeV we are in low coupling regime: the coupling decreases with the energy scale and we have the so–called asymptotic freedom. At high energy scale we can study the physical processes in perturbation theory. On the contrary, for energy scales $\mu \ll \Lambda_{QCD}$ we have confinement, whose consequence is that we can't observe free quarks and gluons, but only confined in color–free hadrons. In this regime we can't use perturbation theory and so we need to introduce non perturbative methods if we want to study the physics at these energies. This is the case of many processes in flavour physics, the branch of physics that studies transitions between quarks of different type, or *flavour*. It is well–described by the *Standard Model* but its origin remains unexplained and it needs to be deeply investigated [16].

The most accurate and extensive non perturbative method, that is the one used in this work, is Lattice QCD (LQCD) [8, 9]. LQCD is based only on first principles and it is basically a discretization of the space–time and consequently of all the fields and of all the interactions. It is defined introducing a 4–dimensional lattice spacing a in a finite volume $V = L^3 \times T$, that guarantees both the UV and IR regularizations of the theory. By introducing a lattice spacing we are introducing an UV cut–off proportional to $1/a$, while by introducing a finite volume we have an IR cut–off proportional to $1/L$.

One of the great advantage of LQCD is that we can calculate physical observables, i.e. expectation values, using numerical simulations. From these observables calculated on the lattice we can evaluate physical quantities of interest by performing a continuum limit. In this work we will use two–point correlation functions calculated on the lattice to evaluate isospin breaking effects on meson masses and decay constants, as explained in details in chapter 2.

In this chapter we will summarize the basic concepts which Lattice QCD (LQCD) relies on starting from the space–time discretization and describing how to discretize fermions and gauge fields in order to formulate a gauge theory on the lattice.

We will then briefly describe how physical quantities are renormalized on the lattice and how to perform numerical simulations.

1.1 4–dimensional discretization

The first step for the implementation of LQCD is to discretize the space–time by introducing a 4–dimensional finite volume $V = L^3 \times T$ and a lattice spacing a, defining the lattice points as

$$x_\mu = an_\mu \quad (\mu = 1, .., 4), \tag{1.1}$$

with integer vector $n_\mu = (n_1, n_2, n_3, n_4)$. LQCD is formulated in the euclidean space where a generic path integral, weighted by an highly oscillating function $e^{\imath S}$ in the Minkowski space where S is the action, is weighted by a real Boltzmann exponential factor e^{-S_E}. The euclidean action is obtained from the Minkowskian one by performing a Wick rotation to imaginary time. Under this rotation the partition function transforms as

$$Z_M = \int \mathcal{D}\phi \; e^{\imath S[\phi]} \rightarrow Z_E = \int \mathcal{D}\phi \; e^{-S[\phi]}, \tag{1.2}$$

with ϕ a generic field defined on the lattice points

$$\phi(x_\mu = an_\mu) = \frac{1}{V} \sum_n e^{\imath p_n \cdot x} \; \tilde{\phi}(p_n), \tag{1.3}$$

and $\tilde{\phi}(p_n)$ is its Fourier transform in momentum space. As we will see in sec. (1.4) this partition function can be evaluated numerically.

Working in a finite volume, we need to impose boundary conditions on the field ϕ. Let us consider for simplicity the case $V = L^4$. By imposing periodic boundary conditions $\phi(0) = \phi(L)$, we find the allowed values for the momentum on the lattice, obtaining

$$e^{\imath p_n \cdot L} = 1 \Rightarrow \; p_n^\mu = \frac{2\pi n^\mu}{L}, \tag{1.4}$$

and $n_\mu \in [-L/2 + 1, L/2]$. Therefore, the values for the momentum on the lattice are limited to the first *Brillouin zone*

$$-\frac{\pi}{a} < p_\mu < \frac{\pi}{a}. \tag{1.5}$$

We see from eq. (1.5) that by introducing a lattice we automatically introduced also a cut–off on the momentum. This means that our theory is UV regularized and this is one of the most important features of the lattice.

The simplest way to discretize a field theory is to define the lattice derivatives, the integration measure and to substitute everything in the continuum action, according to:

$$\begin{aligned} x_\mu &\to n_\mu a, \\ \phi(x) &\to \phi(na) \\ \textstyle\int d^4x &\to a^4 \textstyle\sum_n, \\ \partial_\mu \phi(na) &= \frac{1}{2a}[\phi(na+\hat{\mu}a) - \phi(na-\hat{\mu}a)]. \end{aligned} \tag{1.6}$$

In the next sections we will see however that this naive discretization is not always the correct procedure to define a gauge theory on the lattice.

1.2 Field theory on the lattice

In this section we are going to discuss the discretized action for QCD. There are different ways to discretize both the fermion and the gauge fields on the lattice as long as in the continuum limit we obtain the expected continuum theory.

We will start by discretizing the fermion field in a naive way and we will show that this procedure doesn't give the expected continuum limit, because it introduces unphysical fermion species. To solve this problem we will introduce the Wilson action that, at the prize of explicit chiral symmetry breaking, restores the correct fermionic spectrum in the continuum limit. Furthermore we will see that using the so–called *Wilson twisted–mass action* we will able to reduce the leading discretization effects to $\mathcal{O}(a^2)$.

After the fermions, we will discretize the gluon field and we will derive a lattice gauge theory.

1.2.1 Fermions on the lattice

Consider the free fermionic action in the continuum euclidean space

$$S_D = \int d^4x \; \bar{\psi}(x)(\not{\partial} + m_0)\psi. \tag{1.7}$$

When discretizing this action by applying eq. (1.6), however, one doesn't obtain the expected result in the continuum limit. The action suffers of the so called *doubling problem*, i.e. the existence of additional fermionic species, the so–called *doublers fermions*, that are unphysical particles. This problem can be seen by looking at the naively discretized fermionic propagator [9], obtained from eq. (1.7), which has the form

$$S(p) = \frac{1}{m_0 + \frac{\imath}{a}\gamma^\mu \sin(p_\mu a)}, \tag{1.8}$$

where the range of p is the first Brillouin zone, as in eq. (1.5). When $p_\mu = 0$ and $p_\mu = \pm\pi/a$, we have $\sin(p_\mu a) = 0$ and the propagator close to these points can be re–written as

$$S(p) = \frac{1}{m_0 + \imath\gamma^\mu p_\mu + \mathcal{O}(a^2)}. \tag{1.9}$$

Therefore, one finds that in the momentum space there are 2^d (two for every space–time dimension) regions where eq. (1.9) is valid and has finite continuum limit. Then we have $2^4 = 16$ particles entering the fermion spectrum of which 15 come from the regions on the border of the Brillouin zone and so are unphysical doubler fermions.

The Nielsen–Ninomiya theorem [17] states that the doubling problem necessarily appears in the continuum limit for local, hermitian, translational symmetric theories with exact (continuum) chiral symmetry. The Dirac operator in eq. (1.7) is chiral symmetric since in the chiral limit it anticommutes with the γ_5 matrix.

One way to avoid the doubler problem is to explicitly break chiral symmetry on the lattice. The doublers are generated because the naive theory is free from the chiral anomaly present in the continuum theory. One formulation of the fermion lattice action that follows this strategy is the Wilson action [12] that breaks the chiral symmetry even in the massless limit due to the addition of a new term proportional to so–called the Wilson parameter r. The Wilson action has the form

$$S_f^W = a^4 \sum_{n,m} [\bar{\psi}_\alpha(na) K_{\alpha\beta}(na, ma) \psi_\beta(ma)] - \frac{ar}{2}\, a^4 \sum_n \bar{\psi}(na) \Box \psi(na), \tag{1.10}$$

where

$$K_{\alpha\beta}(na, ma) = \frac{1}{2} \sum_{\hat{\mu}} \left[\frac{1}{a} (\gamma_\mu)_{\alpha\beta}\, (\delta_{m,n+\hat{\mu}} - \delta_{m,n-\hat{\mu}}) + m_0\, \delta_{m,n} \delta_{\alpha\beta} \right], \tag{1.11}$$

and

$$\Box\psi(na) = \frac{1}{a^2} \sum_\mu [\psi(na + \hat{\mu}a) + \psi(na - \hat{\mu}a) - 2\psi(na)]. \tag{1.12}$$

The fermionic propagator obtained from eq. (1.10) is

$$S^{(W)}(p) = \frac{1}{m_0 + \frac{\imath}{a}\gamma^\mu \sin(p^\mu a) + \frac{r}{a}\sum_\mu (1 - \cos(p^\mu a))}. \tag{1.13}$$

It is easy to realize that in the continuum limit the term proportional to r doesn't contribute to the propagator for $p \sim 0$, while for p near the borders of the Brillouin zone, i.e. in the regions where the contribution of the doublers come from, it increase the mass of the doubler fermions by $2r/a$, i.e. by a term proportional to the UV cut–off. In this way, by breaking explicitly the chiral symmetry, we have decoupled the unphysical fermions in the continuum limit, giving them a mass proportional to the cut–off.

In sec. (1.2.3), starting from the Wilson action, we will introduce the Wilson twisted–mass action that besides solving the doubling problem also guarantees automatic $\mathcal{O}(a)$ improvement of physical quantities.

1.2.2 Gauge theory on the lattice

In this section we introduce the gauge fields on the lattice in order to formulate a gauge invariant theory.

Consider a $SU(N_c)$ gauge group, with N_c colors, and a fermionic field $\psi(na)$ defined on the lattice (as explained in sec. (1.2.1)) that transforms under the fundamental representation of $SU(N_c)$ with a local transformation $G(na) \in SU(N_c)$:

$$\begin{aligned} &\psi(na) \to G(na)\ \psi(na) \\ &\bar{\psi}(na) \to \bar{\psi}(na)\ G^{-1}(na), \end{aligned} \tag{1.14}$$

with

$$G(na) = e^{\imath\Lambda(na)} \tag{1.15}$$

and $\Lambda(na) \in SU(N_c)$ an hermitian matrix. The derivative term of the fermion action

$$\partial_\mu \psi(na) = \frac{1}{2a}[\psi(na + \hat{\mu}a) - \psi(na - \hat{\mu}a)] \tag{1.16}$$

involves the field ψ at different points in the space–time. In order to compensate the phase difference between the two points after a local gauge transformation, we have to introduce a parallel transport factor, functions of the gauge field,

$$U_{n,n+\mu} \equiv U_\mu(na) \in SU(N_c) \tag{1.17}$$

which is called *link variable*, or simply *link*, and connects the points na and $na + \hat{\mu}a$, as illustrated in fig. (1.1). The link variables transform under the gauge group as

$$\begin{aligned} &U_\mu(na) \to G(na)\ U_\mu(na)\ G^{-1}(na + \hat{\mu}a) \\ &U_\mu^\dagger(na) \equiv U_{n,n+\mu}^\dagger = U_{n+\mu,n} \to G(na + \hat{\mu}a)\ U_\mu^\dagger(na)\ G^{-1}(na) \end{aligned} . \tag{1.18}$$

It is easily shown that using eq. (1.18), $\psi(na)$ and $(U_\mu(na) \cdot \psi(na + \hat{\mu}a))$ transform in the same way under $SU(N_c)$.

Figure 1.1: Link variables on the lattice. On the left, the *link* $U_\mu(na) = U_{n,n+\mu}$ connects the lattice points n and $(n+\hat{\mu})$. On the right, the hermitian conjugate link is shown with opposite direction.

The Wilson action in eq. (1.10) can be promoted to a gauge invariant fermionic action by introducing the link variables

$$\begin{aligned} S_f^W[U,\psi,\bar{\psi}] = a^4 \Bigg\{ \left(m_0 + \frac{4r}{a} \right) \sum_n \sum_{b=1}^{N_c} \bar{\psi}^b(na)\psi^b(na) + \\ -\frac{1}{2a} \sum_{n,\mu} \sum_{a,b=1}^{N_c} \Big[\bar{\psi}^a(na)\,(r-\gamma_\mu)\,U_\mu^{ab}(na)\psi^b(na+\hat{\mu}a) + \\ +\bar{\psi}^a(na+\hat{\mu}a)\,(r+\gamma_\mu)\,U_\mu^{\dagger ab}(na)\psi^b(na) \Big] \Bigg\}, \end{aligned} \tag{1.19}$$

where a and b are color indexes. We can define the lattice equivalent of the continuum covariant derivate as

$$\begin{aligned} D_\mu\psi(na) &= \frac{1}{2a}[U_{n,n+\hat{\mu}}\ \psi(na+\mu a) - U_{n,n-\hat{\mu}}\ \psi(na-\mu a)] = \\ &= \frac{1}{2}(\nabla_\mu + \nabla^*_\mu)\psi(na), \end{aligned} \tag{1.20}$$

with ∇_μ and ∇^*_μ *forward* and *backward* covariant derivates defined as

$$\begin{aligned} \nabla_\mu\psi(na) &= \frac{1}{a}[U_{n,n+\hat{\mu}}\ \psi(na+\mu a) - \psi(na)] \\ \nabla^*_\mu\psi(na) &= \frac{1}{a}[\psi(na) - U_{n,n-\hat{\mu}}\ \psi(na-\mu a)]. \end{aligned} \tag{1.21}$$

Introducing

$$D_W = \frac{1}{2}\left[\gamma_\mu(\nabla_\mu + \nabla^*_\mu) - ar\nabla^*_\mu\nabla_\mu\right], \tag{1.22}$$

we can write the action in eq. (1.19) in a more compact way as

$$S_f^{(W)}[U,\psi,\bar{\psi}] = a^4 \sum_n \bar{\psi}(na)[D_W + m_0]\psi(na). \tag{1.23}$$

Eq. (1.23) is the Wilson lattice fermionic gauge–invariant action.

In order to formulate a lattice gauge–invariant field theory we have to write also the gauge field kinetic term that has to be invariant under the group transformation and reduces in the continuum limit to the known gauge action S_G

$$S_G[U] = \frac{1}{2}\int d^4x \; Tr[\tilde{G}_{\mu\nu}(x)\tilde{G}^{\mu\nu}(x)], \tag{1.24}$$

where $\tilde{G}_{\mu\nu}$ is the gauge field defined as

$$\tilde{G}_{\mu\nu}(na) = \partial_\mu \tilde{G}_\nu(na) - \partial_\nu \tilde{G}_\mu(na) + \imath g_0 \left[\tilde{G}_\mu(na), \tilde{G}_\nu(na).\right], \tag{1.25}$$

with

$$\tilde{G}_\mu = \sum_{a=1}^{8} G_\mu^a \; t^a, \tag{1.26}$$

and t^a the group generators. To this purpose we have to find the relation between the link $U_\mu(na)$ and the gauge field and use the links to write the kinetic term. Being the parallel transporter, the link should corresponds to the discretized version of the *Schwinger line integral*, defined in the continuum as

$$U(x, y) = P \exp\left[\imath g_0 \; \left(\int_x^y dx_\mu G_\mu(x)\right)\right]. \tag{1.27}$$

When $y - x = \epsilon \ll 1$, we can write the integral as

$$U(x, x+\epsilon) \simeq \exp\left[\imath g_0 \; \sum_\mu \epsilon^\mu G_\mu(x)\right]. \tag{1.28}$$

The previous equation provides us the explicit expression of $U_\mu(na)$ on the lattice, being $a \ll 1$, that is

$$U_\mu(na) = e^{\imath g_0 a G_\mu(na)}, \tag{1.29}$$

where $G_\mu(na)$ is the lattice gauge field. It is easy to verify that by substituting eq. (1.29) into eq. (1.18) we find for the field $G_\mu(na)$ a transformation rule that in the continuum limit tends to the known continuum gauge transformation. Furthermore we find the correct continuum limit also for the covariant derivative in eq. (1.19).

Using eq. (1.29) we can derive the expression of the kinetic term of the gauge field action. The simplest gauge invariant object that we can use is the so–called plaquette, shown in fig. (1.2), that is the trace of the path–ordered product of the link variables

$$U_{\mu\nu}(na) = U_\mu(na)U_\nu(na+\hat{\mu}a)U_\mu^\dagger(na+\hat{\nu}a)U_\nu^\dagger(na). \tag{1.30}$$

Using (1.29) in eq. (1.30), expanding the gauge field

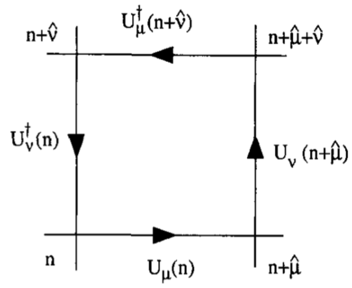

Figure 1.2: Elementary *plaquette* on the plane $\mu - \nu$.

$$G_\mu(na + \hat{\nu}a) \simeq G_\mu(na) + a\ \partial_\nu G_\mu(na), \tag{1.31}$$

and using the Baker-Campbell-Ausdorff rule

$$e^A e^B = e^{A+B+\frac{1}{2}[A,B]+..}, \tag{1.32}$$

one obtains

$$U_{\mu\nu}(na) = e^{\imath g_0 a^2 G_{\mu\nu}(na)}, \tag{1.33}$$

where $G_{\mu\nu}(na)$ in eq. (1.25). One can therefore use the plaquette to write the kinetic term as

$$S_G[U] = \beta \sum_n \sum_{1 \le \mu \le \nu} \left[1 - \frac{1}{2N_c} Tr(U_{\mu\nu}(na) + U^\dagger_{\mu\nu}(na))\right], \tag{1.34}$$

where

$$\beta = \frac{2N_c}{g_0^2}. \tag{1.35}$$

In the continuum limit, using eq. (1.33), one has

$$U_{\mu\nu}(na) + U^\dagger_{\mu\nu}(na) = 2\mathbb{I} - g_0^2 a^4 G^{\mu\nu}(na) G_{\mu\nu}(na) + \mathcal{O}(a^6), \tag{1.36}$$

that leads to

$$\begin{aligned} 1 - \frac{1}{2N_c} Tr\left[U_{\mu\nu}(na) + U^\dagger_{\mu\nu}(na)\right] &\simeq 1 - \frac{1}{2N_c} Tr\left[2\mathbb{I} - g_0^2 a^4 G^{\mu\nu}(na) G_{\mu\nu}(na)\right] = \\ &= \frac{g_0^2}{2N_c} a^4\ Tr\left[G^{\mu\nu}(na) G_{\mu\nu}(na)\right] = \\ &= \frac{1}{\beta} a^4\ Tr\left[G^{\mu\nu}(na) G_{\mu\nu}(na)\right]. \end{aligned} \tag{1.37}$$

For $V \to \infty$ e $a \to 0$, using $\sum_{1 \le \mu \le \nu} = \frac{1}{2} \sum_{\mu,\nu}$, we recover the continuum kinetic action

$$\begin{aligned} S_G[U] &\simeq \frac{1}{2} a^4 \sum_n \sum_{\mu,\nu} Tr\left[G^{\mu\nu}(na) G_{\mu\nu}(na)\right] \\ &\xrightarrow[V\to\infty]{a\to 0} \frac{1}{2} \int d^4x\ Tr\left[\tilde{G}^{\mu\nu}(x) \tilde{G}_{\mu\nu}(x)\right]. \end{aligned} \tag{1.38}$$

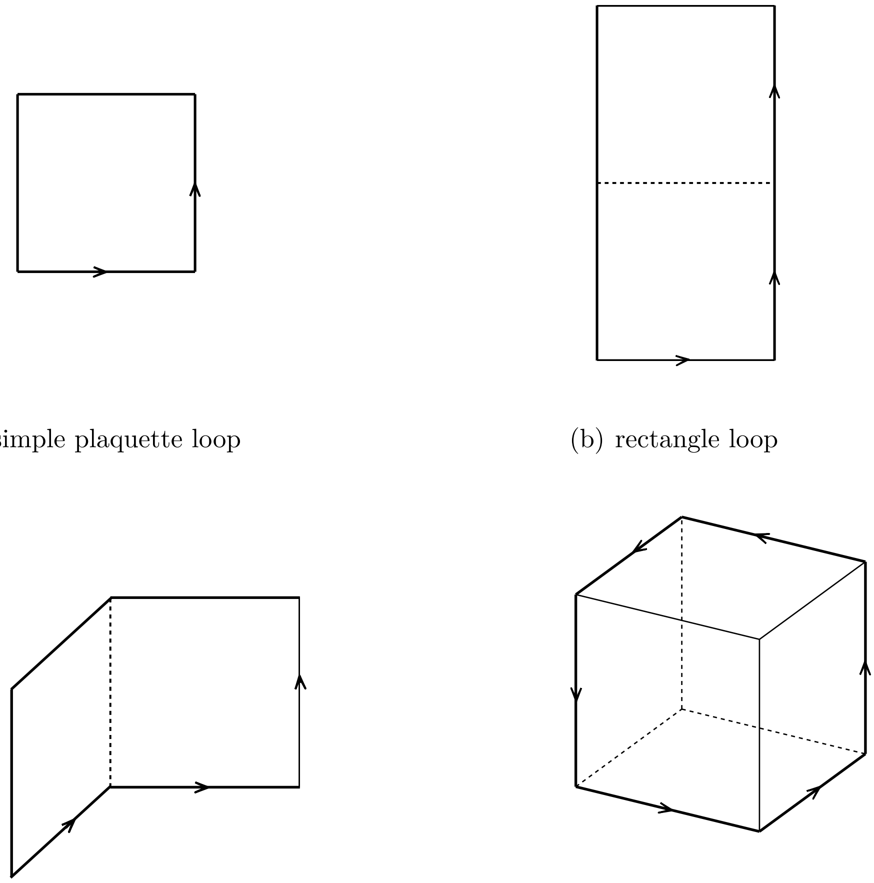

(a) simple plaquette loop (b) rectangle loop

(c) chair-type loop (d) three-dimensional loop

Figure 1.3: Four types of Wilson loops in the action.

We have thus obtain the full lattice action for a $SU(N_C)$ gauge invariant field theory, that is

$$S[U, \psi, \bar{\psi}] = S_G[U] + S_f^{(W)}[U, \psi, \bar{\psi}], \tag{1.39}$$

with S_G defined in eq. (1.34) and $S_f^{(W)}$ in eq. (1.23).

As we have already mentioned, there are many different ways to discretize the action on the lattice, as long as it gives the proper continuum limit. Another choice of gauge action, that is the one that we are going to consider in our calculation is the so called improved *Iwasaki action* [18][19]. In this case the action S_G is expressed in terms of different closed paths of the links, i.e. different types of plaquettes, shown in fig. (1.3). The Iwasaki action is

$$S_G = \frac{1}{g^2}\{c_0 \sum Tr\,(\text{simple plaquette loop}) + c_1 \sum Tr\,(\text{rectangle loop}) + \\ +c_2 \sum Tr\,(\text{chair-type loop}) + c_3 \sum Tr\,(\text{three-dimensional loop}) + \\ +\text{constant}\}. \tag{1.40}$$

Requiring that the action reduces in the continuum limit to the known gauge action we obtain the renormalization condition

$$c_0 + 8c_1 + 16c_2 + 8c_3 = 1. \tag{1.41}$$

By an appropriate choice of the coefficients in eq. (1.40), namely $c_1 = -0.331$, $c_2 = c_3 = 0$, one can obtain an improved gauge lattice action with reduced cut off effects. The explicit expression of the Iwasaki action is thus

$$S_G^{IW} = \frac{\beta}{3}\left[\sum_{x;\mu<\nu}(1-8c_1)P_{\mu\nu}^{1\times1} + c_1\sum_{x;\mu\neq\nu}P_{\mu\nu}^{1\times2}\right], \tag{1.42}$$

where $P_{\mu\nu}^{1\times1}$ is the usual plaquette term and $P_{\mu\nu}^{1\times2}$ contains all loops enclosing two rectangle loops.

1.2.3 Wilson twisted mass fermions

In this work the action used for the fermionic field is the Wilson twisted–mass (Wtm) action [20, 21]. The main advantage of this action is that it provides automatic $\mathcal{O}(a)$ improvement of physical observables in the continuum limit, if only one parameter, the so called Wilson mass, is properly tuned. This means that discretization effects coming from the lattice start from terms proportional to a^2.

Let us see the form of this action. Starting from the Wilson action in eq. (1.10), the Wtm action is defined as

$$S_f^{Wtm}[\chi,\bar{\chi}] = a^4\sum_n \bar{\chi}(na)(D_W + m_0 + \imath\mu_q\gamma_5\tau_3)\chi(na), \tag{1.43}$$

with χ a fermionic doublet in the so–called *twisted* basis, m_0 so–called the bare Wilson mass of the quark, μ_q the so–called *twisted mass* of the quark and D_W the standard Wilson operator is given in eq. (1.22). In the previous equation we have introduced a chirally twisted mass term $\imath\mu_q\gamma_5\tau_3$ in the twisted basis χ and we want to understand the relation between the field χ and the field ψ in the *physical basis*. Once can derive their relation by analyzing the continuum limit of the Wtm action, that is

$$S_f^{Wtm}\Big|_{cont} = \int d^4x\ \bar{\chi}(x)(\gamma^\mu D_\mu + m_q + \imath\mu_q\gamma_5\tau_3)\chi(x) = \\ = \int d^4x\ \bar{\chi}(x)(\gamma^\mu D_\mu + Me^{\imath\alpha\gamma_5\tau_3})\chi(x), \tag{1.44}$$

where

$$M = \sqrt{m_q^2 + \mu_q^2} \tag{1.45}$$

is the *polar mass*, the twisted angle α is defined from

$$\begin{cases} m_q = m_0 - m_{cr} = M\cos\alpha \\ \mu_q = M\sin\alpha. \end{cases} \tag{1.46}$$

In the previous equation, m_{cr} is the so–called *critical mass* that, as we will see in sec. (1.3), has a role in the renormalization of the quark mass. We have called twisted basis the one with the field χ because when the operator D_μ in eq. (1.44) is chirally invariant, as for continuum QCD, the fields ψ and χ are connected by a chiral rotation

$$\begin{cases} \psi = \exp\left(\frac{\imath}{2}w\gamma_5\tau_3\right)\chi \\ \\ \bar{\psi} = \bar{\chi}\exp\left(\frac{\imath}{2}w\gamma_5\tau_3\right), \end{cases} \tag{1.47}$$

and the action (1.44) in the physical (ψ) basis reduces to the standard QCD continuum action. The angle w in eq. (1.47) is the *twisted angle* and τ_3 is the Pauli matrix in the flavour space. If the angle w is properly chosen, the continuum Wtm action and the Wilson action are the same action written in two different bases related by eq. (1.47). If we apply eq. (1.47) to the action in eq. (1.44), being D_μ invariant under chiral transformation, the only variation is in the mass term, and we have

$$Me^{\imath\alpha\gamma_5\tau_3} \to Me^{\imath(\alpha-w)\gamma_5\tau_3}. \tag{1.48}$$

By choosing $w = \alpha$, that is

$$\tan w = \frac{\mu_q}{m_q}, \tag{1.49}$$

then the action in the twisted basis with mass $m_q + \imath\mu_q\gamma_5\tau_3$ is equivalent to the one in the physical basis with mass equal to the polar mass M.

As we have seen in sec. (1.2.1), however, we have introduced the Wilson action in order to get rid of the doubler fermions and this has been achieved this at the price of breaking the chiral symmetry of finite lattice spacing. Therefore, also the Wtm action is not invariant under chiral transformation, and one cannot reabsorb the twisted mass term with a field rotation. This has the consequence that the Wilson actions are equivalent only in the continuum limit but not at finite lattice spacing.

It is useful to understand how the expectation values of general observables $\mathcal{O}$ are related in the two bases. The integral measure is invariant under the chiral transformation in eq. (1.47) and we thus have that

$$\left\langle \mathcal{O}[\psi,\bar{\psi}] \right\rangle_{(M,0)} = \langle \mathcal{O}[\chi,\bar{\chi}] \rangle_{(m_q,\mu_q)}. \tag{1.50}$$

Eq. (1.50) means that the correlation function in the physical basis with mass M is equal, in the continuum limit, to the one calculated in the twisted basis with mass m_q and twisted mass μ_q.

An important feature of the Wtm action is that one can minimize discretization errors by choosing the rotation angle properly. The case of interest is the so called *maximal twist* when

$$w = \frac{\pi}{2}. \tag{1.51}$$

In term of quark masses this is equivalent to $m_q = 0$, as can be seen from eq. (1.49). In this case the only mass term that contributes to the polar mass M is the twisted mass μ_q, since $m_0 = m_{cr}$, see eq. (1.46).

One method to improve on–shell physical observables was suggested by Symanzik [22] and it is based on the cancellation of the discretization effects through the introduction of counter–terms in the action and in the operators. Near the continuum limit, we can expand the action in power series of the lattice spacing, that at $\mathcal{O}(a^2)$ reads like

$$S_{eff} = S_0 + aS_1 + a^2 S_2 + .., \tag{1.52}$$

where S_0 is the continuum action and S_k with $k \neq 0$ are operators defined as

$$S_k = \int d^4x \ \mathcal{L}_k(x). \tag{1.53}$$

with $\mathcal{L}_k(x)$ linear combinations of the local operators $\mathcal{O}_i(x)$ with dimension $4 + k$ and with the same symmetries of the lattice theory.

Consider the twisted mass action at maximal twist with twisted mass μ_q and with S_0 the gauge action in the continuum limit

$$S_0 = \int d^4x \ \bar{\chi}(x) \left[\gamma_\mu D^\mu + \imath\mu_R\gamma_5\tau_3\right] \chi(x). \tag{1.54}$$

In this case, the operators that contribute to S_1 are

$$\mathcal{O}_1 = \imath\bar{\chi}\sigma_{\mu\nu}G_{\mu\nu}\chi \qquad \mathcal{O}_5 = m^2\bar{\chi}\chi, \tag{1.55}$$

with $G_{\mu\nu}$ the gluon tensor. In then follows that a generic correlation function of a multilocal operator Φ in the effective theory,

$$\Phi_{eff} = \Phi_0 + a\Phi_1 + .., \tag{1.56}$$

has the form

$$\langle\Phi\rangle = \langle\Phi_0\rangle_{cont} - a\int d^4y \, \langle\Phi_0\mathcal{L}_1(y)\rangle_{cont} + a\,\langle\Phi_1\rangle_{cont} + \mathcal{O}(a^2), \tag{1.57}$$

where $\langle . \rangle_{cont}$ is calculated using the continuum action S_0. It can be shown [23] with symmetry considerations that in the case of maximal twist the $\mathcal{O}(a)$ term vanishes, and so we have

$$\langle \Phi \rangle = \langle \Phi_0 \rangle_{cont} + \mathcal{O}(a^2). \tag{1.58}$$

The use of twisted mass regularization at maximal twist has the further advantage of simplifying the renormalization of some hadronic matrix element. Of particular interest for the present study is the decay constant f_{PS} of a pseudo–scalar meson composed of two quarks of mass m_1 and m_2 defined as

$$f_{PS}\ p^\mu = \langle 0 | \, A^R_\mu \, | PS \rangle \tag{1.59}$$

where A^R_μ s the renormalized axial current. With twisted mass fermions at maximal twist, making use of the Partially Conserved Vector Current (PCVC) relation, the decay constant can be computed as

$$f_{PS} = (\mu_1 + \mu_2) \frac{\langle 0 | \, P_5 \, | PS \rangle}{M^2_{PS}}, \tag{1.60}$$

where P_5 is the operator $\bar{q}_1 \gamma_5 q_2$ and where there is no need of any renormalization constant.

1.3 Non Perturbative Renormalization: RI/MOM

LQCD is a regularization of QCD both in the UV and in the IR. QCD has divergent bare quantities, like quark masses, the strong coupling and generic operators and these quantities must be renormalized. On the lattice, the connection between bare lattice observables and the renormalized one in the continuum limit is provided by renormalization constants that absorb the divergencies when $a \to 0$.

LQCD quantities can be renormalized using both perturbative and non–perturbative methods. In this work we will use a non–perturbative method, the so–called RI/MOM [24], that is a mass–independent momentum-subtraction renormalization scheme. The RI-MOM renormalization scheme consists in imposing that the forward amputated Green function, computed in the chiral limit in the Landau gauge and at a given (large Euclidean) scale $p^2 = \mu^2$, is equal to its tree-level value. The renormalization conditions are thus imposed at fixed momentum and in the chiral limit where quarks are massless.

Let us consider the case of a bare bilinear operator defined on the lattice

$$\mathcal{O}_\Gamma(na) = \bar{\psi}(na)\ \Gamma\ \psi(na), \tag{1.61}$$

with Γ a combination of γs matrices. Consider an amputated forward Green function $\Lambda_{\mathcal{O}}(pa)$ in momentum space calculated between off–shell quark states

$$\Lambda_{\mathcal{O}}(pa) = \mathcal{S}^{-1}(pa)\ G_{\mathcal{O}}(pa)\ \mathcal{S}^{-1}(pa), \tag{1.62}$$

where $\mathcal{S}(pa)$ is the quark propagator and

$$G_{\mathcal{O}}(pa) = \langle \mathcal{S}(pa)\ \Gamma\ \mathcal{S}(pa) \rangle \tag{1.63}$$

is the forward non-amputated Green function. $G_{\mathcal{O}}(pa)$ has colour and spin indices and it is convenient to introduce

$$\Gamma_{\mathcal{O}}(pa) = \frac{1}{12}\,\mathrm{Tr}\,[P_\Gamma \cdot \Lambda_{\mathcal{O}}(pa)], \tag{1.64}$$

where the trace is over spin and colour indices. In eq. (1.64) P_Γ is a projector chosen in such a way that $\Gamma_{\mathcal{O}}(pa)$ is equal to 1 at tree–level. For example $P_\Gamma = \{\mathbb{I}, \gamma_5, \frac{1}{4}\gamma_\mu, -\frac{1}{4}\gamma_\mu\gamma_5\}$ for $\Gamma = \{\mathbb{I}, \gamma_5, \gamma_\mu, \gamma_\mu\gamma_5\}$.

The renormalization scale μ has to be chosen in the range

$$\Lambda_{QCD} \ll \mu \ll \frac{\pi}{a}, \tag{1.65}$$

where the upper limit is fixed in order to keep discretization effects under control and the lower bound in order to have the possibility of matching with perturbative scheme, as for example $\overline{MS}$.

Being μ the renormalization scale, the renormalization functions are computed by imposing in the chiral limit

$$\Gamma^R_{\mathcal{O}}(p)\Big|_{p^2=\mu^2} = \lim_{a\to 0}\left[Z_\psi^{-1}(a\mu) Z_{\mathcal{O}}(a\mu)\Gamma_{\mathcal{O}}(pa)\right]\Big|_{p^2=\mu^2} = 1, \tag{1.66}$$

that means that the renormalized Green function for $p^2 = \mu^2$ is equal to its tree–level value (i.e. 1 because of the projector P_Γ). Z_ψ is the fermion field renormalization constant while $Z_{\mathcal{O}}$ is the one of the operator. They are both mass independent because they are defined in the chiral limit.

Z_ψ is calculated from the quark propagator by imposing in the chiral limit the renormalization condition

$$\frac{\imath}{12}\,\mathrm{Tr}\left[\frac{\not p\ \mathcal{S}_R^{-1}}{p^2}\right]_{p^2=\mu^2} = Z_\psi^{-1}\frac{\imath}{12}\,\mathrm{Tr}\left[\frac{\not p\ \mathcal{S}^{-1}}{p^2}\right]_{p^2=\mu^2} = 1. \tag{1.67}$$

In our analysis, as explained in sec. (3.1), we used two sets of renormalization constants, that differ in the residual discretization effects evaluation, as explained in ref. [25]. The two methods give different results at fixed lattice cut-off, but the difference disappears in the continuum limit.

We now focus on the renormalization of quark masses. The corresponding renormalization constant is independent of the flavor f and the sign of the Wilson parameter r_f. As we have seen in sec. (1.2.1), the Wtm action is not invariant under chiral transformation. Therefore the Wilson quark m_q term is not protected against additive renormalization. We have

$$m_q = Z_m m_q = Z_m(m_0 - m_{cr}) \tag{1.68}$$

with m_0 the quark bare mass in eq. (1.43) and m_{cr} the *critical mass*. The renormalized mass m_q^R is defined as

$$m_q^R = \lim_{a\to 0}\left[Z_m(a\mu)\cdot m_q\right] = \lim_{a\to 0}\left[Z_m(a\mu)(m_0 - m_{crit})\right]. \tag{1.69}$$

On the other hand, the twisted mass μ_q renormalizes only multiplicatively so that

$$\mu_q^R = \lim_{a\to 0}\left[Z_\mu(a\mu)\cdot \mu_q\right], \tag{1.70}$$

Using the vector and axial currents Ward identities [26, 27] on the lattice, by imposing the proper renormalization of the currents it can be shown that the renormalization constants of the scalar and pseudoscalar densities are related to those of the Wilson and twisted mass respectively. One has

$$Z_m = \frac{1}{Z_S}, \qquad Z_\mu = \frac{1}{Z_P} \tag{1.71}$$

where Z_S and Z_P are the scalar and pseudoscalar operator renormalization constants.

At maximal twist the twisted mass μ_q is the only mass parameter related directly to the physical mass. Thus another advantage of working at maximal twist is that the quark mass renormalizes multiplicatively.

1.4 Numerical simulations

Lattice QCD is particularly suited for the study of QCD at low energy scales. One of the great advantage of formulating a field theory on the lattice, besides providing an ultraviolet cut off, is that it also provides a proper definition of vacuum expectation values. In the case of QCD it reads

$$\langle \mathcal{O}\rangle = \frac{\int \mathcal{D}U\mathcal{D}\bar{\psi}\mathcal{D}\psi\ \mathcal{O}\ e^{-S[U,\bar{\psi},\psi]}}{\int \mathcal{D}U\mathcal{D}\bar{\psi}\mathcal{D}\psi\ e^{-S[U,\bar{\psi},\psi]}}. \tag{1.72}$$

The action S is the discretized QCD action. Fermions are defined as Grassmann variables. Since the action is bilinear in the quark fields,

$$S_f = a^4 \sum_f [\bar{\psi}_f(na)K_{nm}[U]\psi_f(ma)], \tag{1.73}$$

the integration over the Grassmann variables can be performed analytically using

$$\int D\bar{\psi}\mathcal{D}\psi\ e^{-\bar{\psi}_f K[U]\psi_f} = \det K[U]. \tag{1.74}$$

Then, eq. (1.72) can be written in terms of a functional integral over only the gauge field

$$\langle \mathcal{O} \rangle = \frac{\int \mathcal{D}U\ \mathcal{O}\ e^{-S_{eff}[U]}}{\int \mathcal{D}U\ e^{-S_{eff}[U]}}. \tag{1.75}$$

where S_{eff} is the effective action

$$S_{eff} = S_G[U] - \ln\left(\prod_{f=1}^{N_f} \det K_f[U]\right), \tag{1.76}$$

S_G is the gluon action and N_f the number of quark flavours.

Eq. (1.75) is the starting point of lattice numerical simulations, in which the integral over the gauge fields is computed numerically. It would be computationally too expensive (impossible in practice) to calculate directly the integral in eq. (1.75), because the number of integrations is too high. For this reason, the integral is evaluated using statistical methods. The relevant observation is that the contributions of each gauge field configuration to the integral in eq. (1.75) is weighted by the factor $e^{-S_{eff}[U]}$. Therefore, only a small fraction of them gives a significant contribution, being the distribution highly peaked on those configurations that are close to minimize the action. For this reason, in any lattice simulation only a representative sample of gauge configurations is selected, using a method called the *importance sampling*. The set of gauge configuration is generated according to a probability distribution given by the Boltzmann factor $e^{-S_{eff}}$ generated using a *Markov chain*, i.e. a sequence of stochastic variables where each configuration U_i is calculated from the preceding one U_{i-1}. Choosing an appropriate transition probability, for $N \to \infty$ extractions, one generates configurations with the Boltzmann distribution [28].

In all lattice regularizations, lower values of the quark mass correspond to higher densities of low eigenvalues of the fermionic matrix. This makes the computation more and more demanding as the value of m_q is lowered. At the present days, still a large fraction of the simulations, including ours, is performed with light quark masses higher than the physical values. This has to be taken into account by eventually performing a chiral extrapolation to the physical mass during the computations, as explained in chapter. (3).

The lattice regularized theory reproduces the target theory only in the continuum limit. Observables computed at finite lattice spacing differ from its continuum counterpart for finite terms which vanish in this limit, i.e. discretization effects. In order to extract continuum physics it is therefore necessary to compute observables at different values of the lattice spacings and extrapolate them to $a \to 0$.

Up to the late nineties, the computational power was not sufficient to evaluate the fermionic determinant in eq. (1.76), because K is a huge sparse multidimensional matrix with Dirac, colour and space–time indices. Therefore, all lattice computations at that time were performed using the so–called *quenched approximation* which consists in taking

$$\det K[U] \equiv cost. \tag{1.77}$$

In the last decade the development in algorithms and machines made it possible the calculations taking into account the contribution of the fermionic determinant. In the present work we include the effects of four flavors of dynamical quarks ($N_f = 2+1+1$), corresponding to the degenerate up and down quarks, the strange and the charm.

The procedure adopted to evaluate the statistical errors for quantities numerically calculated on the lattice is explained in sec. (A).

Chapter 2

Description of the method

In this chapter we will discuss the method that we used to evaluate leading isospin breaking effects (LIB) on the lattice.

We will first describe the basic ingredients of our strategy, that is a perturbative expansion of euclidean correlation functions in powers of the electric charge e and the mass difference $m_d - m_u$ of the light quark masses, i.e. the parameters that originate the isospin breaking effects. In order to better understand our strategy we will start by describing how to calculate isospin breaking effects due to the u and d mass difference. We will then include the electromagnetic effects and explain how we included electromagnetism in our numerical simulations using a non–compact formulation of QED, i.e. by using as dynamical variable on the lattice the electromagnetic field A_μ.

We will also give some details about the lattice fermion action, in particular of the mixed–action setup used in this work and about interpolating fields considered for the meson operators.

We then illustrate our method explaining how we perform the expansions of the physical observables in $m_d - m_u$ and α_{em} and how to calculate corrections to the lattice path–integral. We will focus on two–point correlation functions, from which we evaluated isospin breaking corrections to meson masses and decay constants, and we will give examples in the case of pions and kaons.

Working on the lattice in finite volume, and being electromagnetism a long range interaction, we need to correct for QED finite volume effects which are by far not negligible. In this chapter we will show how they have been evaluated in our calculation.

2.1 Basic ingredients of LIB on the lattice

In order to better explain the strategy, we are first going to describe how to calculate LIB due to the small mass difference between the *up* and *down* quarks [11]. The introduction of QED isospin breaking effects is somewhat less straightforward and could be better understood if the basic ideas behind our strategy are clear.

The method is based on a perturbative expansion of physical observables in a small parameter, that in the present case is the *up* and *down* quark mass difference

$$m_d - m_u. \tag{2.1}$$

By doing this we will express isospin breaking corrections as a sum of amplitudes calculated in the isospin symmetric theory, multiplying by the small parameter. The advantages of this strategy is that the amplitudes by themselves are not small quantities and can be calculated precisely on the lattice.

Consider a generic euclidean correlation function of an observable $\mathcal{O}$

$$\langle \mathcal{O} \rangle = \frac{\int D\phi\ \mathcal{O}\ e^{-S}}{\int D\phi\ e^{-S}}, \tag{2.2}$$

where $D\phi$ is the measure of the theory and S is the euclidean action. We can rewrite the lagrangian $\mathcal{L}$ and so the action $S = \sum_x \mathcal{L}(x)$, as the sum of a term which is $SU(2)_V$ symmetric plus a term proportional to the u and d mass difference that violates the isospin symmetry:

$$\begin{aligned}
\mathcal{L} &= \mathcal{L}_{kin} + \mathcal{L}_m = \\
&= \mathcal{L}_{kin} + (m_u \bar{u}u + m_d \bar{d}d) = \\
&= \mathcal{L}_{kin} + \frac{m_u + m_d}{2}(\bar{u}u + \bar{d}d) - \frac{m_d - m_u}{2}(\bar{u}u - \bar{d}d) = \\
&= (\mathcal{L}_{kin} + m_{ud}\ \bar{q}q) - \Delta m_{ud}\ \bar{q}\tau^3 q = \\
&= \mathcal{L}_0 - \Delta m_{ud}\ \hat{\mathcal{L}},
\end{aligned} \tag{2.3}$$

where

$$\begin{cases}
\Delta m_{ud} = \dfrac{m_d - m_u}{2} \\
m_{ud} = \dfrac{m_u + m_d}{2} \\
q^T = (u, d).
\end{cases} \tag{2.4}$$

Using eq. (2.3), we have

$$S = \sum_x \mathcal{L}(x) = \sum_x \mathcal{L}_0(x) - \Delta m_{ud} \sum_x \hat{\mathcal{L}}(x) = S_0 - \Delta m_{ud}\ \hat{S}, \tag{2.5}$$

where

$$\hat{S} = \sum_x [\bar{q}\tau^3 q](x) = \sum_x [\bar{u}u - \bar{d}d](x). \tag{2.6}$$

By substituting eq. (2.6) in eq. (2.2) and expanding at first order the exponential of the action with respect to Δm_{ud} we obtain

$$\begin{aligned}
\langle \mathcal{O} \rangle \;\; &\simeq \;\; \frac{\int D\phi \; \mathcal{O} \; (1 + \Delta m_{ud} \; \hat{S}) \; e^{-S_0}}{\int D\phi \; (1 + \Delta m_{ud} \; \hat{S}) \; e^{-S_0}} = \frac{\langle \mathcal{O} \rangle_0 + \Delta m_{ud} \, \langle \mathcal{O}\hat{S} \rangle_0}{1 + \Delta m_{ud} \, \langle \hat{S} \rangle_0} = \\
&= \;\; \langle \mathcal{O} \rangle_0 + \Delta m_{ud} \, \langle \mathcal{O}\hat{S} \rangle_0 \, ,
\end{aligned} \tag{2.7}$$

where $\langle . \rangle_0$ represent the vacuum expectation value evaluated in the isospin symmetric theory and where $\langle \hat{S} \rangle_0 = 0$ because of isospin symmetry.

We can apply eq. (2.7) to the calculation of the u and d propagators

$$\begin{aligned}
G_u(x_1, x_2) \;\; &= \;\; G_\ell(x_1, x_2) + \Delta m_{ud} \, \sum_y G_\ell(x_1, y) \; G_\ell(y, x_2) + \cdots \, , \\
G_d(x_1, x_2) \;\; &= \;\; G_\ell(x_1, x_2) - \Delta m_{ud} \, \sum_y G_\ell(x_1, y) \; G_\ell(y, x_2) + \cdots \, ;
\end{aligned} \tag{2.8}$$

that can be graphically represented as

$$\begin{aligned}
\overset{u}{\longrightarrow} \;\; &= \;\; \longrightarrow \; + \Delta m_{ud} \; -\!\!\otimes\!\!- \; + \cdots \, , \\
\overset{d}{\longrightarrow} \;\; &= \;\; \longrightarrow \; - \Delta m_{ud} \; -\!\!\otimes\!\!- \; + \cdots \, ,
\end{aligned} \tag{2.9}$$

where

$$\begin{aligned}
{}_y \!\longrightarrow\! {}_x \;\; &= \;\; G_\ell(x - y) = \langle \ell(x) \bar{\ell}(y) \rangle \, , \\
\otimes \;\; &= \;\; \sum_z \bar{\ell}(z) \ell(z) \, ,
\end{aligned} \tag{2.10}$$

with ℓ either u or d in the isospin symmetric limit. Using the expansion (2.7) we have written the u and d propagators as a sum of isospin symmetric propagators that thus can be calculated on the lattice, i.e. the simple quark propagator and the propagator with a scalar insertion $\otimes$.

The same procedure can be applied to all correlation functions in order to extract the leading isospin breaking corrections to physical observables such as meson masses and decay constants.

We shall consider the following two point correlation functions of pion and kaon mesons:

$$
\begin{aligned}
C_{\pi^+\pi^-}(t,\vec{p}) &= \sum_{\vec{x}} e^{-i\vec{p}\cdot\vec{x}} \langle\, \bar{u}\gamma_5 d(x)\ \bar{d}\gamma_5 u(0)\,\rangle\ , \\
C_{\pi^0\pi^0}(t,\vec{p}) &= \frac{1}{2}\sum_{\vec{x}} e^{-i\vec{p}\cdot\vec{x}} \langle\, (\bar{u}\gamma_5 u - \bar{d}\gamma_5 d)(x)\ (\bar{u}\gamma_5 u - \bar{d}\gamma_5 d)(0)\,\rangle\,, \\
C_{K^+K^-}(t,\vec{p}) &= \sum_{\vec{x}} e^{-i\vec{p}\cdot\vec{x}} \langle\, \bar{u}\gamma_5 s(x)\ \bar{s}\gamma_5 u(0)\,\rangle\ , \\
C_{K^0K^0}(t,\vec{p}) &= \sum_{\vec{x}} e^{-i\vec{p}\cdot\vec{x}} \langle\, \bar{d}\gamma_5 s(x)\ \bar{s}\gamma_5 d(0)\,\rangle\,,
\end{aligned}
\tag{2.11}
$$

and use eq. (2.9) to expand the u and d propagator in order to calculate isospin breaking corrections.

First order corrections to pion masses and decay constants do vanish, as can be shown by considering the diagrammatic expansion of the correlation functions of the charged pion

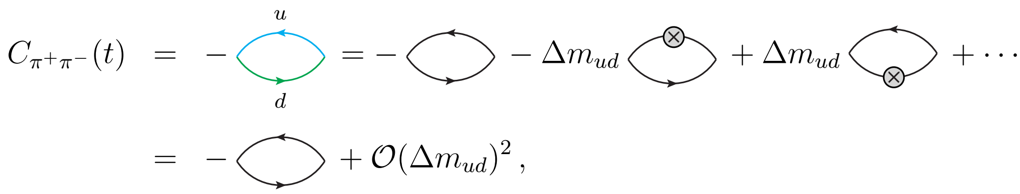
(2.12)

and the connected diagrams entering the neutral pion

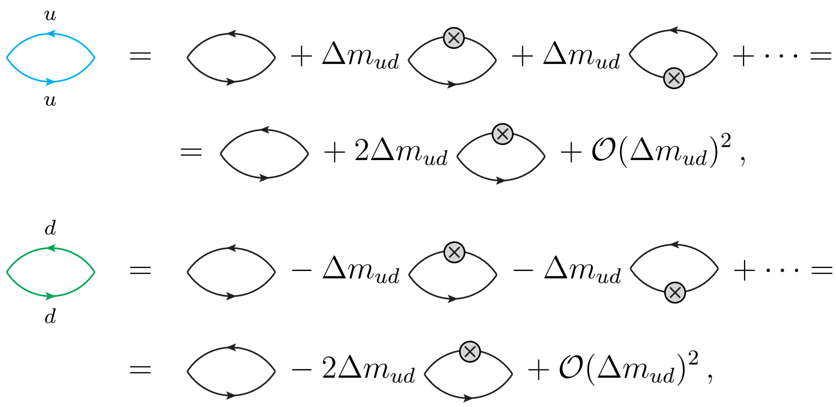
(2.13)

with (connected) two point correlation function

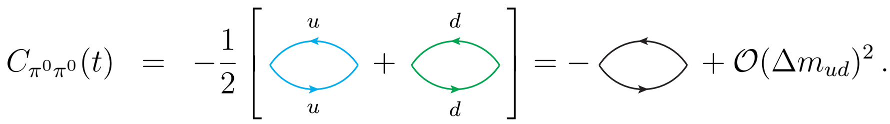
(2.14)

Also the first order corrections for the disconnected diagrams contributing to $C_{\pi^0\pi^0}(t)$ cancel out, a result that can be understood in terms of the isospin quantum numbers. Pion fields are symmetric under $u \leftrightarrow d$ interchange, so isospin corrections have to be quadratic in Δm_{ud}.

In the case of strange particles, and in general for flavoured mesons, first order corrections to masses and decay constants are different from zero. The isospin breaking corrections to the two point correlation functions of kaons are

$C_{K^+K^-}(t) = -$ 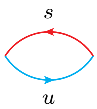

$= -$ 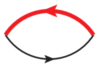 $- \Delta m_{ud}$ 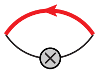 $+ \mathcal{O}(\Delta m_{ud})^2 ,$

$C_{K^0K^0}(t) = -$ 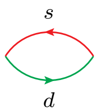

$= -$ 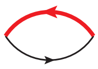 $+ \Delta m_{ud}$ 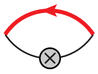 $+ \mathcal{O}(\Delta m_{ud})^2 ,$ (2.15)

i.e. they are proportional to Δm_{ud} and equal but opposite for the neutral and charged kaon.

In the following chapters we are going to discuss the inclusion of QED isospin breaking effects, by performing an expansion in both $m_d - m_u$ and α_{em} for pions and kaons. As we have seen from eq. (2.12) and (2.13) the pion doesn't have first order isospin breaking corrections coming from the u and d mass difference and the leading correction comes from QED. On the contrary, kaons have both types of corrections. In this case we will define a convention to separate QED and QCD effects.

2.2 QED on the lattice

In this section we describe how QED can be regularized on the lattice and we will give some details about the fermionic action used in this work. In particular we will provide a prescription for the definition of the IR regularized finite volume lattice photon propagator, i.e. a way to eliminate the infrared divergence associated with the zero momentum mode. We will also describe the numerical simulations in the full theory and the calculation of the electromagnetic correction to the kaon two–point correlator.

We used the non–compact formulation of lattice QED [29], that consists in treating the electromagnetic gauge potential $A_\mu(x)$ in a fixed (Feynman) gauge as a dynamical variable. The field $A_\mu(x)$ is distributed as a free field with the Maxwell action

$$\begin{aligned} S_{gauge}[A] &= \frac{1}{2} \sum_{x,\mu,\nu} A_\mu(x) \left[-\nabla_\nu^- \nabla_\nu^+ \right] A_\mu(x) = \\ &= \frac{1}{2} \sum_{k,\mu,\nu} \tilde{A}_\mu^\star(k) \left[2 \sin(k_\nu/2) \right]^2 \tilde{A}_\mu(k) \, , \end{aligned} \tag{2.16}$$

which is gaussian distributed in momentum space.

The electromagnetic interaction of quarks is written in terms of the quarks discrete covariant derivatives by introducing the QED links through exponentiation,

$$A_\mu(x) \quad \longrightarrow \quad E_\mu(x) = e^{-ieA_\mu(x)} \ , \tag{2.17}$$

and multiplying the QCD links for the appropriate $U(1)_{em}$ factors,

$$\begin{aligned} \mathcal{D}^+_\mu[U,A]\ \psi_f(x) &= [E_\mu(x)]^{e_f}\ U_\mu(x)\psi_f(x+\mu) - \psi_f(x) \\ \mathcal{D}^-_\mu[U,A]\ \psi_f(x) &= \psi_f(x) - [E_\mu(x)]^{e_f}\ U_\mu(x)\psi_f(x-\mu) \end{aligned} \tag{2.18}$$

where

$$e_f = \begin{cases} +2/3 & \text{for up type quarks} \\ -1/3 & \text{for down type quarks.} \end{cases}$$

Gauge invariance is obtained if the fields transform as

$$\begin{gathered} \psi_f(x) \longrightarrow e^{ie_f e\lambda(x)}\psi_f(x)\ , \qquad \bar{\psi}_f(x) \longrightarrow \bar{\psi}_f(x)e^{-ie_f e\lambda(x)} \\ A_\mu(x) \longrightarrow A_\mu(x) + \nabla^+_\mu \lambda(x)\ , \end{gathered} \tag{2.19}$$

where we define

$$\begin{gathered} \nabla^+_\mu f(x) = f(x+\hat{\mu}) - f(x)\ , \qquad \nabla^-_\mu f(x) = f(x) - f(x-\hat{\mu}) \\ \nabla_\mu = \frac{\nabla^+_\mu + \nabla^-_\mu}{2}\ . \end{gathered} \tag{2.20}$$

In order to calculate isospin breaking corrections we will perform a combined perturbative expansion in $\hat{\alpha}_{em}$ and $m_d - m_u$ and so we need to treat electromagnetism up to order e^2. Being $D_f[U,A]$ the lattice Dirac operator, we have

$$\begin{aligned} &\sum_x \bar{\psi}_f(x)\Big\{D_f[U,A] - D_f[U,0]\Big\}\ \psi_f(x) = \\ &\qquad = \sum_{x,\mu}\left\{(e_f e)A_\mu(x)V^\mu_f(x) + \frac{(e_f e)^2}{2}A_\mu(x)A_\mu(x)T^\mu_f(x) + \dots\right\}\ , \end{aligned} \tag{2.21}$$

where $V^\mu_f(x)$ is the conserved vector current of the quark f while $T^\mu_f(x)$ is the so called "tadpole" vertex. The specific expressions of $V^\mu_f(x)$ and $T^\mu_f(x)$ depend on the particular discretization of the fermion action. We want to notice that the tadpole interaction is characteristic of the lattice regularization and its role is essential in preserving gauge invariance at order e^2. The electromagnetic current and the tadpole vertex to be inserted in the correlators are the sums over all flavours of quarks with the corresponding charge factors,

$$\begin{aligned} J^\mu(x) &= \sum_f e_f e\, V_f^\mu(x) = \sum_f e_f e\, \bar{\psi}_f\, \Gamma_V^\mu[U]\, \psi_f(x)\ , \\ T^\mu(x) &= \sum_f (e_f e)^2\, T_f^\mu(x) = \sum_f (e_f e)^2\, \bar{\psi}_f\, \Gamma_T^\mu[U]\, \psi_f(x)\ . \end{aligned} \tag{2.22}$$

Given a QCD lattice correlator, the leading corrections of order α_{em} are calculated by considering the time ordered product of the original operators with two integrated insertions of $\sum_\mu A_\mu(x)J^\mu(x)$ or with a single insertion of $\sum_\mu A_\mu(x)A_\mu(x)T^\mu(x)$. Later in this section and in sec. (2.5) we will show this expansion for the correlators of pions and kaons.

By having introduced non–compact QED on the lattice, we have to give a prescription for treating the zero mode of the photon propagator. The lattice action of the QED gauge field in Feynman gauge is in eq. (2.16) where $A_\mu(x)$ is a real field while $\tilde{A}_\mu(k)$ denotes its Fourier transform that is a complex field satisfying the condition $\tilde{A}^\star_\mu(k) = \tilde{A}_\mu(-k)$. In order to calculate the photon propagator we have to invert the Laplace operator $\nabla^-_\nu\nabla^+_\nu$ and to do this we have to deal with its kernel. We have regularized the photon propagator by making the zero momentum mode to vanish identically, i.e. $\tilde{A}(k=0)=0$. This has been achieved by sampling the gauge potential directly in coordinate space and calculating the propagator stochastically. We introduced the projecting operator $\mathtt{P}^\perp$

$$\mathtt{P}^\perp\phi(x) = \phi(x) - \frac{1}{V}\sum_y \phi(y)\ , \tag{2.23}$$

that projects a given field on the subspace orthogonal to the zero momentum mode. The regularized photon propagator is then defined as

$$D^\perp_{\mu\nu}(x-y) = \left[\frac{\delta_{\mu\nu}}{-\nabla^-_\rho\nabla^+_\rho}\ \mathtt{P}^\perp\right](x-y)\ , \tag{2.24}$$

and calculated stochastically. The procedure consists in defining a stochastical field that satisfies

$$\langle B(x)\ B(y)\rangle_B = \delta(x-y), \tag{2.25}$$

where $\langle.\rangle_B$ denotes the average over the stochastic distribution.

One then defines

$$C(y) = \sum_z \mathcal{O}(y-z)\cdot B(z), \tag{2.26}$$

where $\mathcal{O}$ does not depend on B. Then

$$\begin{aligned}\langle B(x)C(y)\rangle_B = \langle \sum_z \mathcal{O}(y-z)\cdot B(x)\ B(z)\rangle_B &= \sum_z \mathcal{O}(y-z)\delta(x-z) = \\ &= \mathcal{O}(y-x). \end{aligned} \tag{2.27}$$

Using this simple strategy, we calculated the photon propagator as outlined below:

- we extract four independent real fields $B_\mu(x)$ ($\mu = 0, .., 3$) distributed according to a real Z_2 noise, which thus satisfy

$$\langle B_\mu(x)B_\nu(y)\rangle^B = \delta_{\mu\nu}\ \delta(x-y)\ ; \tag{2.28}$$

- for each field $B_\mu(x)$ we solve numerically the equation of motion in Feynman gauge,

$$[-\nabla^-_\rho \nabla^+_\rho]C_\mu[B;x] = \mathtt{P}^\perp\ B_\mu(x)\ , \tag{2.29}$$

  with solution

$$C_\mu[B;x] = \left[\frac{\delta_{\mu\nu}}{-\nabla^-_\rho \nabla^+_\rho}\ \mathtt{P}^\perp\right] B_\nu(x) = \sum_z D^\perp_{\mu\nu}(x-z)B_\nu(z)\ , \tag{2.30}$$

  where the field $C_\mu[B;x]$ is a functional of B_μ.

- the photon propagator is thus obtained as

$$\langle B_\mu(y)C_\nu[B;x]\rangle^B = \sum_z D^\perp_{\nu\rho}(x-z)\ \langle B_\mu(y)B_\rho(z)\rangle^B = D^\perp_{\mu\nu}(x-y)\ . \tag{2.31}$$

In order to illustrate the full procedure, we consider one contribution to the expansion at order α_{em} of the kaon propagator, namely the diagram with the exchange of a photon between the u and s quark line. We apply eq. (2.21) and consider the insertions of two electromagnetic currents V^μ_f. Then we have

$-e_s e_u \quad e^2$ 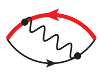 $=$

$$\begin{aligned} &= e_s e_u e^2 \left\langle \sum_{x,y} A_\mu(x)A_\nu(y)\ T\,\langle 0|\ [\bar{u}\gamma_5 s](t)\, V^\mu_s(x)\, V^\nu_u(y)\, [\bar{s}\gamma_5 u](0)\ |0\rangle \right\rangle^A \\ &= e_s e_u e^2 \sum_{x,y} D^\perp_{\mu\nu}(x-y)\ T\,\langle 0|\ [\bar{u}\gamma_5 s](t)\, V^\mu_s(x)\, V^\nu_u(y)\, [\bar{s}\gamma_5 u](0)\ |0\rangle\ , \end{aligned} \tag{2.32}$$

where the red line represents the s quark, while the black one the u quark. The $\langle . \rangle_A$ means the average over the gauge potential A_μ and $D^{\perp}_{\mu\nu}$ is the IR regularized photon propagator. Using eq. (2.31), we write eq. (2.32) as

$-$ 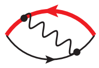

$$
\begin{aligned}
&= \sum_{x,y} D^{\perp}_{\mu\nu}(x-y)\, T\, \langle 0|\ [\bar{u}\gamma_5 s](t)\, V^{\mu}_{s}(x)\, V^{\nu}_{u}(y)\, [\bar{s}\gamma_5 u](0)\ |0\rangle \\
&= \left\langle \sum_{x,y} B_\mu(x) C_\nu[B;y]\ T\, \langle 0|\ [\bar{u}\gamma_5 s](t)\, V^{\mu}_{s}(x)\, V^{\nu}_{u}(y)\, [\bar{s}\gamma_5 u](0)\ |0\rangle \right\rangle^{B} \\
&= -\left\langle \sum_{x,y} B_\mu(x) C_\nu[B;y]\ \mathrm{Tr}\Big\{\gamma_5 S_s[U;t-x]\Gamma^{\mu}_{V} S_s[U;x]\gamma_5 S_{ud}[U;-y]\Gamma^{\nu}_{V} S_{ud}[U;y-t]\Big\} \right\rangle^{B},
\end{aligned}
\tag{2.33}
$$

where $S_f[U]$ is the fermion propagator. We can reduce the calculation of the diagram to the calculation of two single "generalized" quark propagators from $t' = 0$ to $t' = t$. If we define

$$
\begin{aligned}
\{D_f[U]\ \Psi^f_B\}(x) &= \textstyle\sum_\mu B_\mu(x)\Gamma^{\mu}_{V} S_f[U;x], \\
\{D_f[U]\ \Psi^f_C\}(x) &= \textstyle\sum_\mu C_\mu[B;x]\Gamma^{\mu}_{V} S_f[U;x],
\end{aligned}
\tag{2.34}
$$

with $D_f[U]$ the Dirac operator, then using also $S_f[U;x]^\dagger = \gamma_5 S_f[U;x]\gamma_5$, we can write eq. (2.33) as

$-e_s e_u e^2$ 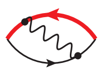

$$
= -e_s e_u e^2 \Big\langle\ \mathrm{Tr}\Big\{\ [\Psi^{ud}_C]^\dagger(t)\ \Psi^{s}_B(t)\ \Big\}\ \Big\rangle^{B}. \tag{2.35}
$$

In this way, solving eq. (2.34) for different values of B_μ and C_μ we can calculate the correlation function in eq. (2.35). In the numerical simulations we used 3 electromagnetic stochastic sources for each QCD gauge configuration.

Following the same strategy we can calculate all other types of diagrams containing insertions of photons required for the evaluation of the isospin breaking effects.

2.3 Fermion lattice action

In this section we are going to describe the fermion lattice action used in our calculation. We will also give the explicit expression of the conserved vector current $V^{\mu}_{f}(x)$ and of the tadpole vertex $T^{\mu}_{f}(x)$ in eq. (2.21).

We chose a mixed–action setup [30, 31], i.e. the sea and the valence quarks have different actions. Our fermion action is of the form

$$
S = S_{sea} + S_{val}. \tag{2.36}
$$

The sea quark action S_{sea} is the Wilson twisted mass action at maximal twist with $N_f = 2+1+1$ sea quarks with the introduction of the electromagnetic field A_μ, as explained in sec. (2.2). The expression of the action is

$$S_{sea} = S_{tm}^{\ell} + S_{tm}^{h}, \tag{2.37}$$

where S_{tm}^{ℓ} and S_{tm}^{h} are the up/down and strange/charm actions respectively.

Up and down sea quarks are arranged in mass–degenerate doublet and the action at maximal twist is of the form [32]:

$$S_{tm}^{\ell} = a^4 \sum\nolimits_x \overline{\psi}(x) \left\{ \frac{1}{2}\gamma_\mu(\mathcal{D}_\mu^+ + \mathcal{D}_\mu^-) - i\gamma_5\tau^3 \left[m_0 - \frac{a}{2}\mathcal{D}_\mu^+\mathcal{D}_\mu^- \right] + \mu_\ell \right\} \psi(x), \tag{2.38}$$

with the covariant derivate $\mathcal{D}_\mu^\pm$ defined in eq. (2.18). μ_l is the light quark mass, i.e. the up and down average mass, and m_0 is the untwisted mass tuned to its critical value m^{cr} as discussed in ref. [33], in order to guarantee the automatic $\mathcal{O}(a)$ improvement.

For the strange and charm doublet we have [34]

$$\begin{aligned} S_{tm}^{h} \; &= \; a^4 \sum\nolimits_x \overline{\psi}(x) \; \left\{ \frac{1}{2}\gamma_\mu(\mathcal{D}_\mu^+ + \mathcal{D}_\mu^-) - i\gamma_5\tau^1 \left[m_0 - \frac{a}{2}\mathcal{D}_\mu^+\mathcal{D}_\mu^- \right] + \right. \\ & \qquad\qquad \left. + \mu_\sigma + \mu_\delta\tau^3 \right\} \; \psi(x), \end{aligned} \tag{2.39}$$

where the twisted masses μ_σ and μ_δ are related to the strange and charm masses by the relation

$$m_{c,s}^{sea} = \frac{1}{Z_P}\left(\mu_\sigma \pm \frac{Z_P}{Z_S}\mu_\delta \right), \tag{2.40}$$

with Z_P and Z_S the pseudo–scalar and scalar quark density operator respectively. In eq. (2.39) the term proportional to τ_3 is used to split the masses of the members of the doublet, and consequently the Wilson term was twisted with the flavour matrix τ_1.

The twisted-mass action (2.37) leads to a mixing in the strange and charm sectors [34, 35], but the non–unitary mixed set up guarantees that K and D mesons do not mix.

In the valence sector we consider a doublet of fermionic fields for each flavour, $\psi_f^T = (\psi_f^+, \psi_f^-)$. For each fermionic doublet a corresponding doublet of bosonic fields (i.e. ghost fields) $\phi_f^T = (\phi_f^+, \phi_f^-)$ is introduced. The ghost doublets are never considered in the calculation of physical observables, but they have the only purpose of canceling the valence quark determinant. The fields within the same doublet have the same mass m_f, the same electric charge e_f, but opposite Wilson parameter r. The valence action reads as

$$S_{val} \;=\; \sum_{f,x} \left\{ \bar{\psi}_f D_f[U,A]\psi_f + \bar{\phi}_f D_f[U,A]\phi_f \right\} \,, \tag{2.41}$$

where the Dirac operator is

$$D_f[U,A] = \frac{1+\tau^3}{2} D_f^+[U,A] + \frac{1-\tau^3}{2} D_f^-[U,A] \ , \tag{2.42}$$

with

$$\begin{aligned} D_f^{\pm}[U,A]\ \psi(x) &= m_f\psi(x) \ \pm\ i\gamma_5(m_f^{cr}+4)\psi(x) \\ &- \sum_\mu \frac{\pm i\gamma_5 - \gamma_\mu}{2} U_\mu(x)[E_\mu(x)]^{e_f}\psi(x+\mu) \\ &- \sum_\mu \frac{\pm i\gamma_5 + \gamma_\mu}{2} U_\mu^\dagger(x-\mu)[E_\mu^\dagger(x-\mu)]^{e_f}\psi(x-\mu) \ . \end{aligned} \tag{2.43}$$

The symbol $\pm$ distinguish between the sign of the Wilson parameter r, that multiplies the γ_5 matrix, and τ^i are the Pauli matrices.

The mixed action setup used allows to compute observables with $O(a^2)$ cutoff effects at the price of introducing unitarity violations that disappear when the continuum limit is performed, because at matched sea and valence renormalized quark masses the resulting continuum theory is unitary. For each correlator, by replicating some of the valence matter fields when needed, the choice made for the action allows to consider only the fermionic Wick contractions that would arise in the continuum theory, avoiding the introduction of (finite) isospin breaking lattice artifacts. The resulting diagrams are then discretized by using for each quark propagator a convenient choice of the sign of the twisted Wilson term, that is the case in which the fields of the two valence quarks have opposite Wilson term. The resulting correlators have reduced cutoff effects and smaller statistical errors [36].

Using the Dirac operator in eq. (2.42) we can calculate the conserved vector current $V_f^\mu(x)$ and of the tadpole vertex $T_f^\mu(x)$ in eq. (2.21), obtaining

$$\begin{aligned} V_f^\mu(x) &= i\left[\bar\psi_f(x)\frac{i\tau^3\gamma_5-\gamma_\mu}{2}U_\mu(x)\psi_f(x+\mu) - \bar\psi_f(x+\mu)\frac{i\tau^3\gamma_5+\gamma_\mu}{2}U_\mu^\dagger(x)\psi_f(x)\right] \ , \\ T_f^\mu(x) &= \bar\psi_f(x)\frac{i\tau^3\gamma_5-\gamma_\mu}{2}U_\mu(x)\psi_f(x+\mu) + \\ &\quad +\bar\psi_f(x+\mu)\frac{i\tau^3\gamma_5+\gamma_\mu}{2}U_\mu^\dagger(x)\psi_f(x) \ . \end{aligned} \tag{2.44}$$

2.4 Electromagnetic corrections on the lattice

Generalizing the strategy described in sec. (2.1), we are going to introduce QED in our calculation of isospin breaking effects on the lattice [10], performing a combined perturbative expansion in the small parameters :

$$\frac{\hat{m}_d - \hat{m}_u}{\Lambda_{QCD}} \quad \sim \quad \hat{\alpha}_{em} = \frac{e^2}{4\pi} \quad \sim \quad \mathcal{O}(\epsilon), \tag{2.45}$$

neglecting contributions of order $\mathcal{O}(\epsilon^2)$.

In order to calculate $\mathcal{O}(\hat{\alpha}_{em})$ corrections, we use the non–compact formulation of QED on the lattice, as described in sec. (2.2). At this order we have to consider corrections to correlation functions containing two insertions of the electromagnetic current or one insertion of the tadpole vertex, multiplied by the IR regularized photon propagator and integrated over the space–time volume. In the first case the correction to a given correlator is proportional to

$$T\langle\mathcal{O}(x_i)\rangle \quad \longrightarrow \quad T\int d^4y d^4z \; D_{\mu\nu}(y-z) \; \langle\mathcal{O}(x_i) J^\mu(y) J^\nu(z)\rangle \; , \tag{2.46}$$

where $T\langle\mathcal{O}(x_i)\rangle$ is the T–product of a certain number of local operators, $D_{\mu\nu}(y-z)$ is the photon propagator in a fixed QED gauge and $J^\mu(x)$ is the sum of the electromagnetic currents of all the flavours, as in eq. (2.22). In sec. (2.2) we have already given a proper definition of the finite volume infrared regularized photon propagator so that eq. (2.46) is infrared regularized. On the other hand, because of the contact interactions of the electromagnetic currents, eq. (2.22) is ultraviolet divergent and need to be regularized. The introduction of the electromagnetism induce a (divergent) shift of the quark masses, of the strong coupling of QCD and, because we are working with Wilson twisted mass fermions, also of the critical masses.

By neglecting for now the critical mass term and the tadpole vertex contribution, consider the short distance expansion of the product of electromagnetic currents, which reads

$$J^\mu(x) J_\mu(0) \quad \sim \quad c_1(x) 1 + \sum_f c_m^f(x) m_f \bar{\psi}_f \psi_f + c_{g_s}(x) G_{\mu\nu} G^{\mu\nu} + \cdots \; . \tag{2.47}$$

The coefficients c_1, c_m^f and c_{g_s} are divergent quantities and need to be properly renormalized. In particular the terms proportional to c_m^f can be reabsorbed by a redefinition of the quark mass m_f while the term proportional to c_{g_s} can be reabsorbed by a redefinition of the strong coupling constant (i.e. the lattice spacing). The term proportional to c_1 corresponds to the vacuum polarization and the associated divergence cancels by taking the fully connected part of the right hand side of eq. (2.46).

Let us consider a generic "physical" observable $\mathcal{O}$ in the full theory,

$$\mathcal{O}(\vec{g}) \;=\; \mathcal{O}(e^2, g_s^2, m_u, m_d, m_s) \;=\; \langle\mathcal{O}\rangle^{\vec{g}} \; , \tag{2.48}$$

where we have used the following compact vector notation for the bare parameters of the theory

$$\vec{g} = \left(e^2, g_s^2, m_u, m_d, m_s\right) \tag{2.49}$$

and where the notation $\langle\cdot\rangle^{\vec{g}}$ means that the path–integral average is performed in the full theory. Our method consists in expanding any observable $\mathcal{O}(\vec{g})$ with respect to the isosymmetric QCD result $\mathcal{O}(\vec{g}^0)$ according to

$$\begin{aligned}\mathcal{O}(\vec{g}) &= \mathcal{O}(\vec{g}^0) + \left\{ e^2 \frac{\partial}{\partial e^2} + \left[g_s^2 - (g_s^0)^2\right] \frac{\partial}{\partial g_s^2} + \left[m_f - m_f^0\right] \frac{\partial}{\partial m_f} \right\} \mathcal{O}(\vec{g}) \Big|_{\vec{g}=\vec{g}^0} \\ &= \langle \mathcal{O} \rangle^{\vec{g}^0} + \Delta\mathcal{O} \,, \end{aligned} \tag{2.50}$$

where

$$\vec{g}^0 = \Big(0, (g_s^0)^2, m_{ud}^0, m_{ud}^0, m_s^0\Big) \,, \tag{2.51}$$

is the compact vector notation in the case of isospin symmetry, i.e. $e^2 = 0$ and $m_u = m_d$. The notation $\langle\cdot\rangle^{\vec{g}^0}$ means that the path–integral average is performed in the isosymmetric theory.

The bare parameters $\vec{g}^0$ can be fixed by matching the renormalized couplings of the two theories at a given scale $\mu^\star$ [37]. More precisely, first the parameters $\hat{g}_i(\mu) = Z_i(\mu) g_i$ are fixed by using an hadronic prescription. Then the renormalized couplings of the isosymmetric theory $\hat{g}_i^0(\mu) = Z_i^0(\mu) g_i^0$ at the scale $\mu^\star$ are fixed by imposing the following matching conditions

$$\begin{aligned} &\hat{g}_s^0(\mu^\star) = \hat{g}_s(\mu^\star) \,, \\ &\hat{m}_{ud}^0(\mu^\star) = \hat{m}_{ud}(\mu^\star) = \frac{\hat{m}_d(\mu^\star) + \hat{m}_u(\mu^\star)}{2} \,, \\ &\hat{m}_s^0(\mu^\star) = \hat{m}_s(\mu^\star) \,. \end{aligned} \tag{2.52}$$

In this work we rely on this prescription by matching the couplings renormalized in the $\overline{MS}$ scheme at $\mu^\star = 2$ GeV.

By using the property that a physical observable is a Renormalization Group Invariant (RGI) quantity, i.e.

$$\mathcal{O}(g_i) = \mathcal{O}(\hat{g}_i) \,, \qquad \mathcal{O}(g_i^0) = \mathcal{O}(\hat{g}_i^0) \,, \tag{2.53}$$

the perturbative expansion of eq. (2.50) can be expressed in terms of the renormalized couplings according to

$$\begin{aligned}\mathcal{O}(\hat{g}_i) &= \mathcal{O}\left(\hat{g}_i^0\right) + \\ &+ \left\{ \hat{e}^2 \frac{\partial}{\partial \hat{e}^2} + \left[\hat{g}_s^2 - \left(\frac{Z_{g_s}}{Z_{g_s}^0}\hat{g}_s^0\right)^2\right] \frac{\partial}{\partial \hat{g}_s^2} + \left[\hat{m}_f - \frac{Z_{m_f}}{Z_{m_f}^0}\hat{m}_f^0\right] \frac{\partial}{\partial \hat{m}_f} \right\} \mathcal{O}(\hat{g}_i) \Big|_{\hat{g}_i = \frac{Z_i}{Z_i^0}\hat{g}_i^0} \end{aligned} \tag{2.54}$$

From the comparison of the previous equation with eq. (2.47) we find in the differential operator language the divergent terms proportional to $Z_{m_f}/Z^0_{m_f}$ and $Z_{g_s}/Z^0_{g_s}$ that correspond to the short distance expansion counter–terms c^f_m and c_{g_s} respectively. In practice, these counter–terms do appear because the renormalization constants (the bare parameters) of the full theory are different from the corresponding quantities of isosymmetric QCD, the theory in which we perform the numerical simulations. Once the counter–terms have been properly tuned, our procedure can be interpreted as the expansion of the full theory in the renormalized parameters $\hat{\alpha}_{em}$ and $\hat{m}_d - \hat{m}_u$.

In eq. (2.47) we didn't take into account the shift of the critical mass induced by electromagnetism in the presence of a Wilson term in the fermionic action. To do this we re–write eq. (2.47) modifying both the left and the right side to include the tadpole contribution to the electromagnetic current

$$
\begin{aligned}
J^\mu(x)J_\mu(0) \;&+\; \sum_\mu T^\mu(x) \\
&\sim\; c_1(x)\mathbb{1} \;+\; \sum_f c^f_k(x)\bar{\psi}_f i\gamma_5\tau^3\psi_f \;+ \\
&+\; \sum_f c^f_m(x) m_f\bar{\psi}_f\psi_f \;+\; c_{g_s}(x)G_{\mu\nu}G^{\mu\nu} \;+\; \cdots\,. \qquad (2.55)
\end{aligned}
$$

In the previous equation, $T^\mu(x)$ is the tadpole contribution and c^f_k is the critical mass counter–term coefficient. In order to determine the counter–term associated with the electromagnetic shift of the critical mass, we adopted a method commonly used to implement the maximal twist condition in simulations of isosymmetric QCD. Starting from the Dirac operators in eq. (2.42) and eq. (2.43) for a given flavour doublet, we can separately tune the critical mass of each valence quark by imposing the following vector Wilson Twisted Identity (WTI)

$$
W_f(\vec{g}) = \nabla_\mu \langle \left[\bar{\psi}_f\gamma^\mu\tau^1\psi_f\right](x)\ \left[\bar{\psi}_f\gamma^5\tau^2\psi_f\right](0)\ \rangle^{\vec{g}} = 0\,, \qquad f = \{u,d,s\}\,. \qquad (2.56)
$$

The explicit formulae corresponding to its expansion in powers of e can be obtained applying the Δ operator of eq. (2.50). To do this let us consider the general expression of eq. (2.50) taking into account also the critical mass shift. Given a general observable in the full theory, we have

$$
\mathcal{O}(\vec{g}) \;=\; \mathcal{O}(e^2, g_s^2, m_u, m_d, m_s, m_u^{cr}, m_d^{cr}, m_s^{cr})\,, \qquad (2.57)
$$

where we have enlarged the parameter space of the theory

$$
\vec{g} = \left(e^2, g_s^2, m_u, m_d, m_s, m_u^{cr}, m_d^{cr}, m_s^{cr}\right)\,. \qquad (2.58)
$$

By calling m_0^{cr} the single critical mass parameter of the symmetric theory, we see that isosymmetric QCD simulations correspond to

$$\vec{g}^0 = \left(0, (g_s^0)^2, m_{ud}^0, m_{ud}^0, m_s^0, m_0^{cr}, m_0^{cr}, m_0^{cr}\right) . \tag{2.59}$$

The value of m_0^{cr} has been precisely determined in ref. [33] in the isosymmetric theory by requiring the validity of the vector Ward–Takahashi identity of eq. (2.56) with $m_f^0 = m_{ud}^0$,

$$W_{ud}(\vec{g}^0) = 0 \qquad \longrightarrow \qquad m_0^{cr} . \tag{2.60}$$

Our gauge ensembles have been generated at this well defined value of critical mass for each $\beta^0 = 6/(g_s^0)^2$. The LIB corrections to any observable can be obtained by making an expansion, at fixed lattice spacing, with respect to the differences $m_f^{cr} - m_0^{cr}$ which represents a regularization specific isospin breaking effect induced by the electromagnetic interactions. We can then write the generalization of eq. (2.50), that we will use in the rest of this work for calculating LIB on the lattice

$$\Delta\mathcal{O} \;=\; \left\{e^2\frac{\partial}{\partial e^2} + \left[g_s^2 - (g_s^0)^2\right]\frac{\partial}{\partial g_s^2} + [m_f - m_f^0]\frac{\partial}{\partial m_f} + [m_f^{cr} - m_0^{cr}]\frac{\partial}{\partial m_f^{cr}}\right\}\mathcal{O}(\vec{g})\Big|_{\vec{g}=\vec{g}^0} \tag{2.61}$$

In sec. (2.5) we will use eq. (2.61) to expand the lattice path–integral.

2.5 Expansion of the lattice–path integral

In this section we are going to apply the method described in sec. (2.4) in order to calculate the LIB (Leading Isospin Breaking) corrections to pions and kaons.

We first want to describe the general method used for the calculation of LIB corrections to general observables, applying the strategy described in sec. (2.4).

The starting point is the path–integral representation of an observable $\mathcal{O}$ in the full theory,

$$\mathcal{O}(\vec{g}) \;=\; \langle\mathcal{O}\rangle^{\vec{g}} = \frac{\int dAe^{-S_{gauge}[A]}\, dU\; e^{-\beta S_{gauge}[U]}\; \prod_{f=1}^{n_f}\det\left(D_f^{\pm}[U,A;\vec{g}]\right)\; \mathcal{O}[U,A;\vec{g}]}{\int dAe^{-S_{gauge}[A]}\; dU\; e^{-\beta S_{gauge}[U]}\; \prod_{f=1}^{n_f}\det\left(D_f^{\pm}[U,A;\vec{g}]\right)} , \tag{2.62}$$

where $S_{gauge}[A]$ has been given in eq. (2.16) and is a functional of the gauge potential A_μ, $S_{gauge}[U]$ is the QCD gauge action with $\beta = 6/g_s^2$ and is a functional of the link variables $U_\mu(x)$, and $D_f^{\pm}[U,A;\vec{g}]$ are the Dirac operators defined in eq. (2.43). We want to express eq. (2.62) in terms of the isospin symmetric path integral

$$\mathcal{O}(\vec{g}^0) \;=\; \langle\mathcal{O}\rangle^{\vec{g}^0} \;=\; \frac{\int dU\; e^{-\beta^0 S_{gauge}[U]}\; \prod_{f=1}^{n_f}\det\left(D_f^{\pm}[U;\vec{g}^0]\right)\; \mathcal{O}[U]}{\int dU\; e^{-\beta^0 S_{gauge}[U]}\; \prod_{f=1}^{n_f}\det\left(D_f^{\pm}[U;\vec{g}^0]\right)} , \tag{2.63}$$

that is our starting point in the calculation, i.e. what we calculate on the lattice. We can do this noting that we need to introduce appropriate factors that takes into account the variations induced by the introduction of electromagnetism. This can be easily done defining

$$R[U,A;\vec{g}] = e^{-(\beta-\beta^0)S_{gauge}[U]}\ r[U,A;\vec{g}]\ ,$$

$$r[U,A;\vec{g}] = \prod_{f=1}^{n_f} r_f[U,A;\vec{g}] \ = \ \prod_{f=1}^{n_f} \frac{\det\left(D_f^{\pm}[U,A;\vec{g}]\right)}{\det\left(D_f^{\pm}[U;\vec{g}^0]\right)}\ , \tag{2.64}$$

and the functional average $\langle . \rangle^A$ on the photon field

$$\langle \mathcal{O} \rangle^A = \frac{\int dA\ e^{-S_{gauge}[A]}\ \mathcal{O}[A]}{\int dA\ e^{-S_{gauge}[A]}}. \tag{2.65}$$

Using eq. (2.64) and eq. (2.65), the path–integral in eq. (2.62) can be written as

$$\langle \mathcal{O} \rangle^{\vec{g}} \ = \ \frac{\left\langle R\mathcal{O} \right\rangle^{A,\vec{g}^0}}{\left\langle R \right\rangle^{A,\vec{g}^0}} \ = \ \frac{\left\langle\ \left\langle\ R[U,A;\vec{g}]\ O[U,A;\vec{g}]\ \right\rangle^A\ \right\rangle^{\vec{g}^0}}{\left\langle\ \left\langle\ R[U,A;\vec{g}]\ \right\rangle^A\ \right\rangle^{\vec{g}^0}}\ , \tag{2.66}$$

that is a path–integral with respect to isospin symmetric quantities.

We can know use eq. (2.61) to evaluate the LIB corrections by applying the operator Δ in eq. (2.50) to eq. (2.66), obtaining

$$\begin{aligned} \Delta\mathcal{O} \ &= \ \left\langle \Delta(R\mathcal{O}) \right\rangle^{A,\vec{g}^0} - \left\langle \Delta R \right\rangle^{A,\vec{g}^0} \left\langle \mathcal{O} \right\rangle^{\vec{g}^0} = \\ &= \ \left\langle \Delta\mathcal{O}[U,A;\vec{g}]\Big|_{\vec{g}=\vec{g}^0} \right\rangle^{A,\vec{g}^0} + \\ &\quad + \left\{ \left\langle \Delta\left(R\mathcal{O} - \mathcal{O}\right)[U,A;\vec{g}]\Big|_{\vec{g}=\vec{g}^0} \right\rangle^{A,\vec{g}^0} - \left\langle \Delta R[U,A;\vec{g}]\Big|_{\vec{g}=\vec{g}^0} \right\rangle^{A,\vec{g}^0} \left\langle \mathcal{O}[U;\vec{g}^0] \right\rangle^{\vec{g}^0} \right\}. \end{aligned} \tag{2.67}$$

In the previous expression we put in curly brackets the contributions coming from the reweighting factor in eq. (2.64) and, consequently, from the sea quark determinants. In the following we will refer to these contributions as vacuum polarization terms or disconnected terms. In order to apply the delta operator Δ, it is useful to observe that

$$\left.\frac{\partial \left\langle \mathcal{O} \right\rangle^A (e^2)}{\partial(e^2)}\right|_{e^2=0} \ = \ \left\langle \frac{1}{2} \left.\frac{\partial^2 \mathcal{O}[A;e]}{\partial e^2}\right|_{e=0} \right\rangle^A\ , \tag{2.68}$$

and to write down the expressions and the related graphical representations of the derivates in eq. (2.61) applied to the quark propagator and to the Dirac operator. Assuming that the derivatives have been evaluated at $\vec{g} = \vec{g}_0$ and that the integral $\langle . \rangle_A$ has been already performed, we have that

$$\frac{1}{2}\frac{\partial^2 S_f}{\partial e^2} = S_f \frac{\partial D_f}{\partial e} S_f \frac{\partial D_f}{\partial e} S_f - \frac{1}{2} S_f \frac{\partial^2 D_f}{\partial e^2} S_f \quad = \quad e_f^2$$ 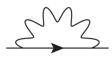 $$+\, e_f^2$$ 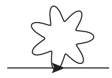 , (2.69)

$$\frac{\partial S_f}{\partial m_f} = -S_f \frac{\partial D_f}{\partial m_f} S_f \quad = \quad - -\!\!\otimes\!\!- \ , \tag{2.70}$$

$$\frac{\partial S_f^{\pm}}{\partial m_f^{cr}} = -S_f^{\pm} \frac{\partial D_f^{\pm}}{\partial m_f^{cr}} S_f^{\pm} \quad = \quad \mp -\!\!\otimes\!\!- \ . \tag{2.71}$$

In the previous expression we have explicitly shown the two electromagnetic corrections to the quark propagator, with the second one that is the tadpole insertion, and the mass and critical mass corrections. The Dirac operator is the one in eq. (2.42). The insertion $-\!\!\otimes\!\!-$ corresponds to the insertion of the scalar operator, while the critical mass $-\!\!\otimes\!\!-$ to the pseudoscalar operator γ_5 and in this case the sign depends on the sign of the Wilson parameter. When deriving the Dirac operator with respect of e we have to calculate

$$\begin{aligned} \frac{\partial (E_\mu(x))^{e_f}}{\partial e} &= \frac{\partial}{\partial e} e^{-\imath e e_f A_\mu(x)} = (-\imath e_f) A_\mu(x) (E_\mu(x))^{e_f} \\ \frac{\partial^2 (E_\mu(x))^{e_f}}{\partial e^2} &= (-\imath e_f)^2 A_\mu(x) A_\mu(x) (E_\mu(x))^{e_f} . \end{aligned} \tag{2.72}$$

Using the previous equation, we can see that from $\frac{\partial D_f}{\partial e}$ we obtain the field A_μ, and consequently the photon propagator by multiplying two derivatives calculated in two space–time points. That is the first term in eq. (2.69). From $\frac{\partial^2 D_f}{\partial e^2}$ we obtain the product of the field A_μ in the same space–time point, from which it originates the photon propagator in the second term of eq. (2.69). Eqs. (2.70) and (2.71) come from the derivative of D_f with respect to the fermion mass m_f and the critical mass m_f^{cr} respectively. As one can see from the expression of D_f, the m_f–term is proportional to the identity, while the m_f^{cr}–term is proportional to $\imath\gamma_5 r_f$, with $r_f = \pm 1$ Wilson parameter.

The disconnected contributions coming from the reweighting factor can be derived from eq. (2.71) and are

$$\frac{\partial R}{\partial g_s^2} = \frac{6}{(g_s^0)^4} S_{gauge}[U] = \boxed{G_{\mu\nu}G^{\mu\nu}} \ ,$$

$$\frac{1}{2}\frac{\partial^2 r_f}{\partial e^2} = \frac{1}{2}\mathrm{Tr}\left(S_f \frac{\partial^2 D_f}{\partial e^2}\right) - \frac{1}{2}\mathrm{Tr}\left(S_f \frac{\partial D_f}{\partial e} S_f \frac{\partial D_f}{\partial e}\right) + \frac{1}{2}\mathrm{Tr}\left(S_f \frac{\partial D_f}{\partial e}\right)\mathrm{Tr}\left(S_f \frac{\partial D_f}{\partial e}\right)$$

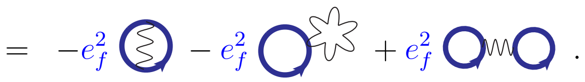

(2.73)

Let see a concrete application of these equations in the calculation of the correction to the $S_f^{\pm}$ quark propagator, that we will use in the next sections to directly calculate isospin breaking corrections. Applying eq. (2.71) and eq. (2.73) we have

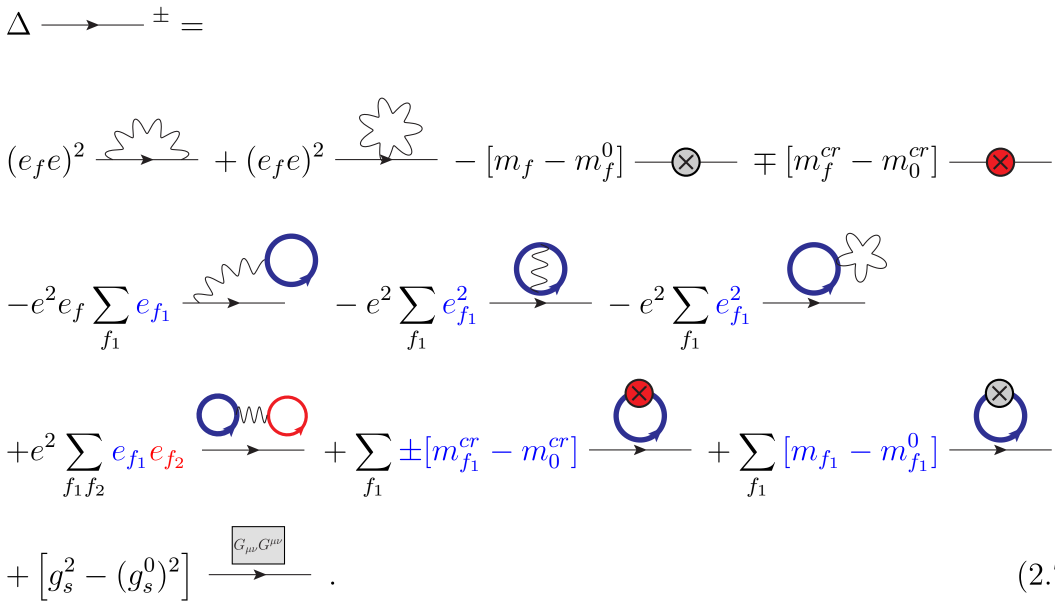

(2.74)

Here quark propagators of different flavours have been drawn with different colors and different lines. We can see that we have the two electromagnetic contributions and the mass insertions of eq. (2.71), and the disconnected contributions containing sea quark loops proportional to e_{f_1} and e_{f_2} of eq. (2.73). Quark disconnected diagrams are noisy and difficult to calculate and for this reason we used the so called electro–quenched approximation, i.e. the limit in which the electric charges of the sea quarks are neglected. We use this approximation in the calculation of the kaon corrections but not in the pion ones because, as we will see, in this case the contributions of the sea quarks cancel out in the difference between the charged and neutral pions. The electro–quenched expansion corresponds to $S_{sea}^{e=0}$ and it is obtained by setting

$$\begin{aligned} g_s &= g_s^0 \\ r_f[U, A, \vec{g}_0] &= 1. \end{aligned} \tag{2.75}$$

In this case eq. (2.74) simply becomes

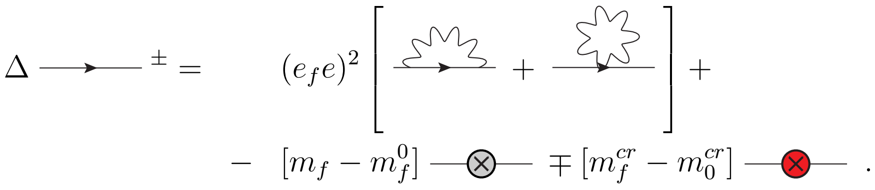

(2.76)

2.5.1 LIB to hadron two–point functions

The meson mass and the decay constants are extracted from the two–point correlation function.

Before calculating the correction to the two–point functions, we need to specify the source operators and the notation adopted for the diagrams that enter the evaluation of the isospin breaking corrections.

In sec. (2.3) we have described the fermonic lattice action and anticipated that, in order to minimize cutoff effects and optimize the numerical signal, we work in a mixed action setup and extract both charged and neutral meson masses from two–point correlators of twisted Wilson quarks having opposite chirally rotated Wilson terms. In other words, we have two types of fermions with opposite values of the Wilson term, i.e.

$$\psi_f^{\pm}(x). \tag{2.77}$$

We then define the scalar and pseudoscalar local operators

$$\begin{aligned} S_{fg}^{\pm\pm}(x) &= \bar{\psi}_f^{\pm}(x)\psi_g^{\pm}(x) \ , \\ P_{fg}^{\pm\pm}(x) &= \bar{\psi}_f^{\pm}(x)\gamma^5\psi_g^{\pm}(x) \ , \end{aligned} \tag{2.78}$$

where f and g indicates the flavour of the quarks and $\pm$ the sign of the Wilson term.

Using these operators we can for example decode the following diagrammatic expression

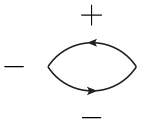

$$= T\langle\, P^{+-}_{12}(x)\; P^{-+}_{21}(0)\,\rangle\;,$$

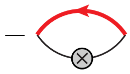

$$= \sum_y T\langle\, P^{+-}_{12}(x)\; S^{--}_{23}(y)\; P^{-+}_{31}(0)\,\rangle\;,$$

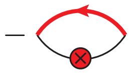

$$= i\sum_y T\langle\, P^{+-}_{12}(x)\; P^{--}_{23}(y)\; P^{-+}_{31}(0)\,\rangle\;. \tag{2.79}$$

where we have always chosen opposite values for the Wilson parameters of quarks in the mesons. Lines of the same color are quarks with the same mass. In terms of quark propagators we have

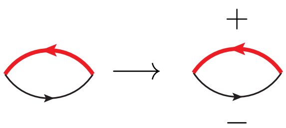

$$= \mathrm{Tr}\left\{\, \gamma^5\; S^{+}_{f_1}[U;\vec{g}^0]\; \gamma^5\; S^{-}_{f_2}[U;\vec{g}^0]\,\right\}\;. \tag{2.80}$$

It useful to define also the electromagnetic vector current and the tadpole insertion in eq. (2.22) by specifying the sign of the Wilson parameters. We have the different combinations

$$
\begin{aligned}
\left[V^{++}_{fg}\right]^{\mu}(x) &= i\left[\bar\psi^{+}_{f}(x)\frac{+i\gamma_5-\gamma_\mu}{2}U_\mu(x)\psi^{+}_{g}(x+\mu)-\bar\psi^{+}_{f}(x+\mu)\frac{+i\gamma_5+\gamma_\mu}{2}U^{\dagger}_{\mu}(x)\psi^{+}_{g}(x)\right]\;,\\
\left[V^{--}_{fg}\right]^{\mu}(x) &= i\left[\bar\psi^{-}_{f}(x)\frac{-i\gamma_5-\gamma_\mu}{2}U_\mu(x)\psi^{-}_{g}(x+\mu)-\bar\psi^{-}_{f}(x+\mu)\frac{-i\gamma_5+\gamma_\mu}{2}U^{\dagger}_{\mu}(x)\psi^{-}_{g}(x)\right]\;,\\
\left[T^{++}_{fg}\right]^{\mu}(x) &= \bar\psi^{+}_{f}(x)\frac{+i\gamma_5-\gamma_\mu}{2}U_\mu(x)\psi^{+}_{g}(x+\mu)+\bar\psi^{+}_{f}(x+\mu)\frac{+i\gamma_5+\gamma_\mu}{2}U^{\dagger}_{\mu}(x)\psi^{+}_{g}(x)\;,\\
\left[T^{--}_{fg}\right]^{\mu}(x) &= \bar\psi^{-}_{f}(x)\frac{-i\gamma_5-\gamma_\mu}{2}U_\mu(x)\psi^{-}_{g}(x+\mu)+\bar\psi^{-}_{f}(x+\mu)\frac{-i\gamma_5+\gamma_\mu}{2}U^{\dagger}_{\mu}(x)\psi^{-}_{g}(x)\;.
\end{aligned}
\tag{2.81}
$$

Using eq. (2.78) and eq. (2.81) we can write down some of the electromagnetic corrections that we are going to use in our calculation. We have some examples of these corrections

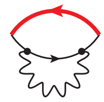

$$- \quad = \quad \sum_{yz} T\langle\, P_{12}^{+-}(x)\, \left[V_{23}^{--}\right]^{\mu}(y)\, \left[V_{34}^{--}\right]^{\nu}(z)\, P_{41}^{-+}(0)\,\rangle\, D_{\mu\nu}(y,z)\ ,$$

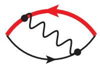

$$- \quad = \quad \sum_{yz} T\langle\, P_{12}^{+-}(x)\, \left[V_{23}^{--}\right]^{\mu}(y)\, P_{34}^{-+}(0)\, \left[V_{41}^{++}\right]^{\nu}(z)\,\rangle\, D_{\mu\nu}(y,z)\ ,$$

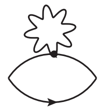

$$- \quad = \quad \frac{1}{2}\sum_{y} T\langle\, P_{12}^{+-}(x)\, P_{23}^{-+}(0)\, \left[T_{31}^{++}\right]^{\mu}(y)\,\rangle\, D_{\mu\mu}(y,y)\ , \tag{2.82}$$

and the other combinations can be easily derived using the same convention. We also show an example of a disconnected diagram

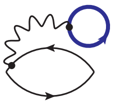

$$= \quad \sum_{yz} T\langle\, P_{12}^{+-}(x)\, P_{23}^{-+}(0)\, \left[V_{31}^{++}\right]^{\mu}(y)\, \left[V_{44}^{\pm\pm}\right]^{\nu}(z)\,\rangle\, D_{\mu\nu}(y,z)\ . \tag{2.83}$$

Having in mind our notation for the Feynman diagrams, we can now look at the corrections to the two–point function and how to obtain the LIB corrections to mass and to decay constant.

Two–point correlation functions of a generic hadron H can be written as a sum of single particle states $|n\rangle$ with the same quantum numbers. Each term is suppressed at large euclidean times as $e^{-M_n t}$ and proportional to the matrix element

$$G_H^n = \langle 0|\mathcal{O}_H|n\rangle\ . \tag{2.84}$$

Consider a generic meson H, and the interpolating operator $\mathcal{O}_H$ with the appropriate quantum numbers, of the form

$$O_H = \bar{\psi}_{f_1}^{+}\Gamma\psi_{f_2}^{-}\ . \tag{2.85}$$

As already said, the resulting correlators have reduced cutoff effects (proportional to $a^2\mu$) and smaller statistical errors with respect to the other possible choices of O_H (see refs. [30, 31]). In the case of the connected fermionic Wick contraction arising in the neutral pion two–point functions we use

$$O_{\pi^0}^{conn} = (\bar{u}^{+}\gamma^5 u^{-} - \bar{d}^{+}\gamma^5 d^{-})/\sqrt{2}. \tag{2.86}$$

The two–point correlation function calculated with the operator $\mathcal{O}_H$ is

$$\begin{aligned} C_{HH}(t) &= \langle\, \mathcal{O}_H(t)\, \mathcal{O}_H^{\dagger}(0)\,\rangle = \sum_n \frac{|G_H^n|^2}{2M_n}\, e^{-M_n t} = \\ &= \frac{|G_H^0|^2}{2M_0}\, e^{-M_0 t}\left(1 + \sum_{n>0} C_n\, e^{-(M_n - M_0)t}\right)\ , \end{aligned} \tag{2.87}$$

with

$$C_n := \frac{M_0}{M_n} \frac{|G_H^n|^2}{|G_H^0|^2}. \tag{2.88}$$

As can be seen in eq. (2.87), the contribution of the excited states is suppressed by $e^{-(M_n - M_0)t}$. Therefore for $t \gg \dfrac{1}{M_n - M_0}$ the correlation function behaves as

$$C_{HH}(t) \xrightarrow[t\to\infty]{} \frac{|G_H^0|^2}{2M_0}\, e^{-M_0 t}. \tag{2.89}$$

From eq. (2.89) it can be seen that we can use two–point correlation functions to obtain the meson mass M_0 and the matrix element G_H^0 needed to evaluate the meson decay constant. In particular we have

$$M_0 = \ln\left[\frac{C_{HH}(t-1)}{C_{HH}(t)}\right]. \tag{2.90}$$

The matrix element G_H^0 we can be obtained from a simultaneous fit of the correlation function using eq. (2.89), which provides both M_0 and G_H^0.

On the lattice with a finite temporal extension, the correlation function in the large time limit has the form

$$C_H(t) \xrightarrow[t\to\infty]{} \frac{|G_H^0|^2}{2M_0} (e^{-M_0 t} + \eta\, e^{-M_0(T-t)}), \tag{2.91}$$

where η is the eigenvalue of the time reversal transformation of the product of the two operators. For $\eta = +1$ eq. (2.89) becomes

$$C_{HH}(t) = \frac{|G_H^0|^2}{M_0}\, e^{-M_0 \frac{T}{2}} \cosh\left[\left(t - \frac{T}{2}\right) M_0\right]. \tag{2.92}$$

In order to evaluate the isospin breaking corrections for the meson mass and decay constant we need the expression of ΔC defined as

$$\begin{aligned} C_{HH}(t;\vec{g}) &= C_{HH}(t;\vec{g}_0) + \Delta C_{HH}(t) = \\ &= C_{HH}(t;\vec{g}_0) \cdot \left[1 + \frac{\Delta C_{HH}(t)}{C_{HH}(t;\vec{g}_0)}\right], \end{aligned} \tag{2.93}$$

where we have used for the action parameters the compact notation of eq. (2.58) and eq. (2.59). Denoting $C_{HH}(t;\vec{g}_0) \equiv C_{HH}^0$, we can evaluate the LIB correction to the correlator, obtaining

$$\frac{\Delta C_{HH}}{C_{HH}^0}(t) = 2\cdot \delta G_H^0 - \Delta M_0 \left\{ \left(\frac{T}{2} + \frac{1}{M_0}\right) - \left(\frac{T}{2} - t\right) \cdot \tanh\left[M_0 \left(\frac{T}{2} - t\right)\right]\right\}, \tag{2.94}$$

where

$$\delta G_H^0 \equiv \frac{\Delta G_H^0}{G_H^0}. \tag{2.95}$$

In the following we will indicate with the compact notation

$$\partial_t \frac{\Delta C_{HH}}{C^0_{HH}} = M_0 \tag{2.96}$$

the evaluation of the mass M_0 through the fit of the two–point correlation function using eq. (2.94).

2.5.2 LIB corrections to the pion mass

In this section we calculate the LIB corrections to the pion mass using the same strategy employed to obtain the corrections to the quark propagator.

Consider the case of charged pions. We can start from the correlator

$$C_{\pi^+\pi^-}(t;\vec{g}) = \langle\ [\bar{u}^+\gamma^5 d^-](t,\vec{p}=0)\ [\bar{d}^-\gamma^5 u^+](0)\ \rangle^{\vec{g}}\ , \tag{2.97}$$

and apply the Δ operator defined in eq. (2.61). We have

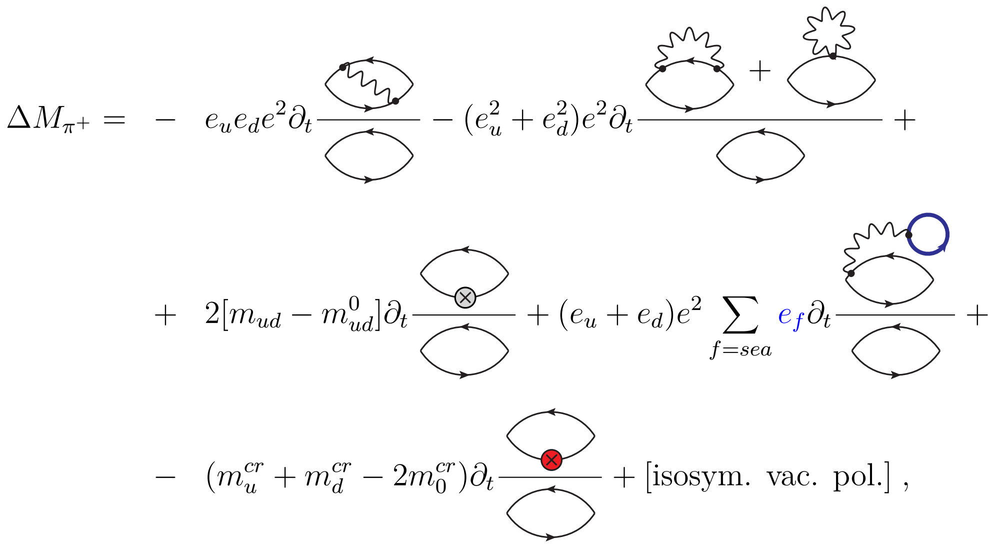

(2.98)

where $m_{ud} = (m_d + m_u)/2$ is the bare isosymmetric light quark mass and when ∂_t is defined in eq. (2.96).

In the case of the neutral pion we have

$$\Delta M_{\pi^0} = - \frac{e_u^2 + e_d^2}{2} e^2 \partial_t$$

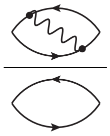

$$- (e_u^2 + e_d^2) e^2 \partial_t$$

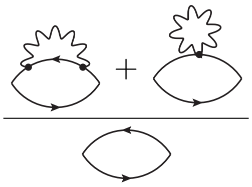

$$+ \quad 2[m_{ud} - m_{ud}^0] \partial_t$$

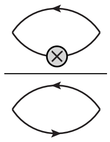

$$+ (e_u + e_d) e^2 \sum_{f=sea} e_f \partial_t$$

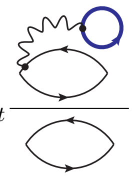

$$+ \quad - \quad (m_u^{cr} + m_d^{cr} - 2m_0^{cr}) \partial_t$$

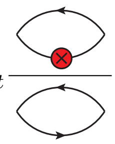

$$+ \frac{(e_u - e_d)^2}{2} e^2 \partial_t$$

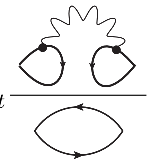

$$+ \quad [\text{isosym. vac. pol.}] \ . \tag{2.99}$$

The contributions coming from the sea quarks have been drawn in blue and with different line and we have not explicitly written down the vacuum polarization contributions of eq. (2.73), but they are the same for the charged and neutral pions. By taking the difference between eq. (2.98) and eq. (2.99) we obtain

$$M_{\pi^+} - M_{\pi^0} = \frac{(e_u - e_d)^2}{2} e^2 \partial_t$$

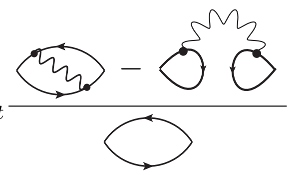

$$. \tag{2.100}$$

All the isosymmetric vacuum polarization diagrams cancel in the difference, together with the disconnected sea quark loop contributions. Note in particular the cancellation of the corrections proportional to $m_{ud} - m_{ud}^0$ and to the variation of the strong coupling. This is a general feature: at first order of the perturbative expansion in α_{em} and $m_{ud} - m_{ud}^0$, the isosymmetric corrections coming from the variation of the strong gauge coupling (the lattice spacing), of m_{ud} and of the heavier quark masses do not contribute to observables that vanish in the isosymmetric theory, like the mass splitting $M_{\pi^+} - M_{\pi^0}$. Furthermore, α_{em} at this order doesn't need to be renormalized. For these reasons, the pion mass splitting is a theoretical clean observable.

The calculation of the disconnected diagram in eq. (2.99) is computationally expensive and it has been postponed to a future calculation. On the other hand this diagram is of order $\mathcal{O}(\alpha_{em} m_{ud})$ so it is numerically comparable with higher order corrections that we have not included in the expansion. From the phenomenological point of view we are introducing a systematical error comparable with higher order corrections.

In sec. (3.2) we will show our result for the mass difference in eq. (2.100) neglecting the disconnected diagram contribution.

2.5.3 Critical mass

In this section we discuss the evaluation IB corrections to the critical mass, that are needed in order to evaluate the kaon mass difference. As mentioned before, we calculate these corrections by imposing the WTI in eq. (2.56). By applying Δ in eq. (2.61) to eq. (2.56), which can be written as

$$W_f(\vec{g}) = -\nabla_0$$

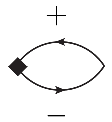

$$=$$

$$= -\nabla_0 \ \mathrm{Tr}\Big\{ \gamma^0 \ S_f^+[U, A; \vec{g}; t, \vec{p} = 0] \ \gamma^5 \ S_f^-[U, A; \vec{g}; -t, \vec{p} = 0] \Big\} = 0 \ , \quad (2.101)$$

one obtains the following expression for Δm_f^{cr}

$$\Delta W_f = 0 \quad \longrightarrow \quad \Delta m_f^{cr} = -\frac{e_f^2}{2} e^2$$

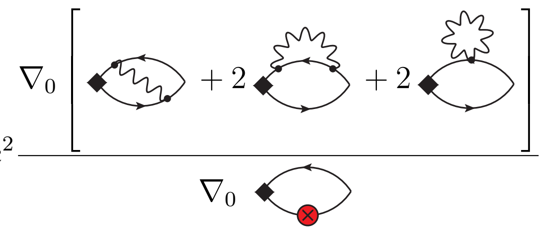

$$. \quad (2.102)$$

A great advantage of eq. (2.102) is that it holds at finite quark masses and does not require therefore any chiral extrapolation.

In sec. (3.3) we will show numerical results for the corrections to critical mass using this strategy.

2.5.4 LIB correction to the kaon mass

By repeating the analysis performed for the pions to the kaon two–point functions, one obtains for the charged kaon K^+

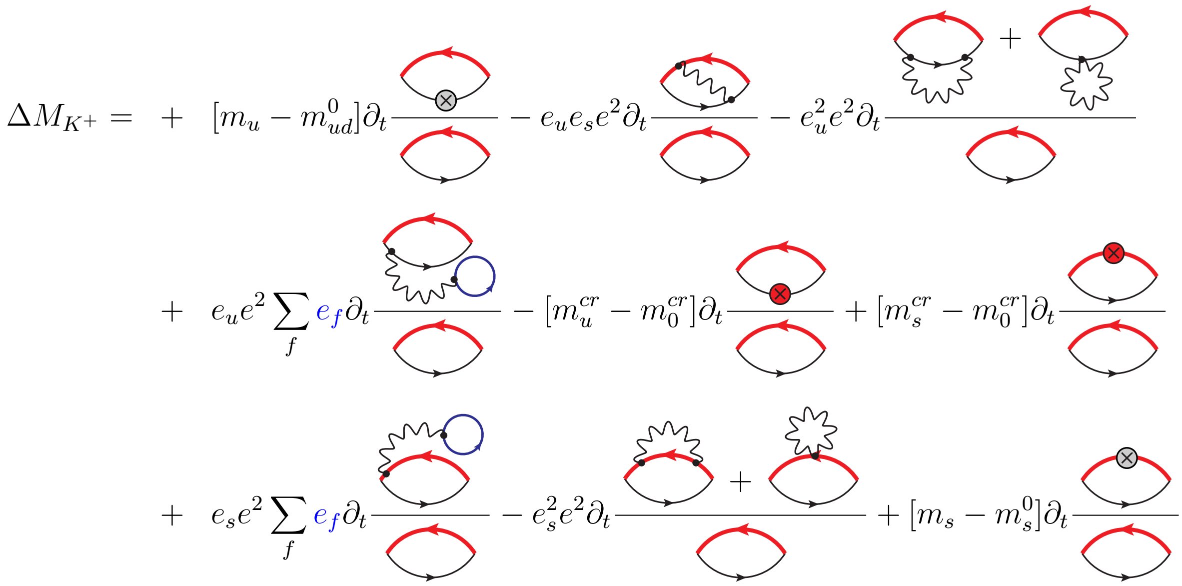

$$+ \quad [\text{isosymmetric vac. pol.}] \,, \tag{2.103}$$

and for the neutral K^0

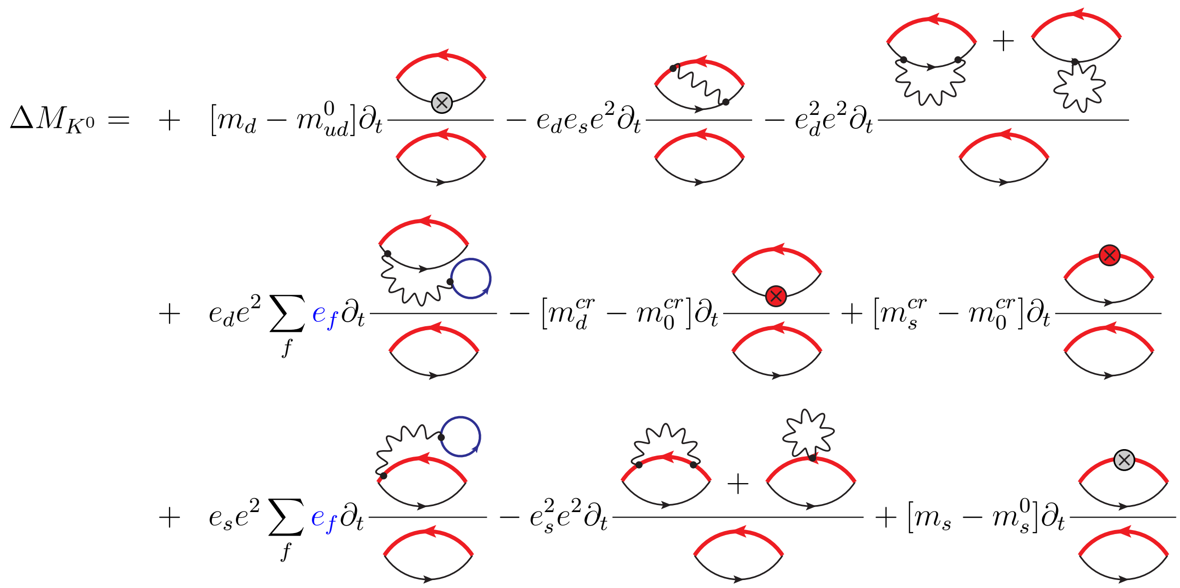

$$+ \quad [\text{isosymmetric vac. pol.}] \,. \tag{2.104}$$

In the previous expressions the strange quark propagator has been drawn in red. By taking the difference of eq. (2.103) and eq. (2.104) one finds

$M_{K^+} - M_{K^0} \;=\; (e_u^2 - e_d^2)e^2\partial_t$ 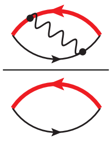 $-\,(e_u^2 - e_d^2)e^2\partial_t$ 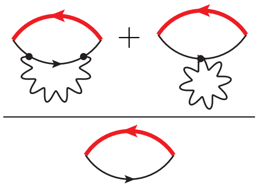

$-\;\; 2\Delta m_{ud}\partial_t$ 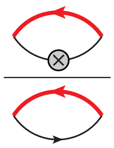 $-\,(\Delta m_u^{cr} - \Delta m_d^{cr})\partial_t$ 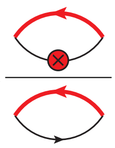

$+\;\; (e_u - e_d)e^2 \sum_f e_f \partial_t$ 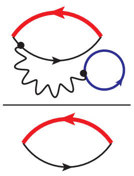 ,

(2.105)

where Δm_{ud} is defined in eq. (2.4), $\Delta m_f^{cr} = m_f^{cr} - m_0^{cr}$ and we used the relation $e_s = -(e_u + e_d)$.

In this case the sea quark disconnected contribution does not cancel out. Being the calculation of the quark loop diagram computationally expensive, we used for our numerical result the electro–quenced approximation.

From the experimental point of view the kaon mass splitting, in sec. (3.3) we have determined the up and down mass difference.

2.5.5 Kaon decay constant

In this section we will show how to evaluate isospin breaking correction due to the up–down mass difference to the kaon decay constant.

Consider a leptonic decay of a pseudoscalar meson $M \to \ell\nu$, than the decay constant is defined by the following relation

$$\langle 0|\, \bar{q}_1 \gamma^\mu \gamma^5 q_2 \,|M(p)\rangle = \imath p^\mu f_M, \tag{2.106}$$

where the axial current is calculated between the constituent quark q_1 and q_2 of the meson M. Consider the twisted mass Ward identity of a renormalized operator $\hat{\mathcal{O}}$ [36] at maximal twist

$$\langle \partial_\mu \hat{A}^\mu_{fg}(x)\hat{\mathcal{O}}(y)\rangle = (\hat{m}_f + \hat{m}_g)\langle \hat{P}_{fg}(x)\hat{\mathcal{O}}(y)\rangle + \mathrm{O}(a), \tag{2.107}$$

with P_{fg} and A_{fg} the renormalized pseudo–scalar and axial density respectively for quarks of flavours f and g and renormalized masses $\hat{m_f}$ and $\hat{m_g}$. The second member in eq. (2.107) is renormalization group invariant because the pseudo–scalar density renormalized with the RC Z_P, while the quark mass with $1/Z_P$. We can then use eq. (2.107) without further renormalization, obtaining for the decay constant the relation

$$f_K = (m_s + m_{ud})\,\frac{G_K}{M_K^2}, \tag{2.108}$$

where $G_K = \langle 0|\,\bar{s}\gamma_5 l(0)\,|K\rangle$.

The variation of f_K is

$$\delta f_K \equiv \frac{f_K^0 - f_K +}{2 f_K} = \delta G_K - 2\delta M_K + \frac{\Delta m_{ud}}{m_s + m_{ud}}, \tag{2.109}$$

with

$$\delta M_K = \frac{\Delta M_K}{M_K}, \qquad \delta G_K = \frac{\Delta G_K}{G_K}. \tag{2.110}$$

δG_K and δM_K can be calculated from two–point correlation function by performing a fit using eq. (2.94).

The quantity δf_K is of particular interest, because it provides the isospin breaking correction due to the up–down mass difference to the ratio K_{ℓ_2}/Π_{ℓ_2} decay rate, for which we will present results in sec. (3.4).

In our calculation we included only IB effects due to the up–down mass difference. In the presence of electromagnetism it is not possible to give a physical definition of the decay constant, because of the contributions from diagrams in which the photon is emitted by the meson and absorbed by the charged lepton. Thus the physical width is not just given in terms of the matrix element of the axial current and can only be obtained by a full calculation of the electromagnetic corrections at a given order. In order to cancel the infrared divergences and obtain results for physical quantities, radiative corrections from virtual and real photons must be combined. In ref. [38] the authors propose a strategy to include electromagnetic effects in processes for which infrared divergences are present but which cancel in the standard way between diagrams containing different numbers of real and virtual photons.

2.6 QED finite volume effects (FVE)

The long-range nature of the electromagnetic interaction, i.e. the vanishing mass of the photon, induces finite-volume effects (FVE) which only fall off like inverse powers of the linear extent of the lattice. These are far more severe than the QCD finite-volume effects for stable particles, which are exponentially suppressed, and require to be accurately corrected. Furthermore the FVE depend on the specific prescription used to subtract the zero mode of the photon.

For the evaluation of the FVE we will follow the strategy described in ref. [13]. Let us consider the spacetime of the four–torus $\mathbb{T}^4$ and the case where only the four-momentum zero-mode of the photon field is eliminated, i.e. $A^\mu(0) \equiv 0$ that is how we defined the photon propagator in sec. (2.2), which we denote as QED_{TL}.

Power–like FVE arise from the exchange of a photon around the torus, and they are obtained by comparing results obtained in finite volume (FV) with those of infinite volume (IV) QED.

The FV correction to the mass m of a point particle of spin 0 and of charge q in units of e on a torus is given by the difference of the FV self energy, $\Sigma_0(p, T, L)$, and its IV counterpart, $\Sigma_0(p)$, on shell:

$$\begin{aligned} \Delta m_0^2(T,L) \equiv m_0^2(T,L) - m^2 &= (qe)^2 \Delta\Sigma_0(p = im, T, L) \\ &\equiv (qe)^2 \left[\Sigma_0(p = im, T, L) - \Sigma_0(p = im)\right] , \end{aligned} \tag{2.111}$$

where $p = im$ is a shorthand for $p = (im, \vec{0})$. Notice that this difference is infrared and UV finite. On shell the IV integral is IR finite and in finite volume the sums are IR finite because the FV formulations of QED that we consider are regulated by the spacetime volume. Moreover, for large k^2, the difference of the FV sums and IV integrals is UV finite.

Being interested in the expansion at $\mathcal{O}(\alpha_{em})$, we can calculate eq. (2.111) at one loop. At this order, the self–energy difference can be written as

$$\Delta\Sigma(p, T, L) = \left[{\sum\!\!\!\!\!\!\!\!\int_k}' - \int \frac{d^4k}{(2\pi)^4} \right] \sigma_0(k, p) \ , \tag{2.112}$$

where k is the momentum of the photon in the loop and ${\sum\!\!\!\!\!\!\!\int}'_k$ is defined as

$${\sum\!\!\!\!\!\!\!\!\int_k}' \equiv \frac{1}{TL^3} \sum_{k_\mu \in BZTL^{4*}} \ . \tag{2.113}$$

The integrand $\sigma_0(k, p)$ of the self energy is

$$\sigma_0(k,p) = 4\sigma_T(k) - \sigma_{S_0}(k,p) - 4p^2\sigma_{S_1}(k,p) - 4p_\mu, \sigma_{S_2,\mu}(k,p) \tag{2.114}$$

with

$$\begin{aligned} \sigma_T(k) &= \tfrac{1}{k^2} \ , & \sigma_{S_0}(k,p) &= \tfrac{1}{[(p+k)^2+m^2]} \ , \\ \sigma_{S_1}(k,p) &= \tfrac{1}{k^2[(p+k)^2+m^2]} \ , & \sigma_{S_2,\mu}(k,p) &= \tfrac{k_\mu}{k^2[(p+k)^2+m^2]} \ . \end{aligned} \tag{2.115}$$

Using eq. (2.111), eq. (2.112) and eq. (2.113) it is found that the FV corrections to a boson of spin 0 in terms of the infinite-volume mass m are given by [13]

$$m_0^2(T,L) \sim_{T,L\to+\infty} m^2 \left\{1 - q^2\alpha\left[\frac{k}{mL}\left(1+\frac{2}{mL}\left[1-\frac{\pi}{2k}\frac{T}{L}\right]\right)\right]\right\}. \tag{2.116}$$

At this order the result is valid for both point–like and composite particles.

An other important observation is that the coefficient of the leading $1/L$ and $1/L^2$ corrections to the mass m of a particle of charge qe is the same for spin-1/2 fermions and spin-0 bosons at $\mathcal{O}(\alpha_{em})$, i.e. these coefficients are always the same, independent of the spin and the point–like or composite nature of the particle: they are fixed by QED Ward-Takahashi identities.

Chapter 3

Analysis and results

In this chapter we are going to illustrate the analyses performed as described in Chapter (2) for different physical quantities.

We are first going to describe the lattice set up used in the calculation and some details about the estimates of the systematic errors.

We will then show results for the pions mass difference $M_{\pi^+} - M_{\pi^0}$ that in the expansion at first order in Δm_{ud} and α_{em} is a pure QED effect.

We will apply the method in the kaon sector and, using as experimental input the mass difference $M_{K^+} - M_{K^0}$, we will calculate $m_d - m_u$, an important physical quantity that can be used to predict isospin breaking effects for other observables, such as the neutron–proton mass splitting.

Finally we will show results for the QCD isospin breaking effects on the ratio of the K_{ℓ_2} and Π_{ℓ_2} decay rates, computed from the isospin breaking effects on the kaon decay constant.

3.1 Simulation details and analysis overlook

We used data obtained from numerical simulations with $N_f = 2+1+1$ sea quarks performed by *European Twisted Mass Collaboration* (ETMC). In table (3.1) we present the details of the lattice setup. Further details can be found in [39].

We performed the numerical simulations at three different lattice spacing in order to eventually perform the continuum limit. We fixed the lattice spacing through the coupling β, fixed at the values

$$\beta = \{1.90, 1.95, 2.10\}, \tag{3.1}$$

that correspond to lattice spacings

$$a = \{0.0885(36), 0.0815(30), 0.0619(18)\}\ fm. \tag{3.2}$$

β	$a\ (fm)$	$V^3 \times T$	$Z_{P,M1}(2\ GeV)$	$Z_{P,M2}(2\ GeV)$	$a\mu_{sea}$	$M_\pi\ (MeV)$	$M_\pi L$	N_g
1.90	0.0885(36)	$32^3 \times 64$	0.529(7)	0.574(4)	0.0030	245	3.53	150
					0.0040	282	4.06	90
					0.0050	314	4.53	150
1.90	0.0885(36)	$24^3 \times 48$	0.529(7)	0.574(4)	0.0040	282	3.05	150
					0.0060	344	3.71	150
					0.0080	396	4.27	150
					0.0100	443	4.78	150
1.95	0.0815(30)	$32^3 \times 64$	0.509(4)	0.546(2)	0.0025	239	3.16	150
					0.0035	281	3.72	150
					0.0055	350	4.64	150
					0.0075	408	5.41	75
1.95	0.0815(30)	$24^3 \times 48$	0.509(4)	0.546(2)	0.0085	435	4.32	150
2.10	0.0619(18)	$48^3 \times 96$	0.516(2)	0.545(2)	0.0015	211	3.19	90
					0.0020	243	3.66	90
					0.0030	296	4.46	90

Table 3.1: Details of lattice setup used in the $N_f = 2+1+1$ numerical simulations. We present the values of β and the lattice spacing a, the lattice extension $V^3 \times T$ in lattice unit, the RC Z_P in the $\overline{MS}$ scheme at $\mu = 2$ GeV for the two sets of results M1 and M2, the values of the sea quark mass $a\mu_{sea}$, the corresponding values of M_π and $M_\pi L$ and the number of gauge configurations N_g used.

Simulations are also performed at different volumes to study finite size effects. In particular for $\beta = 1.90$ we have data at the same sea quark mass $a\mu_l = 0.0040$ but at different volumes, which allow us to better investigate volume effects.

In our numerical simulations pions are heavier than the physical one, because simulations at the physical point, i.e. to the physical value of the pion mass, are computationally expensive. This means that in order to evaluate physical results we need to perform an extrapolation to the physical point. In tab. (3.1) are shown the pion masses M_π used in the simulation, with range from 211 MeV up to 443 MeV.

Furthermore, working on the lattice, we also need to perform an extrapolation to the continuum limit, where the lattice spacing $a \to 0$. In our numerical simulations we used Wilson twisted mass action at maximal twist that provides an automatic $\mathcal{O}(a)$ improvement of physical quantities calculated on the lattice. For this reason, when performing the continuum limit, we include in our fit function a term proportional to a^2 of the form

$$A \cdot a^2. \tag{3.3}$$

For the fermionic lattice action we worked in a mixed action approach, i.e. we used different actions for sea and valence quarks

$$S = S_{sea} + S_{val}, \tag{3.4}$$

where S_{sea} is the action for the sea quarks and S_{val} is the action for the valence quarks. In particular for the sea quark action we used Wilson twisted mass action at maximal twist, while for the valence quarks we used the Osterwalder–Seiler action, that is a Wilson twisted mass action with a Wilson parameter r_f for every quark of flavour f. For the gauge field we used the Iwasaki action [18]. Further details about the actions can be found in sec. (2.3) and sec. (1.2.2).

In tab. (3.1) the number of gauge configurations N_g generated in the numerical simulations are also given. Following the method described in app. (A) we divided the configurations in 15 jacknives with which we generated bootstrap samples of 100 elements. The associated uncertainties were calculated using eq. (g).

The analysis has been performed using two sets of renormalization constants Z_P, namely M1 and M2. The first method (M1) aims at removing $\mathcal{O}(a^2p^2)$ effects, while in the second method (M2) the renormalization constants are taken at a fixed reference value of $p^2 = \mu^2$. The use of the two sets of renormalization constants is expected to lead to the same final results once the continuum limit for the physical quantity of interest is performed.

For the input parameters, such as the isospin-symmetric m_{ud} mass, the lattice spacings, the chiral constants f_0 and b_0, we used 8 different sets of values determined in ref. [39] using the same sets of gauge configurations used for this work. Those samples are calculated using different strategies of analysis in order to have under control systematic errors from various sources.

In our study we estimated the systematic uncertainty associated with the chiral extrapolation by studying the dependence on the light quark mass m_l using two types of fit ansatze based on Chiral Perturbation Theory (ChPT) or on polynomial expressions. ChPT at NLO is expected to be more accurate in the region of small m_l, but to suffer from possible higher order corrections at larger values where the polynomial expansion is expected to be more accurate. For the discretization effects we tried two different procedures in the extrapolation to the continuum limit adopting two different choices for the scaling variables: the Sommer parameter r_0 in lattice units and the mass $aM_{s's'}$ of a fictitious pseudoscalar meson made of two stange-like valence quarks, trying to exploit cancellation of discretization effects in ratios like $M_K/M_{s's'}$ [39].

The different analyses are labeled by a letter from A to D (as in ref. [39]) which indicates the different methods used for the determination of the input parameters, see table (3.2), and a number (1 or 2) indicating the Z_P set used (M1 or M2).

The final result for an observable x is calculated assigning the same weight to results from the different sets, each one characterized by a central value x_i and a standard deviation σ_i. Therefore, central value and error of the observable x are obtained respectively from the mean value of the $N = 8$ sets,

$$\bar{x} = \frac{1}{N}\sum_{i=1}^{N} x_i, \tag{3.5}$$

	A	B	C	D
Chiral extrap.	ChPT	Polynomial	ChPT	Polynomial
Scaling variable	r_0/a	r_0/a	$aM_{s's'}$	$aM_{s's'}$

Table 3.2: Details of the samples used for the input parameters in the analysis, as labeled in ref. [39]. Each set of input parameters, from A to D, has been calculated in [39] using different chiral extrapolations and scaling variables as indicated.

and the expression

$$\sigma^2 = \frac{1}{N}\sum_{i=1}^{N}\sigma_i^2 + \frac{1}{N}\sum_{i=1}^{N}(x_i - \bar{x})^2, \tag{3.6}$$

where σ_i is calculated as in eq. (g). The second term in eq. (3.6), which represents the spread among the mean value of the observable x and the central values of the different samples, is thus the systematic error which accounts for the uncertainties due to the chiral extrapolation, the cutoff effects and the renormalization constants Z_P.

The input parameters taken from ref. [39] and used in the analysis are

$$f_0 = 121.1(4)\ \text{MeV}, \quad b_0 = 2571(97)\ \text{MeV}, \quad m_{ud} = 3.70(17)\ \text{MeV}. \tag{3.7}$$

3.2 $M_{\pi^+} - M_{\pi^0}$

Using the strategy described in sec. (2.4) and using results in sec. (2.5.2), we are going to calculate the mass difference between π^0 and π^+. This difference at first order in the expansion in Δm_{ud} and α_{em} is a pure QED isospin breaking effect. Indeed, being the pions symmetric with respect to the $u \leftrightarrow d$ exchange, the leading QCD correction is quadratic in Δm_{ud}. By taking the difference of the diagrammatic expansion in Δm_{ud} and α_{em} between the charged and the neutral pions, the only terms that survive are those in eq. (2.100). As already pointed out, the calculation of the disconnected diagram in eq. (2.100) is computationally expensive and it has been postponed to a future calculation. On the other hand, from the phenomenological point of view we are introducing a systematical error comparable with higher order corrections.

Neglecting the disconnected diagram and considering the difference $M^2_{\pi^+} - M^2_{\pi^0}$ we have

$$M^2_{\pi^+} - M^2_{\pi^0} = (e_u - e_d)^2 e^2 M_\pi\ \partial_t R_\pi^{exch}(t), \tag{3.8}$$

where M_π is the isosymmetric pion mass and

$$R_\pi^{exch}(t) =$$ 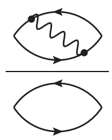 . (3.9)

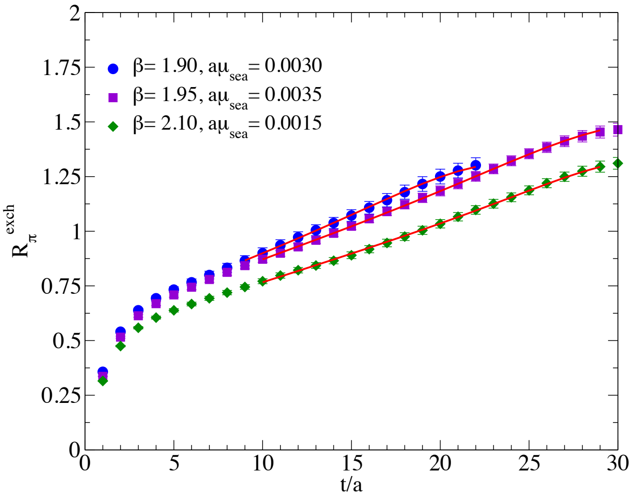

Figure 3.1: R_π^{exch} defined in eq. (3.9) for different values of β and sea quark masses as a function of t/a. We performed a fit according to eq. (2.94) in order to extract the pion mass splitting ΔM.

Using eq. (2.94) we calculated $\partial_t R_\pi^{exch}(t)$, i.e. we extracted the value of ΔM. The fit result is shown in fig. (3.1). Then, using eq. (3.8) we calculated $M^2_{\pi^+} - M^2_{\pi^0}$, obtaining the result shown in fig. (3.2(a)).

Our pions are heavier than the physical ones and our lattice data need to be extrapolated to the chiral limit. Furthermore, QED is a long range interaction and we have to cope with the associated power-law finite volume effects.
We first subtracted QED volume effects using eq. (2.116). As can be seen in fig. (3.2(b)) these corrections are large, of the order of $\sim 30\%$ for the smallest volumes $24^3 \times 48$.
We performed the chiral and continuum limit directly to the finite volume corrected data. In the chiral extrapolation we used partially quenched chiral perturbation theory including electromagnetism [40][41] at $\mathcal{O}(\alpha_{em})$ that takes into account the effects of including electromagnetic loop corrections in the theory and how the chiral logs are effected by including the electromagnetic charges of the sea quarks. In the calculation QED is defined on a finite volume by considering the same infrared regularization used in our analysis, i.e. the removal of the zero modes of the electromagnetic field. We considered the correction to the meson's mass square because this is a finite quantity in the chiral limit. Consider a meson composed by i and j valence quarks with charges q_i and q_j respectively, then [41]

$$M^2_{ij} = \chi_{ij} + \frac{4Ce^2}{f_0^2} q^2_{ij} + \Delta M^2 ij(\infty) + \Delta M^2_{ij}(L), \tag{3.10}$$

where $\chi_{ij} = b_0(m_i + m_j)$, $q_{ij} = q_i - q_j$, b_0 and f_0 are the QCD LECs at LO, C is the

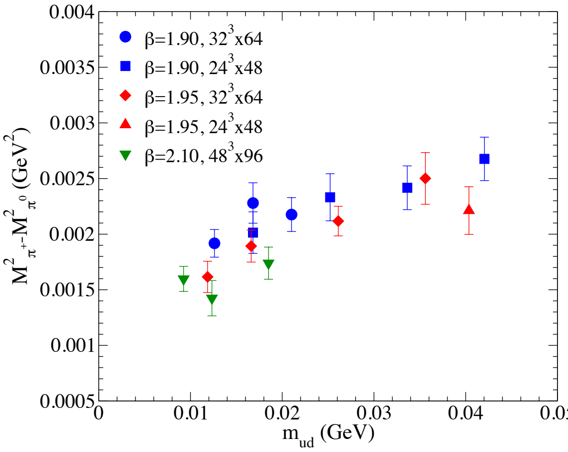

(a)

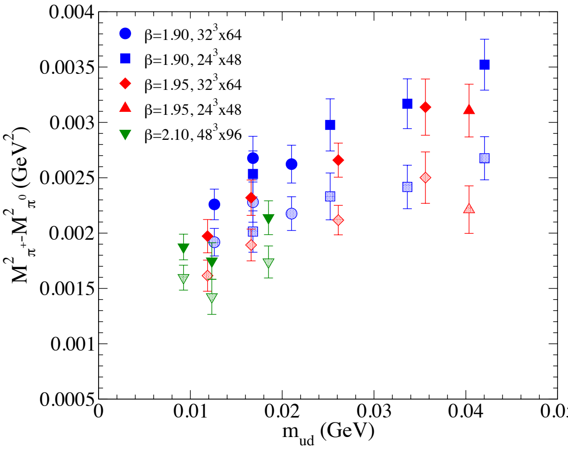

(b)

Figure 3.2: Lattice results for the mass splitting $M^2_{\pi^+} - M^2_{\pi^0}$ calculated using eq. (3.8). We show in different colours data corresponding to different values of β as a function of the isosymmetric light quark mass m_{ud}. In the panel (b) we also show the data after the subtraction of QED finite volume effects (FVE) using eq. (2.116).

EM LEC at LO and

$$\Delta M^2_{ij}(\infty) = [\Delta M^2_{ij}]_{logs} + e^2 K(\mu) q^2_{ij}\chi_{ij}, \qquad \text{with}$$

$$\begin{aligned}\left[\Delta M^2_{ij}\right]_{logs} &= -\tfrac{3e^2}{16\pi^2} q^2_{ij}\ \chi_{ij}\log\left(\tfrac{\chi_{ij}}{\mu^2}\right) + \\ &-\tfrac{8e^2 C}{16\pi^2 f_0^4} q_{ij}\cdot \textstyle\sum_{n=1}^{N_f}\left[(q_i - q_n^{sea})\chi_{in}\log\left(\tfrac{\chi_{in}}{\mu^2}\right) + (q_n^{sea} - q_j)\chi_{nj}\log\left(\tfrac{\chi_{nj}}{\mu^2}\right)\right].\end{aligned} \tag{3.11}$$

In the previous expression N_f is the number of quark flavours considered in the calculation, $\Delta M^2_{ij}(L)$ represents the finite size scaling correction of eq. (2.116), while $\Delta M^2_{ij}(\infty)$ contains the chiral logs. We can notice that the EM effects at leading order in α_{em} generate chiral logs and volume corrections proportional to $q_i - q_j$ and therefore they vanish in the case of neutral mesons.

Applying eq. (3.10) and eq. (3.11) to the pion FVE corrected mass difference we find

$$\begin{aligned}M^2_{\pi^+} - M^2_{\pi^0} = 16\pi\alpha_{em} f_0^2\cdot C\left[1 - \left(4 + \frac{3}{4C}\right)\cdot\xi\log\xi + \frac{K}{4C}\cdot\xi\right] + \\ + \hat{A}\cdot a^2.\end{aligned} \tag{3.12}$$

where we added the a^2 term and where we used $\xi = \chi_{ij}/\mu^2$. We performed the fit for all the sets using the fit function in eq. (3.12). Fit result is shown in fig. (3.3(a)). The discretization effects are of order $\sim 40\%$ comparing the continuum limit with the smallest lattice spacing.

In order to keep discretization effects better under control we determined $M^2_{\pi^+} - M^2_{\pi^0}$ dividing by $\left(\frac{M_\pi^2}{2\cdot b_0 \cdot m_l}\right)^\gamma$. We chose this quantity, rather than simply M_π^2, because it is finite in the chiral limit.

We considered different values of γ, namely

$$\gamma = \{1, 1.5, 2\}. \tag{3.13}$$

The QED finite volume effects are not modified, while the $SU(2)$ chiral expansions for this quantity reads

$$\begin{aligned} \frac{M^2_{\pi^+} - M^2_{\pi^0}}{\left(\frac{M_\pi^2}{2b_0 m_l}\right)^\gamma} = 16\pi\alpha_{em} f_0^2 \cdot C\left\{1 - \left[(4+\gamma) + \frac{3}{4C}\right]\cdot \xi \log \xi + \frac{K}{4C}\cdot \xi\right\} + \\ + \hat{A}_\gamma \cdot a^2. \end{aligned} \tag{3.14}$$

In fig. (3.3) we present the fit results for the various values of γ. We observe a large cancellation of discretization effects and the amount of these effects, that we evaluated comparing the continuum result with the one for the smallest lattice spacing, are

$$\begin{aligned} \gamma &= 0 \quad \sim 40\% \\ \gamma &= 1 \quad \sim 13\% \\ \gamma &= 1.5 \ \sim 4\% \\ \gamma &= 2 \quad \sim 3\%. \end{aligned}$$

This also can be seen by comparing the values of coefficients $\hat{A}_\gamma$ of eq. (3.14) of the term proportional to a^2. For the analysis A_1, the coefficients are:

$$\begin{aligned} \gamma = 0: &\quad \hat{A}_\gamma = 0.00377(130)\ \text{GeV}^4 \\ \gamma = 1: &\quad \hat{A}_\gamma = 0.00142(80)\ \text{GeV}^4 \\ \gamma = 1.5: &\quad \hat{A}_\gamma = 0.00045(72)\ \text{GeV}^4 \\ \gamma = 2: &\quad \hat{A}_\gamma = -0.00039(74)\ \text{GeV}^4. \end{aligned}$$

For example, the parameter $\hat{A}_\gamma$ in the case $\gamma = 1$ is three times smaller than the one with $\gamma = 0$ while for $\gamma = 1.5$ it is eight times smaller. The uncertainty is calculated using eq.(3.6) and corresponds to the statistical+fitting error and the systematic uncertainties on the determinations of the renormalization constants, the lattice spacing and the parameters in eq. (3.7).

To calculate the final result for $M^2_{\pi^+} - M^2_{\pi^0}$ we used the experimental value $M_{\pi_0} =$ 135 MeV, approximating $M_{\pi^+} + M_{\pi^0}$ at the tree level value, and the values for b_0 and m_{ud} given in eq. (3.7). In tab. (3.3) we present the results for $M^2_{\pi^+} - M^2_{\pi^0}$ for different

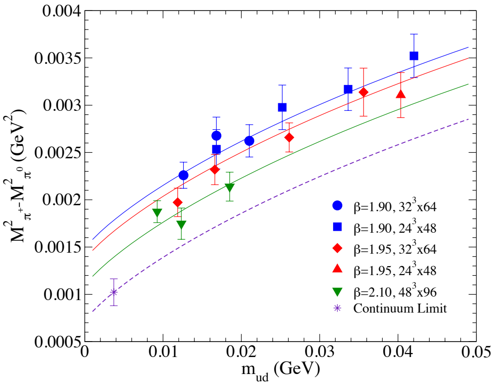

(a) $\gamma = 0$

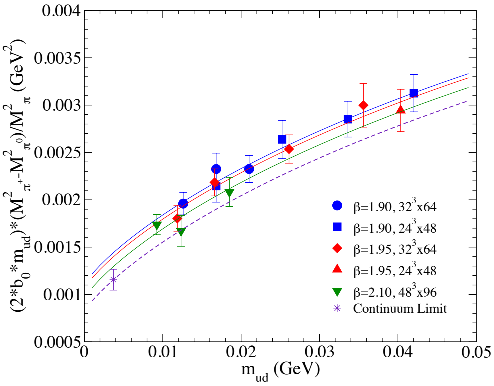

(b) $\gamma = 1$

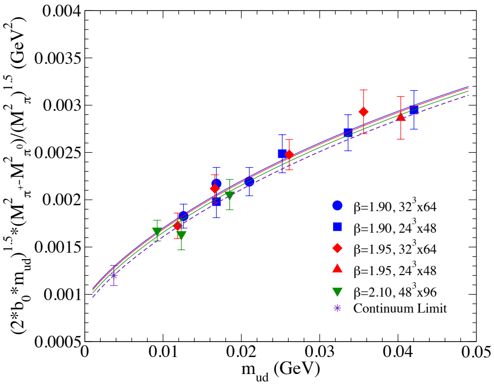

(c) $\gamma = 1.5$

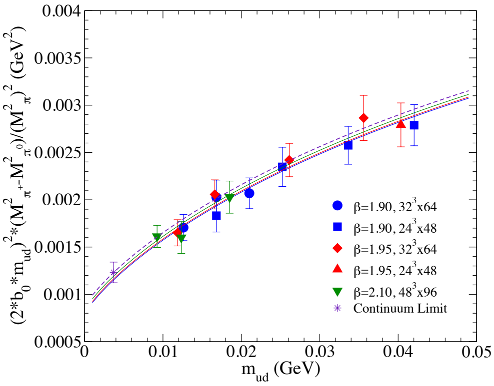

(d) $\gamma = 2$

Figure 3.3: Fit result for the values of γ in eq. (3.13). The dashed violet line is the continuum limit. General fit function is reported in eq. (3.14), but for the case $\gamma = 0$ it is equivalent of eq. (3.12). It can be seen that discretization effects are strongly reduced using a proper value for γ.

values of γ and for all the analyses. From these values we also obtain the following results for $M_{\pi^+} - M_{\pi^0}$:

$$(M_{\pi^+} - M_{\pi^0})|_{\gamma=0} = 3.82(51) \text{ MeV}$$
$$(M_{\pi^+} - M_{\pi^0})|_{\gamma=1} = 4.18(40) \text{ MeV}$$
$$(M_{\pi^+} - M_{\pi^0})|_{\gamma=1.5} = 4.28(39) \text{ MeV}$$
$$(M_{\pi^+} - M_{\pi^0})|_{\gamma=2} = 4.33(41) \text{ MeV}.$$

As our best estimate we chose the one obtained with $\gamma = 1.5$ because the discretization effects are of the oder $\sim 4\%$, strongly suppressed in comparison with the original

	$\gamma = 0$	$\gamma = 1$	$\gamma = 1.5$	$\gamma = 2$
A_1	1022(142) MeV^2	1125(107) MeV^2	1153(102) MeV^2	1167(103) MeV^2
B_1	1022(130) MeV^2	1083(102) MeV^2	1094(100) MeV^2	1093(103) MeV^2
C_1	1065(139) MeV^2	1158(106) MeV^2	1186(100) MeV^2	1199(100) MeV^2
D_1	1028(130) MeV^2	1115(100) MeV^2	1140(96) MeV^2	1153(98) MeV^2
A_2	1009(143) MeV^2	1139(105) MeV^2	1175(99) MeV^2	1194(99) MeV^2
B_2	1017(131) MeV^2	1097(101) MeV^2	1112(99) MeV^2	1112(102) MeV^2
C_2	1063(139) MeV^2	1182(104) MeV^2	1221(97) MeV^2	1241(95) MeV^2
D_2	1025(1230) MeV^2	1139(99) MeV^2	1175(94) MeV^2	1194(96) MeV^2
Average	**1031(137)** MeV^2	**1130(107)** MeV^2	**1157(106)** MeV^2	**1169(109)** MeV^2

Table 3.3: Results for $M^2_{\pi^+} - M^2_{\pi^0}$ as obtained from different analyses and different values of γ. The uncertainty is the statistical+fitting error and the systematic uncertainties on the renormalization constants, the lattice spacing and the parameters in eq. (3.7). It is calculated using eq.(3.6).

ones that were $\sim 40\%$. In tab. (3.4) we present the fit coefficients obtained in the case $\gamma = 1.5$.

We finally obtain our final result:

$$\boxed{\begin{aligned} M_{\pi^+} - M_{\pi^0} &= 4.28(36)(14)\ \text{MeV} \\ &= 4.28(39)\ \text{MeV} \end{aligned}} \tag{3.15a}$$

where we have shown the two contributions to the uncertainty obtained from eq. (3.6). The total error is the sum in quadrature.

We can compare eq. (3.15) with our previous $N_f = 2$ result [10] and with the experimental value [2]

$$\begin{aligned} M_{\pi^+} - M_{\pi^0} &= 5.33(76)\ \text{MeV} && N_f = 2 \\ M_{\pi^+} - M_{\pi^0} &= 4.28(39)\ \text{MeV} && N_f = 2+1+1 \\ M_{\pi^+} - M_{\pi^0} &= 4.5936(5)\ \text{MeV} && \mathit{Experimental}. \end{aligned}$$

The results at $N_f = 2$ and $N_f = 2+1+1$ are compatible within the uncertainties. Furthermore the latter is reduced from 14% to 9%. Our result is fully compatible with the experimental one. This also suggests that the disconnected diagram of eq. (2.100), which has been neglected in the calculation, gives a contribution of $\mathcal{O}(\alpha_{em} m_{ud})$ smaller than the current uncertainties.

	C	K	$\hat{A}$ (GeV^4)
A_1	0.157(17)	4.35(49)	0.00046(72)
B_1	0.169(17)	4.31(49)	0.00044(69)
C_1	0.162(17)	4.40(48)	0.00046(77)
D_1	0.161(17)	4.35(49)	0.00043(72)
A_2	0.162(17)	4.19(47)	-0.00009(63)
B_2	0.162(17)	4.17(47)	-0.00009(61)
C_2	0.168(17)	4.26(46)	-0.00013(68)
D_2	0.167(16)	4.20(47)	-0.00013(64)

Table 3.4: Fit parameters obtained using eq. (3.14) with $\gamma = 1.5$ for the set as explained in tab. 3.2. The uncertainty is the statistical+fitting error and the systematic uncertainties on the renormalization constants, the lattice spacing and the parameters in eq. (3.7), calculated using eq.(3.6). As we will see in sec. (3.3), the parameter C will be used in the kaon sector analysis.

3.3 $m_d - m_u$

In this section we are going to analize the kaon sector and to calculate the quark mass difference $m_d - m_u$ from the study of the charged–neutral kaon mass splitting $M_{K^+} - M_{K^0}$.

As in the case of the pion, we will follow the strategy described in sec. (2.4). In the difference $(\Delta M_{K^+} - \Delta M_{K^0})$, the isosymmetric vacuum polarization diagrams cancel as well as the counter–terms corresponding to the variation of the average up–down quark mass $m_{ud} - m_{ud}^0$ and of the strange quark mass $m_s - m_s^0$. In the kaon case, however, the contribution proportional to the sea quark charge difference $e_u - e_d$ doesn't cancel out, as can be seen in eq. (2.105). This contribution vanishes in the $SU(3)$ limit and/or in the so called electro–quenched approximation (i.e. the limit in which the electric charges of the sea quarks are neglected) that we are going to use in the present analysis.

The remaining contributions are:

$R_K^m =$ 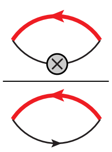 ,

$R_K^k =$ 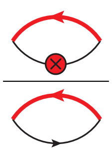 ,

$R_K^{exch} =$ 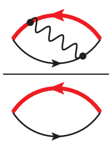 ,

$R_K^{self} =$ 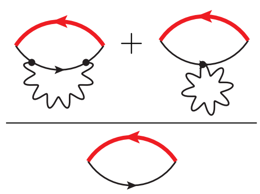 , (3.16)

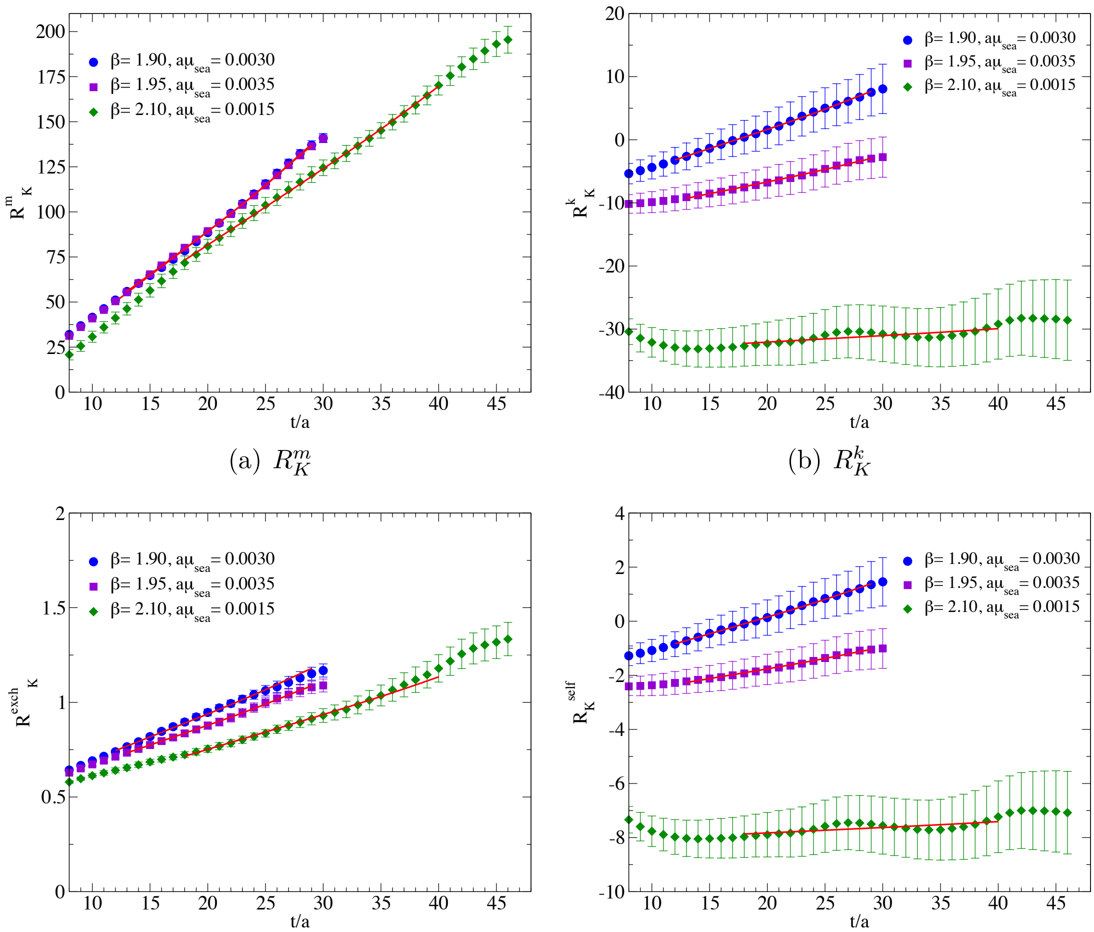

(a) R_K^m (b) R_K^k

(c) R_K^{exch} (d) R_K^{self}

Figure 3.4: Contribution to $M_{K^+} - M_{K^0}$ defined in eq. (3.16) for different values of the lattice spacing and as a function of time. Fit function in eq. (2.94).

and the kaon mass difference can be written as

$$\begin{aligned} M_{K^+} - M_{K^0} = \; & -2\Delta m_{ud}\; \partial_t R_K^m - (\Delta m_u^{cr} - \Delta m_d^{cr})\; \partial_t R_K^k + \\ & + (e_u^2 - e_d^2) e^2 \; \partial_t \left[R_K^{exch} - R_K^{self} \right] \; . \end{aligned} \tag{3.17}$$

In fig. (3.4) we present the fit results for the various correlations $R_K^i(t)$ perform using eq. (2.94) from which we obtained the corresponding contributions to ΔM_i. From this fit we also calculated δG, i.e. the variation $\Delta \langle 0 | \bar{s}\gamma_5 l(0) | K \rangle$, that we will use in sec. (3.4) to calculate δf_K.

From this analysis we determine the parameter Δm_{ud} using the experimental value of $M_{K^+} - M_{K^0}$. Then, the mass difference Δm_{ud} can be used to predict the isospin breaking mass splitting of other hadrons, as for example the neutron–proton mass difference or the isospin breaking effect on the kaon decay constant, see sec. (3.4).

It is useful to introduce a renormalization prescription to separate QED and QCD isospin breaking corrections. To this purpose, we need to express eq. (3.17) in terms of the renormalized light quark masses. In QED the parameters m_{ud} and Δm_{ud} mix under renormalization. The u and d quarks have different renormalization constants, $Z_{m_u}(\mu)$ and $Z_{m_d}(\mu)$, because they have different electric charges. We can write

$$\Delta m_{ud} = \frac{1}{2}\left(\frac{\hat{m}_d}{Z_{m_d}} - \frac{\hat{m}_u}{Z_{m_u}}\right) \quad = \quad \frac{\Delta\hat{m}_{ud}}{Z_{ud}} + \frac{\hat{m}_{ud}}{\mathcal{Z}_{ud}} \,, \tag{3.18}$$

where we have defined

$$\frac{1}{Z_{ud}} = \frac{1}{2}\left(\frac{1}{Z_{m_d}} + \frac{1}{Z_{m_u}}\right) \,, \qquad\qquad \frac{1}{\mathcal{Z}_{ud}} = \frac{1}{2}\left(\frac{1}{Z_{m_d}} - \frac{1}{Z_{m_u}}\right) \,. \tag{3.19}$$

The mixing does not occur in the isosymmetric theory where the quarks are neutral with respect to electromagnetic interactions and we have

$$\frac{1}{Z^0_{ud}} = Z^0_{\bar{\psi}\psi} \,, \qquad\qquad \frac{1}{\mathcal{Z}^0_{ud}} = 0 \,. \tag{3.20}$$

In the maximally twisted mass regularization for fermions, adopted in the present study, $Z^0_{\bar{\psi}\psi} = Z^0_P$ and we have used the values of this renormalization constants collected in tab. (3.1). By neglecting contributions of $O(e^2\Delta m_{ud})$, eq. (3.18) can be rewritten as

$$\Delta m_{ud} = Z^0_{\bar{\psi}\psi}\ \Delta\hat{m}_{ud} + \frac{\hat{m}_{ud}}{\mathcal{Z}_{ud}} \,. \tag{3.21}$$

For the renormalization constant $\mathcal{Z}_{ud}$, we considered the one loop perturbative result in the $\overline{MS}$ scheme that can be obtained from ref. [42], namely

$$\frac{1}{\mathcal{Z}_{ud}(\overline{MS},\mu)} = \frac{(e_d^2 - e_u^2)e^2}{32\pi^2}\left[\ 6\log(a\mu) - 22.596\ldots\ \right] Z^0_{\bar{\psi}\psi} \,. \tag{3.22}$$

Using eq. (3.21), the kaon mass difference of eq. (3.17) can be written as

$$M_{K^+} - M_{K^0} = \left[M_{K^+} - M_{K^0}\right]^{QED}(\mu) + \left[M_{K^+} - M_{K^0}\right]^{QCD}(\mu) \,, \tag{3.23}$$

where

$$\begin{aligned}
\left[M_{K^+} - M_{K^0}\right]^{QED}(\mu) = &\ -2\hat{m}_{ud}\,\tfrac{\partial_t R^m_K}{\mathcal{Z}_{ud}} - (\Delta m_u^{cr} - \Delta m_d^{cr})\partial_t R^k_K + \\
&+ (e_u^2 - e_d^2)e^2\partial_t\left[R^{exch}_K - R^{self}_K\right] , \\
\left[M_{K^+} - M_{K^0}\right]^{QCD}(\mu) = &\ -2\Delta\hat{m}_{ud}\left(Z^0_{\bar{\psi}\psi}\ \partial_t R^m_K\right) \,.
\end{aligned} \tag{3.24}$$

In the QED part we have included the contribution from the electromagnetic shift of the critical masses, proportional to $(\Delta m_u^{cr} - \Delta m_d^{cr})$, and two contributions proportional to the u and d square charges difference $(e_u^2 - e_d^2)e^2$. The QCD part is proportional to the renormalized u and d mass difference $\Delta\hat{m}_{ud}$, which is the quantity that we are going to calculate.

By having introduced a renormalization prescription to separate QED and QCD contributions we can express our results in terms of $\varepsilon_\gamma(\mu)$, which quantify the violation of the Dashen theorem [3]

$$\begin{aligned} \varepsilon_\gamma(\mu) &= \frac{\left[M_{K^+}^2 - M_{K^0}^2\right]^{QED}(\mu) - \left[M_{\pi^+}^2 - M_{\pi^0}^2\right]^{QED}(\mu)}{M_{\pi^+}^2 - M_{\pi^0}^2} \\ &= \frac{\left[M_{K^+}^2 - M_{K^0}^2\right]^{QED}(\mu)}{M_{\pi^+}^2 - M_{\pi^0}^2} - 1 \quad + \quad O(\hat{\alpha}_{em}\Delta\hat{m}_{ud}) \,. \end{aligned} \tag{3.25}$$

In order to compute $\varepsilon_\gamma(\mu)$ we first need to calculate the correction Δm_f^{cr} to the critical mass that enters $\left[M_{K^+} - M_{K^0}\right]^{QED}$ in eq. (3.24). We used eq. (2.102) and we performed a constant fit in time, as shown in fig. (3.6(a)). We also present in fig. (3.6(b)) the dependance of $\frac{\Delta m_f^{cr}}{(e \cdot e_f)^2}$ on the isospin average quark mass m_{ud} for different values of β. As expected the critical mass counter–terms depend very mildly on the light quark mass. The small dependence is due to statistical fluctuations and (small) cutoff effects.

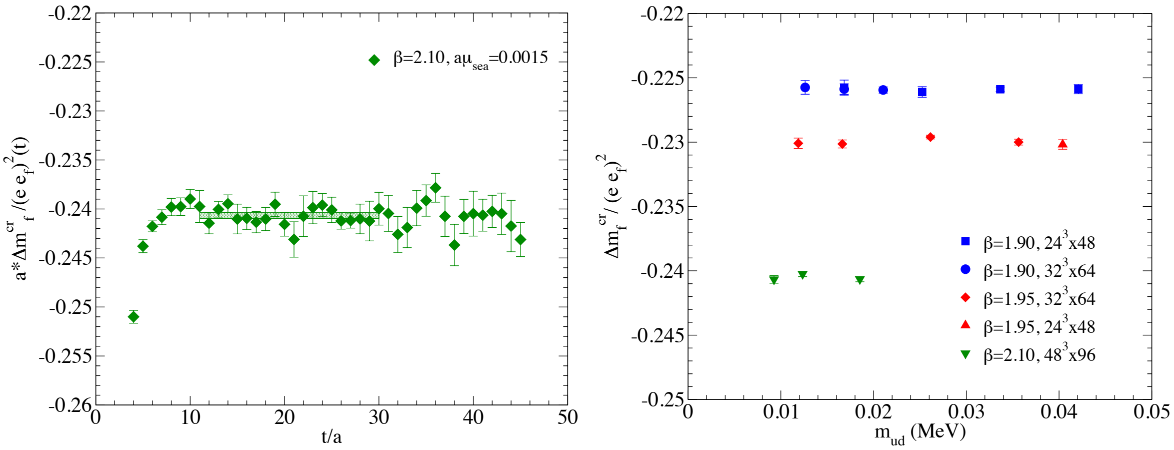

(a) (b)

Figure 3.5: QED correction to the critical mass $\frac{\Delta m_f^{cr}}{(e \cdot e_f)^2}$ calculated using eq. (2.102). On the left panel we show the constant fit in time for $\beta = 2.10$, $a\mu_{sea} = 0.0015$. On the right panel the results of the fits for different values of β presented as a function of the light quark mass. As expected, the critical mass counter–terms depend very mildly on m_{ud}, the small dependence being due to statistical fluctuations and (small) cutoff effects.

We finally calculated $\varepsilon_\gamma(\mu)$ using eq. (3.24), with $M_{\pi^+}^2 - M_{\pi^0}^2$ computed as described in sec. (3.2). We present the results in fig. (3.6). We subtracted QED volume effects using eq. (2.116). In this case the finite volume effects are smaller because they partially cancel in the ratio of the two mass differences.

For the continuum and chiral extrapolations we applied the ChPT expressions in eq. (3.10) and eq. (3.11), obtaining for ε

$$\varepsilon(\mu) = \left(\frac{4}{3} + \frac{3}{4C}\right) \cdot \cdot \left\{ -\frac{M_K^2}{(4\pi f_0)^2} \cdot \left[\log\left(\frac{M_K^2}{\mu^2}\right) + K_0\right] + \frac{M_\pi^2}{(4\pi f_0)^2} \cdot \left[\log\left(\frac{M_\pi^2}{\mu^2}\right) + K_1\right]\right\}, \tag{3.26}$$

where the LEC C is the same of the pion sector. By considering that $M_K^2 = b_0 \cdot (m_s + m_{ud})$ and that the m_{ud} dependence of $\log\left(\frac{M_K^2}{\mu^2}\right)$ is negligable, the terms proportional to $\frac{M_K^2}{(4\pi f_0)^2}$ can be absorbed in a re–definition of the constant K_1 and into a new constant K_2. In this way eq. (3.26) can be re–written as

$$\varepsilon(\mu) = \left(\frac{4}{3} + \frac{3}{4C}\right) \cdot \left\{ \frac{M_\pi^2}{(4\pi f_0)^2} \cdot \left[\log\left(\frac{M_\pi^2}{\mu^2}\right) + K_1\right] + K_2 \right\}. \tag{3.27}$$

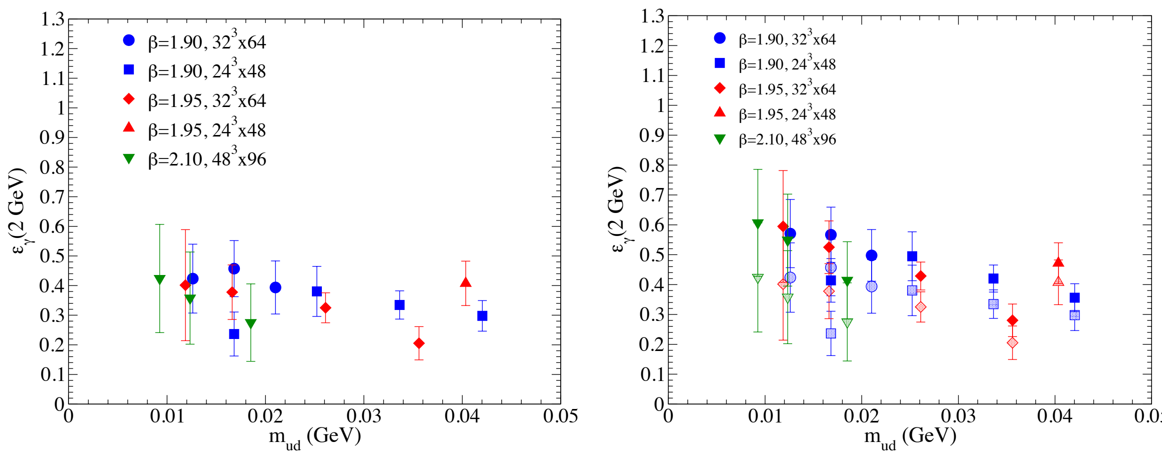

(a) Data without VE corrections (b) Full points are QED VE corrected.

Figure 3.6: The parameter $\varepsilon_\gamma(2\ \mathrm{GeV})$ of eq. (3.25). In the left panel we present in different colours data corresponding to different values of β as a function of the average light quark mass m_{ud}. In the right panel we show the effect of subtracting QED FVE according to eq. (2.116).

In the analysis we used the electro–quenched approximation, the limit in which the electric charges of the sea quarks are neglected. In order to estimate the systematical uncertainty we will consider the complete expression for ϵ, that is

$$\varepsilon(\mu) = \left(\frac{4}{3} + 2e_u^{sea} + 2e_d^{sea} + \frac{3}{4C}\right) \cdot \left\{ \frac{M_\pi^2}{(4\pi f_0)^2} \cdot \left[\log\left(\frac{M_\pi^2}{\mu^2}\right) + K_1 \right] + K_2 \right\}. \tag{3.28}$$

We used the fitting function of eq. (3.27) and the result is shown in fig. (3.7). We included a term proportional to a^2 but we found a coefficient compatible with zero. We used the value of the LEC C determined in the pion analysis in the case $\gamma = 1.5$ and presented in tab. (3.4).

We obtained

$$\varepsilon_\gamma(2\ \mathrm{GeV}) = 0.75(5), \tag{3.29}$$

where the uncertainty is the statistical+fitting error. The systematic uncertainties from the renormalization constants and the lattice spacing are negligible. Another source of systematic uncertainty comes from the electro–quenched approximation, that we estimated by using the chiral formula for ε_γ in eq. (3.28). We computed the ratio $\varepsilon_\gamma(e_d^{sea} + e_u^{sea} = 1/3)/\varepsilon_\gamma(e_d^{sea} + e_u^{sea} = 0)$ by taking C from the fit and by neglecting the variation of K_1 and K_2. Then we added in quadrature the resulting $\sim 11\%$ uncertainty, obtaining

$$\boxed{\varepsilon_\gamma(2\ \mathrm{GeV}) = 0.75(5)(8) = 0.75(9)}\ . \tag{3.30}$$

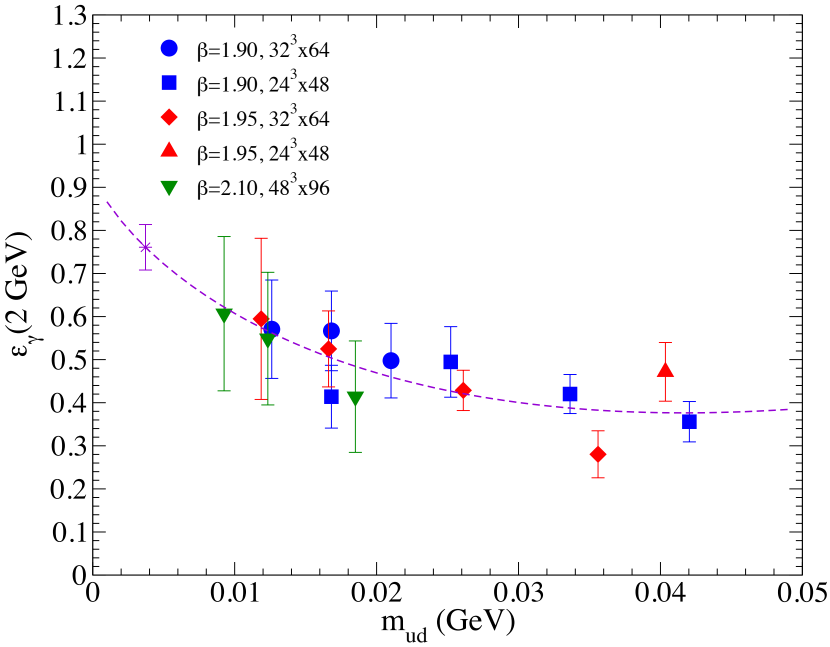

Figure 3.7: Chiral extrapolation of ε_γ(2 GeV). The dashed line is the chiral limit.

The total error is the sum in quadrature of the two contributions. Our result is compatible with the estimate for this quantity provided in ref. [10] for $N_f = 2$, that is $\varepsilon_\gamma \sim 0.79(25)$.

Using result for $M_{\pi^+} - M_{\pi^0}$ in eq. (3.15), ε_γ(2 GeV) of eq. (3.30) and the experimental value $M_{K^+} - M_{K^0} = -3.937$ MeV[2], we can evaluate separately the QED and QCD contributions of eq. (3.24) to the kaons mass difference, finding:

$$[M_{K^+} - M_{K^0}]^{QED} (2\text{ GeV}) = 2.04(17)(07)(10)\text{ MeV} = 2.04(21)\text{ MeV} \qquad (3.31)$$

$$[M_{K^+} - M_{K^0}]^{QCD} (2\text{ GeV}) = -5.98(17)(07)(09)\text{ MeV} = -5.98(20)\text{ MeV} \qquad (3.32)$$

where the first error is the statistical and fitting error, the uncertainty on the lattice spacing and on the renormalization constants while the second one is the systematic error calculated from the different sets of input values used in the analysis computed according to eq. (3.6). The third error in eq. (3.31) is the systematic error due to the electro–quenched approximation. The total error is the sum in quadrature of the three contributions.

Using the result for $[M_{K^+} - M_{K^0}]^{QCD}$ we can compute the quark mass difference $m_d - m_u$, from eq. (3.24). We extrapolated $Z^0_{\bar\psi\psi}\partial_t R^m_K = Z_P \partial_t R^m_K$ to the continuum limit and to the physical light quark mass using a simple polynomial function of the form

$$A + B \cdot m_{ud} + C \cdot a^2, \qquad (3.33)$$

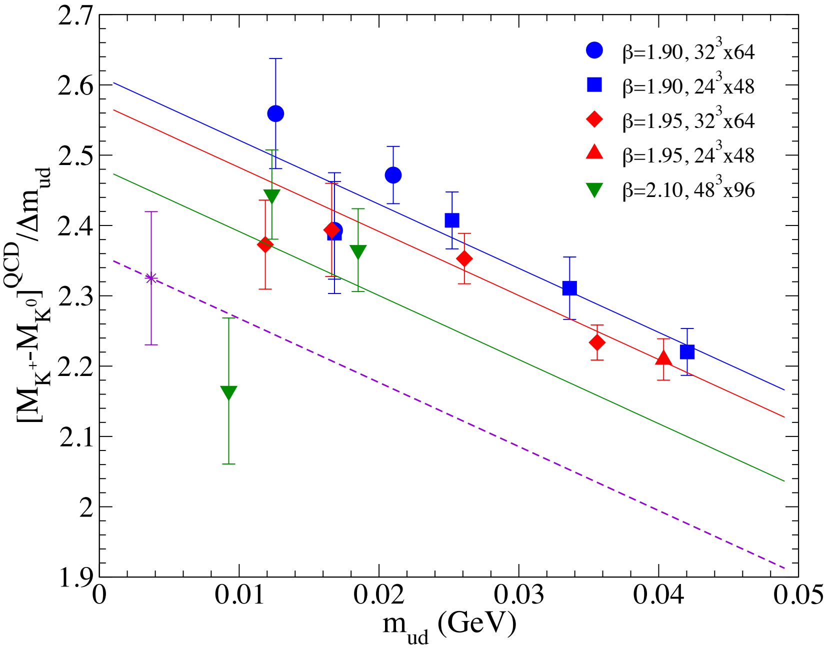

Figure 3.8: Chiral and continuum extrapolation for $Z_P \partial_t R_K^m = \frac{[M_{K^+} - M_{K^0}]_{QCD}}{\Delta m_{ud}}$ calculated using eq. (3.33). The dashed line is the continuum limit.

as shown in fig. (3.8). We finally obtained for the *up* and *down* quark mass difference with $N_f = 2 + 1 + 1$ the value

$$\boxed{[m_d - m_u](\overline{MS}, 2 \text{ GeV}) = 2.56(12)(03)(03) \text{ MeV} = 2.56(13) \text{ MeV}} \tag{3.34}$$

where the first error is the statistical and fitting error, the uncertainty on the lattice spacing and on the renormalization constants, the second is the systematic error, calculated as in eq. (3.6), and the third one is due to the electro–quenched approximation. The final uncertainty is the quadrature of the contributions. We can compare this result with the previous one obtained at $N_f = 2$ [10]:

$$[m_d - m_u](\overline{MS}, 2 \text{ GeV})|_{N_f=2} = 2.39(19) \text{ MeV} \tag{3.35}$$

noting that they are compatible within the error.

3.4 K_{ℓ_2}/Π_{ℓ_2} decay rate

In this section we will calculate the QCD isospin breaking effect in the kaon decay constant $f_{K^0} - f_{K^+}$, and using this result we compute the QCD isospin breaking effects on the ratio of the K_{ℓ_2} and Π_{ℓ_2} decay rates.

As mentioned in sec. (2.5.5), in this case we calculated only the QCD contribution to the isospin breaking effects, because in the presence of electromagnetism it is not possible to give even a physical definition of the decay constant. In ref. [38] the authors propose a strategy that can be implemented in future calculation for the evaluation of the QED contributions.

Using the same strategy described in sec. (2.4) we calculated the expansion at first order in Δm_{ud} and α_{em} of f_K defined in eq. (2.108), finding (see eq. (2.109))

$$\frac{\delta f_K}{\Delta m_{ud}} = \frac{\delta G_K}{\Delta m_{ud}} - 2\frac{\delta M_K}{\Delta m_{ud}} + \frac{1}{m_s + m_{ud}}, \tag{3.36}$$

with

$$\delta M_K = \frac{\Delta M_K}{M_K}, \qquad \delta G_K = \frac{\Delta G_K}{G_K}, \tag{3.37}$$

where M_K is the isosymmetric kaon mass. The corrections ΔM_K and $\Delta G_K = \Delta \langle 0| \bar{s}\gamma_5 l(0) |K\rangle$, are computed from eq. (2.94) using only the QCD contribution to the isospin breaking effects, that is:

$$R_K^m =$$

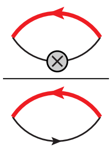

(3.38)

The result of this fit has been presented in fig. (3.4) where we reported the fit with which we calculated δG_K and ΔM_K using eq. (2.94). In fig. (3.9) we illustrate the lattice results for the slope $\frac{\delta f_K}{\Delta m_{ud}}$ as a function of the light quark mass and at the different values of the lattice spacings. We also show the result of the extrapolation to the physical point and to the continuum limit, preformed employing the $SU(2)$ Chiral Perturbation Theory prediction plus a quadratic dependence from the lattice spacing, obtaining

$$\frac{\delta f_K}{\Delta m_{ud}} = A + B \cdot a^2 + C \cdot (m_{ud} - \mu) + D \cdot m_{ud} \log\left(\frac{m_{ud}}{\mu}\right). \tag{3.39}$$

By using the value of $m_d - m_u$ derived in eq. (3.34), we then obtained for δf_K the result

$$\boxed{\delta f_K = \frac{f_{K^0} - f_{K^+}}{2 f_K} = 0.00397(35)(08) = 0.00397(36)\ \text{MeV}}\ , \tag{3.40}$$

where the first error is the statistic error and the second is the systematic one, coming from the lattice spacing and the renormalization constant calculated with eq. (3.6).

From the fact that at first order in Δm_{ud} the pion doesn't get corrections and that

$$\frac{f_{K^+} - f_K}{f_K} = \frac{f_{K^+} - f_{K^0}}{2 f_K} \tag{3.41}$$

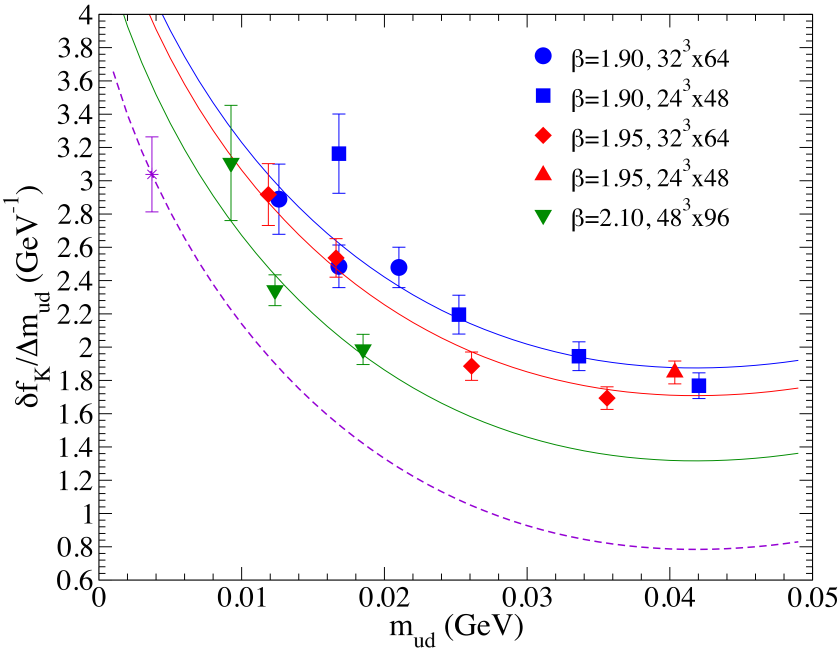

Figure 3.9: Chiral and continuum extrapolation of $\frac{\delta f_K}{\Delta m_{ud}}$ calculated using eq. (3.39). The dashed line is the curve corresponding to the continuum limit.

we can calculate the QCD isospin breaking effects on the ratio K_{ℓ_2}/Π_{ℓ_2} using the previous result

$$\left[\frac{f_{K^+}/f_{\pi^+}}{f_K/f_\pi} - 1\right]^{QCD} (\overline{MS}, 2\ \text{GeV}) = -0.00397(36). \tag{3.42}$$

Our result is higher than the estimate obtained in ref. [14] by using chiral perturbation theory, namely

$$\left[\frac{f_{K^+}/f_{\pi^+}}{f_K/f_\pi} - 1\right]^{QCD}_{\chi PT} (\overline{MS}, 2\ \text{GeV}) = -0.0022(6). \tag{3.43}$$

Comparing our result with the one computed at $N_f = 2$ [10]

$$\left[\frac{f_{K^+}/f_{\pi^+}}{f_K/f_\pi} - 1\right]^{QCD}_{N_f=2} (\overline{MS}, 2\ \text{GeV}) = -0.0040(3)(2), \tag{3.44}$$

we can see that they are perfectly compatible.

Conclusions

In this work we calculated isospin breaking corrections to pion and kaon masses, to the $K_{\ell 2}$ decay rate, as well as the u and d quark mass splitting. We performed LQCD numerical simulations with $N_f = 2+1+1$ sea quark, using gauge configurations produced by the ETM collaboration and computed two–point correlation functions to determine physical quantities in the continuum and chiral limits.

Our method is based on a perturbative expansion in $\Delta m_{ud} = m_d - m_u$ and α_{em} in order to evaluate isospin breaking corrections by starting from simulations in the isosymmetric QCD theory.

The main source of systematic errors in our calculation is the one associated with the chiral extrapolation, required because our pions are heavier than the physical ones. Another important source of systematics errors comes from finite volume effects, which are only power suppresed because QED is a long–ranged interaction.

One of our main result is the pion mass splitting, that receives at the leading order only the QED contribution. Considering that α_{em} doesn't renormalize at this order, this splitting is a very clean observable. However, it receives a disconnected contribution coming from the π_0 that is numerically very expensive to evaluate and presumably very small (being of $\mathcal{O}(\alpha m_{ud})$) and that we neglected in the calculation. We found

$$M_{\pi^+} - M_{\pi^0} = 4.28(39) \text{ MeV} .$$

Kaons masses receive both QED and QCD contributions. We implemented a renormalization prescription to separate QED from QCD isospin breaking corrections allowing to determine the electromagnetic contribution to the kaon mass splitting and the associated value of the Dashen's theorem breaking parameter ε_γ. In this case we used the electro–quenched approximation which consists in neglecting the charges of the sea quarks. Our result for $M_{K^+} - M_{K^0}$ is

$$[M_{K^+} - M_{K^0}]^{QED} (2 \text{ GeV}) = 2.04(21) \text{ MeV}$$

$$[M_{K^+} - M_{K^0}]^{QCD} (2 \text{ GeV}) = -5.98(20) \text{ MeV},$$

from which we also obtained

$$[m_d - m_u](\overline{MS}, 2 \text{ GeV}) = 2.56(13) \text{ MeV} .$$

The uncertainties in the above result contain also an estimation of the error due to the electro–quenched approximation, that is $\sim 11\%$.

Finally we studied the kaon decay constant correction, from which we evaluated the correction to the ratio of K_{ℓ_2} and Π_{ℓ_2} the decay rates, namely

$$\left[\frac{f_{K^+}/f_{\pi^+}}{f_K/f_\pi} - 1\right]^{QCD} (\overline{MS}, 2\ \text{GeV}) = -0.00397(36)\ .$$

The work presented in this thesis has allowed to determine some isospin breaking effects in meson physics with unprecedented precision. Still further important improvements and developments are possible:

- In our calculation we neglected contributions coming from disconnected diagrams. The only way to really understand the associated systematic error is to actually calculate them on the lattice. We can only notice that, within the quoted uncertainties, our results are compatible with the experimental ones (when present) and with previous lattice determinations;

- Another source of systematic error is the chiral extrapolation. Only recently, thanks to the increased computational power, the first lattice computations at physical light quark mass have been presented. However, still a large majority of the simulations, including ours, is performed with light quark masses higher than their physical values. An important improvement of the present work would consist in performing the same calculation with simulations at the physical point;

- In the study of the kaon decay constant we considered isospin breaking effects due only to the up–down mass splitting. In the presence of electromagnetism it is not possible to give even a physical definition of the decay constant, because of the contributions from diagrams in which the photon is emitted by the meson and absorbed by the charged lepton. Thus the physical width is not expressed just in terms of the matrix element of the axial current but it is obtained by a full calculation of the electromagnetic corrections at a given order. In ref. [38] the authors propose a strategy to include electromagnetic effects in processes for which infrared divergences are present in the intermediate steps of the calculation and cancel, as well known, between diagrams containing different numbers of real and virtual photons. By implementing this strategy one can evaluate on the lattice the whole QED effects to the decay amplitude;

- The same method presented in this thesis could be also applied to the case of baryons, in order to calculate for example the proton and neutron mass splitting and other hadron quantities, with the strategy described in ref. [11]. Numerical simulations are already in progress.

Appendix A

Statistical uncertainties

The physical quantities we are interesting in are calculated from two point correlation functions, obtained from numerical simulations as briefly described in chapter 1.4. In these simulations one calculates the path–integral using statistical methods, i.e. as an average on appropriate weighted configurations. For the central limit theorem, if the number of configurations $N \to \infty$, than the average on all configurations has a gaussian distribution and we have

$$\sigma^2_{\langle\mathcal{O}\rangle_N} = \frac{C}{N} \cdot \sigma^2_{\langle\mathcal{O}\rangle}, \tag{a}$$

where $C = 1$ if the configurations were independent. Since however the gauge configurations are generated as part of a Markov chain, they are correlated, each element being related to the previous one. A method that can be used in this case to evaluate the statistical errores is the *jacknife method*, in which the uncertainty is calculated using subgroups of data that are uncorrelated.

Let us consider an observable $\mathcal{O}$ calculated using N gauge configurations and N_J subgroups of configurations each composed by $n_J = N/N_J$ elements. Let us then calculate the average within each subgroup,

$$\overline{\mathcal{O}}_s = \frac{1}{n_J} \sum_{i=1}^{n_J} \mathcal{O}(U_i^s), \quad s = 1, .., N_J, \tag{b}$$

where $\mathcal{O}(U_i^s)$ denotes the observable calculated on the configuration i of the subgroup s. The N_J averages are treated as N_J measures of the observable. If n_J is large enough to guarantee that the configurations are not correlated, then the N_J measures are also independent. In many cases n_J is not large enough to ensure the independence of the measurements. In this case we can use the jacknife method. Using the N_J averages of eq. (b), we calculate N_J jacknife averages $\mathcal{O}_s^J$ by excluding, for the average s the subgroup $i = s$,

$$\mathcal{O}_s^J = \frac{1}{N_J - 1} \sum_{i \neq s, i=1}^{N_J} \overline{\mathcal{O}}_i, \quad s = 1, .., N_J. \tag{c}$$

The central values of the observable is provided by the arithmetic average over the N_J jacknives averages, which is equivalent to the average over all the N gauge configurations,

$$\langle \mathcal{O}_J \rangle_{jack} = \frac{1}{N_J} \sum_{i=1}^{N} \mathcal{O}_s^J = \frac{1}{N} \sum_{i=1}^{N} \mathcal{O}(U_i). \tag{d}$$

The jacknife averages of eq. (c) then also provides an estimate of the statistical errors given by

$$\sigma_J(\mathcal{O}) = \sqrt{(N_J - 1)\ |\langle \mathcal{O}_J^2 \rangle_{jack} - \langle \mathcal{O}_J \rangle_{jack}^2|}, \tag{e}$$

with

$$\left\langle \mathcal{O}_J^2 \right\rangle_{jack} = \frac{1}{N_J} \sum_{s=1}^{N_J} (\mathcal{O}_s^J)^2. \tag{f}$$

When calculating a physical observable on the lattice, we have to combine data from different numerical simulations, for example at different lattice spacing and different quark masses. We can do this by starting from the jacknives calculated as in eq. (c) and using the *boostrap* procedure. Bootstrapping is the practice of evaluating properties of an estimator (such as its variance) by measuring those properties when sampling from an approximating distribution. One standard choice for an approximating distribution is the empirical distribution of the observed data. In the case where a set of observations can be assumed to be from an independent and identically distributed population, this can be implemented by constructing a number of resamples of the observed dataset (and of equal size to the observed dataset), each of which is obtained by random sampling with replacement from the original dataset. Let us consider two observables $\mathcal{A}$ and $\mathcal{B}$ that we have to compare and calculated from two independent numerical simulations. We want to combine these two observables, for example in a fit, in order to obtain a third physical quantity $\mathcal{C}$, which derives from the other two. We have at our disposal for the input quantities the jacknife averages $\mathcal{A}_s^J$ and $\mathcal{B}_s^J$ with $s = 1, ..N_J$ as in eq. (c). As the two sets are independent, because they are obtained from different numerical simulations, we can choose to combine whatever of the N_J^2 couples $(\mathcal{A}_s^J, \mathcal{B}_{s'}^J)$. Following the boostrap procedure, one generates following a random distrubition a N_{boot} of jacknife indices $(i,j)_b$ couples, with $b = 1, ..N_{boot}$. Then one proceeds evaluating for each couple b the observable $\mathcal{C}_b$. The mean value of $\mathcal{C}$ will be equal to the ensemble average. The uncertainty is calculated as

$$\sigma_b(\mathcal{O}) = \sqrt{(N_J - 1)|\langle \mathcal{C}_b^2 \rangle_{boot} - \langle \mathcal{C}_b \rangle_{boot}^2|}, \tag{g}$$

with

$$\langle \mathcal{C}_b \rangle_{boot} = \frac{1}{N_{boot}} \sum_{b=1}^{N_{boot}} \mathcal{C}_b. \tag{h}$$

Bibliography

[1] Antonin Portelli. Inclusion of isospin breaking effects in lattice simulations. *PoS*, LATTICE2014:013, 2015.

[2] K. A. Olive et al. Review of Particle Physics. *Chin. Phys.*, C38:090001, 2014.

[3] R. Dashen. Chiral $SU(3) \otimes SU(3)$ as a Symmetry of the Strong Interactions. *Phys.Rev.*, 183:1245, 1969.

[4] Nazario Tantalo. Lattice calculation of isospin corrections to Kl2 and Kl3 decays. In *7th Workshop on the CKM Unitarity Triangle (CKM 2012) Cincinnati, Ohio, USA, September 28-October 2, 2012*, 2013.

[5] N. Cabibbo. Unitary Symmetry and Leptonic Decays. *Phys. Rev. Lett.*, 10:531–533, 1963.

[6] Sinya Aoki et al. Review of lattice results concerning low-energy particle physics. *Eur. Phys. J.*, C74:2890, 2014.

[7] Guido Altarelli. A QCD primer. *AIP Conf. Proc.*, 631:70–111, 2002.

[8] H. J. Rothe. Lattice gauge theories: An Introduction. *World Sci. Lect. Notes Phys.*, 43:1–381, 1992. [World Sci. Lect. Notes Phys.82,1(2012)].

[9] Rajan Gupta. Introduction to lattice QCD: Course. In *Probing the standard model of particle interactions. Proceedings, Summer School in Theoretical Physics, NATO Advanced Study Institute, 68th session, Les Houches, France, July 28-September 5, 1997. Pt. 1, 2*, pages 83–219, 1997.

[10] G.M. de Divitiis et al. Leading isospin breaking effects on the lattice. *Phys.Rev.*, D87(11):114505, 2013.

[11] G.M. de Divitiis, P. Dimopoulos, R. Frezzotti, V. Lubicz, G. Martinelli, et al. Isospin breaking effects due to the up-down mass difference in Lattice QCD. *JHEP*, 1204:124, 2012.

[12] Kenneth G. Wilson. Confinement of Quarks. *Phys. Rev.*, D10:2445–2459, 1974.

[13] Sz. Borsanyi, S. Durr, Z. Fodor, C. Hoelbling, S.D. Katz, et al. Ab initio calculation of the neutron-proton mass difference. *Science*, 347:1452–1455, 2015.

[14] Vincenzo Cirigliano and Helmut Neufeld. A note on isospin violation in Pl2(gamma) decays. *Phys. Lett.*, B700:7–10, 2011.

[15] Michael E. Peskin and Daniel V. Schroeder. *An Introduction to quantum field theory*. 1995.

[16] V. Lubicz. The Role of lattice QCD in flavor physics. *Nucl. Phys. Proc. Suppl.*, 140:48–57, 2005. [,48(2004)].

[17] Holger Bech Nielsen and M. Ninomiya. Absence of Neutrinos on a Lattice. 1. Proof by Homotopy Theory. *Nucl. Phys.*, B185:20, 1981. [Erratum: Nucl. Phys.B195,541(1982)].

[18] Y. Iwasaki. Renormalization Group Analysis of Lattice Theories and Improved Lattice Action. II. Four-dimensional non-Abelian SU(N) gauge model. 2011.

[19] Silvia Necco. Universality and RG improved gauge actions. *Nucl. Phys. Proc. Suppl.*, 119:452–454, 2003. [,452(2002)].

[20] Andrea Shindler. Twisted mass lattice QCD. *Phys. Rept.*, 461:37–110, 2008.

[21] Stefan Sint. Lattice QCD with a chiral twist. In *Workshop on Perspectives in Lattice QCD Nara, Japan, October 31-November 11, 2005*, 2007.

[22] K. Symanzik. Continuum Limit and Improved Action in Lattice Theories. 2. O(N) Nonlinear Sigma Model in Perturbation Theory. *Nucl. Phys.*, B226:205, 1983.

[23] Martin Luscher, Stefan Sint, Rainer Sommer, and Peter Weisz. Chiral symmetry and O(a) improvement in lattice QCD. *Nucl. Phys.*, B478:365–400, 1996.

[24] G. Martinelli, C. Pittori, Christopher T. Sachrajda, M. Testa, and A. Vladikas. A General method for nonperturbative renormalization of lattice operators. *Nucl. Phys.*, B445:81–108, 1995.

[25] M. Constantinou et al. Non-perturbative renormalization of quark bilinear operators with N_f = 2 (tmQCD) Wilson fermions and the tree-level improved gauge action. *JHEP*, 08:068, 2010.

[26] M. Crisafulli, V. Lubicz, and A. Vladikas. Improved renormalization of lattice operators: A Critical reappraisal. *Eur. Phys. J.*, C4:145–171, 1998.

[27] Marco Bochicchio, Luciano Maiani, Guido Martinelli, Gian Carlo Rossi, and Massimo Testa. Chiral Symmetry on the Lattice with Wilson Fermions. *Nucl. Phys.*, B262:331, 1985.

[28] Simon Duane, A.D. Kennedy, Brian J. Pendleton, and Duncan Roweth. Hybrid monte carlo. *Physics Letters B*, 195(2):216 – 222, 1987.

[29] A. Duncan, E. Eichten, and H. Thacker. Electromagnetic splittings and light quark masses in lattice QCD. *Phys. Rev. Lett.*, 76:3894–3897, 1996.

[30] R. Frezzotti and G. C. Rossi. Chirally improving Wilson fermions. II. Four-quark operators. *JHEP*, 10:070, 2004.

[31] M. Constantinou et al. B_K-parameter from $N_f = 2$ twisted mass lattice QCD. *Phys. Rev.*, D83:014505, 2011.

[32] Roberto Frezzotti, Pietro Antonio Grassi, Stefan Sint, and Peter Weisz. Lattice QCD with a chirally twisted mass term. *JHEP*, 08:058, 2001.

[33] R. Baron et al. Light hadrons from lattice QCD with light (u,d), strange and charm dynamical quarks. *JHEP*, 06:111, 2010.

[34] R. Frezzotti and G. C. Rossi. Twisted mass lattice QCD with mass nondegenerate quarks. *Nucl. Phys. Proc. Suppl.*, 128:193–202, 2004. [,193(2003)].

[35] Remi Baron et al. Computing K and D meson masses with $N_f = 2{+}1{+}1$ twisted mass lattice QCD. *Comput. Phys. Commun.*, 182:299–316, 2011.

[36] R. Frezzotti and G. C. Rossi. Chirally improving Wilson fermions. 1. O(a) improvement. *JHEP*, 08:007, 2004.

[37] J. Gasser, A. Rusetsky, and I. Scimemi. Electromagnetic corrections in hadronic processes. *Eur. Phys. J.*, C32:97–114, 2003.

[38] N. Carrasco, V. Lubicz, G. Martinelli, C. T. Sachrajda, N. Tantalo, C. Tarantino, and M. Testa. QED Corrections to Hadronic Processes in Lattice QCD. *Phys. Rev.*, D91(7):074506, 2015.

[39] N. Carrasco *et al.* "up, down, strange and charm quark masses with $n_f = 2+1+1$ twisted mass lattice qcd". *Nucl. Phys.*, B887:19–64, 2014. arXiv:1403.4504 [hep-lat].

[40] Johan Bijnens and Niclas Danielsson. Electromagnetic Corrections in Partially Quenched Chiral Perturbation Theory. *Phys. Rev.*, D75:014505, 2007.

[41] Masashi Hayakawa and Shunpei Uno. QED in finite volume and finite size scaling effect on electromagnetic properties of hadrons. *Prog. Theor. Phys.*, 120:413–441, 2008.

[42] Sinya Aoki, Kei-ichi Nagai, Yusuke Taniguchi, and Akira Ukawa. Perturbative renormalization factors of bilinear quark operators for improved gluon and quark actions in lattice QCD. *Phys.Rev.*, D58:074505, 1998.